	<p>Research and Development Programme on Seismic Ground Motion</p> <p>CONFIDENTIAL <i>Restricted to SIGMA scientific partners and members of the consortium, please do not pass around</i></p>	<p>Ref : SIGMA-2013-D4-94 Version : 01</p> <p>Date : Page :</p>
--	--	---




# SITE SPECIFIC PROBABILISTIC STUDY FOR PO PLAIN AREA

(Deliverable D4-94)

AUTHORS			REVIEW			APPROVAL		
NOM	DATE	VISA	NOM	DATE	VISA	NOM	DATE	VISA
E. Faccioli (Research POLIMI)			J. Savy (SRC Consulting)	In written review attached		M. Corigliano		
			G. Woo	In written review attached				

*DISSEMINATION: Authors; Steering Committee; Work Package leaders, Scientific Committee, Archiving.*

	<p>Research and Development Programme on Seismic Ground Motion</p> <p>CONFIDENTIAL</p> <p><i>Restricted to SIGMA scientific partners and members of the consortium, please do not pass around</i></p>	<p>Ref : SIGMA-2013-D4-94 Version : 01</p> <hr/> <p>Date : October 2013 Page :</p>
--	---	--

**Executive Summary**


This report gives an updated description of the work in progress that the technical integration team is implementing. The final report will be delivered after the discussions at the next scientific committee meeting.

The work shown is intended as an update and an extension of the previous year work (phase I).

The report is organized in 11 chapters that recall in the introduction the main findings of the previous year work.


In the Appendices, additional results and graphs are provided.

DRAFT

	<p>Research and Development Programme on Seismic Ground Motion</p> <p>CONFIDENTIAL</p> <p><i>Restricted to SIGMA scientific partners and members of the consortium, please do not pass around</i></p>	<p>Ref : SIGMA-2013-D4-94 Version : 01</p> <p>Date : October 2013 Page :</p>
--	---	--


## CONTENTS

<b>1.</b>	<b>PHASE I WP4 WORK .....</b>	<b>5</b>
<b>2.</b>	<b>PHASE II WORK .....</b>	<b>6</b>
<b>3.</b>	<b>CATALOGUE AND MAGNITUDE CONVERSIONS.....</b>	<b>7</b>
3.1.	UPDATING OF WORKING CATALOGUE .....	8
3.2.	UPDATING OF GR PARAMETERS .....	9
3.3.	COMPARING OLD AND NEW G-R PARAMETERS .....	14
<b>4.</b>	<b>UPDATING OF GMPES.....</b>	<b>18</b>
<b>5.</b>	<b>THE SINGLE STATION SIGMA APPROACH.....</b>	<b>19</b>
5.1.	METHOD OF GROUND MOTION RESIDUAL ANALYSIS .....	19
5.2.	NON ERGODIC USE OF GMPES IN HAZARD ANALYSES .....	20
5.3.	ADOPTED CORRECTION COEFFICIENTS .....	21
5.4.	COMPARING NON-ERGODIC AND ERGODIC HAZARD ESTIMATION.....	23
<b>6.</b>	<b>MODEL-BASED DESCRIPTION: FAULTS + BACKGROUND.....</b>	<b>27</b>
6.1.	DISS DATABASE OF FAULT SOURCES .....	27
6.2.	BACKGROUND SEISMIC ACTIVITY .....	30
6.3.	FAULTS.....	33
6.4.	RECURRENCE TIME .....	35
6.5.	COMPARING AS MODELING VERSUS FS+BG .....	36
6.6.	MODELLING FAULTS WITH AN ALTERNATIVE APPROACH.....	39
6.6.1.	<i>Generalized description of ground motion attenuation (GAF) .....</i>	<i>40</i>
6.6.2.	<i>Finite fault stochastic modeling: EXSIM code .....</i>	<i>41</i>
6.6.3.	<i>Approach used for hazard computations with Composite Sources (CSS).....</i>	<i>41</i>
6.6.4.	<i>Accounting for site response .....</i>	<i>43</i>
6.6.5.	<i>Results .....</i>	<i>45</i>
<b>7.</b>	<b>GRIDDED SEISMICITY .....</b>	<b>47</b>
<b>8.</b>	<b>LOGIC TREE.....</b>	<b>50</b>
<b>9.</b>	<b>ACCOUNTING FOR SITE EFFECTS.....</b>	<b>53</b>
<b>10.</b>	<b>RESULTS OF LOGIC TREE FOR GROUND TYPE A .....</b>	<b>55</b>
<b>11.</b>	<b>RESULTS OF LOGIC TREE FOR GROUND TYPE C AND B.....</b>	<b>63</b>

	<p style="text-align: center;">Research and Development Programme on Seismic Ground Motion</p> <p style="text-align: center;">CONFIDENTIAL <i>Restricted to SIGMA scientific partners and members of the consortium, please do not pass around</i></p>	<p>Ref : SIGMA-2013-D4-94 Version : 01</p> <hr/> <p>Date : October 2013 Page :</p>
--	--	--

12.	<b>CONCLUSIONS (TENTATIVE)</b> .....	<b>70</b>
13.	<b>REFERENCES</b> .....	<b>72</b>

DRAFT

	<p>Research and Development Programme on Seismic Ground Motion</p> <p>CONFIDENTIAL</p> <p><i>Restricted to SIGMA scientific partners and members of the consortium, please do not pass around</i></p>	<p>Ref : SIGMA-2013-D4-94 Version : 01</p> <p>Date : October 2013 Page :</p>
--	---	--

## **1. Phase I WP4 work**


The work done in the first phase of Sigma (Phase I) by the POLIMI team concerned SH in the Po Plain region of Northern Italy and was addressed to exploring the influence of the (mostly) epistemic uncertainties associated to three key input elements to the analysis, namely:

- the model of extended seismic source zones (SSZs)
- the description of earthquake occurrence in time
- the ground motion attenuation relations.

The work significantly benefitted from the results of earlier Italian research projects, carried out between 2004 and 2010, which provided an initial reference model of SSZs, the probabilities of earthquakes of different magnitudes occurring in a given time window, needed to compute the hazard from various recurrence models, and the basic tool for PSHA (the CRISIS2008 code, updated in 2012).

A significantly updated SSZ representation was developed, which contained also a subduction-like zone to account for the deeper events, never previously considered.

For the purpose of establishing a baseline hazard evaluation, an initial, rather simple logic tree was designed, consistent with the stated scope of the work, and used for PSHA. The results of the analyses carried out at the three representative sites in the region (Casaglia, Novellara and Tortona) indicated that the variability introduced by the different gridded seismicity models (including stationary and non-stationary ones) tended to be larger than that carried by the GMPEs and the SSZ description. In absolute terms, in the range of the peak values, the current NTC 2008 code spectra on rock tended to be on the low side of the predicted standard percentile prediction band. Mean peak UH spectrum values on rock reached or exceeded 1g for 10000 years and were significantly higher for the sites on ground type C, like NVL and CAS. A comparison of the 475 year predicted spectrum with the spectrum observed during the strong  $M_w$  6.1 shock of May 20, 2012, at an additional site (MRN) on the deep Po Plain sediments, showed that peak predicted levels were realistic, but not the spectral bandwidth, presumably because of the strong influence of site effects on such sediments.

	<p>Research and Development Programme on Seismic Ground Motion</p> <p>CONFIDENTIAL</p> <p><i>Restricted to SIGMA scientific partners and members of the consortium, please do not pass around</i></p>	<p>Ref : SIGMA-2013-D4-94 Version : 01</p> <p>Date : October 2013 Page :</p>
--	---	--

## 2. Phase II work

In this second stage a few tasks just sketched in the first phase were now more deeply inspected.

In particular, concerning fault sources, these were previously treated only through one of the gridded, non-stationary seismicity descriptions. To this end, the necessary input takes into account both the tectonic setting of the May – June 2012 sequence of strong earthquakes occurring in the region and the interpretations thereof expected from other Italian research groups of SIGMA (notably INGV). Another topic taken into account is the dispersion in activity rates introduced by magnitude conversions. A special care has been devoted to the updating of the catalogue as well.

Moreover, a planned use of the “single-station”, non-ergodic sigma has been introduced in the hazard calculations, based on the analyses of the acceleration records available for the sites of interest.

Concerning GMPEs selection, a significant updating is introduced with respect to phase I; in accordance with the SHARE project general criteria (Delavaud et al. 2012) for active shallow crustal regions (ASCR), we used the most updated, published versions of the equations adopted therein.

Finally, concerning site effects, different approaches have been explored and compared in terms of hazard curves and spectra.

The flow chart of Figure 1 sketches the new tasks explored in this phase.

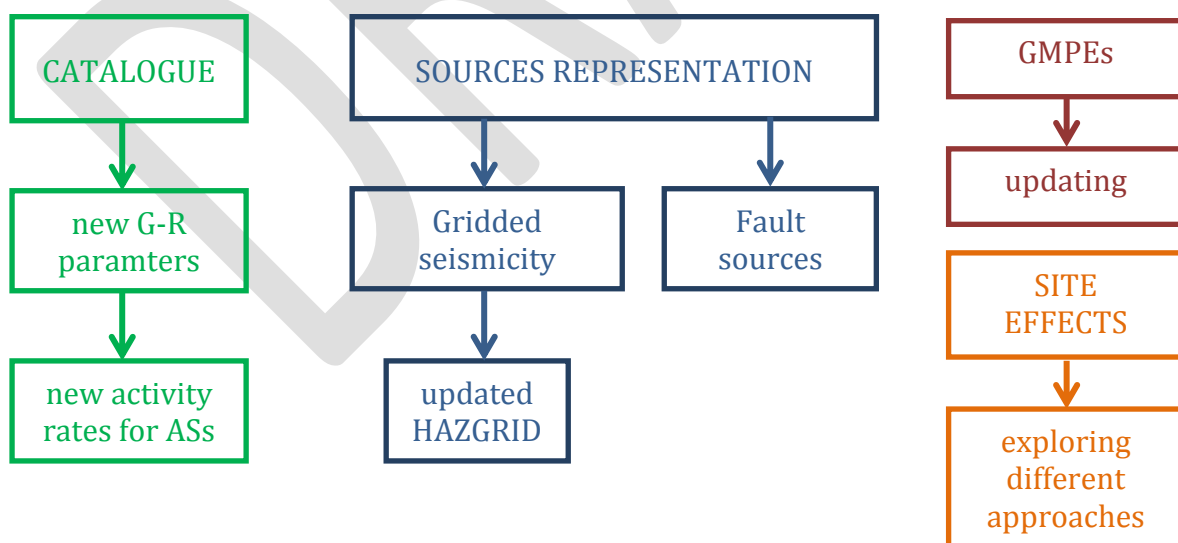


Figure 1 – Flowchart of new activities.

### 3. Catalogue and magnitude conversions

Phase I working catalogue was updated to the end of January 2012. The conversion law adopted to translate  $M_L$  values to  $M_w$  ones was the one of CPT11 (Rovida et al. 2011).

In order to verify the reliability of this law, a selected set of magnitude data was assembled, representative of the very recent Po Plain seismicity, with  $M_L$  values taken from the INGV Seismic Bulletin or Iside database and corresponding  $M_w$  values from INGV moment tensor solutions (<http://cnt.rm.ingv.it/tdmt.html>, Pondrelli et al., 2011). The data (blue dots in Figure 2) were fit with a straight line as shown in the figure. For comparison purposes, other existing correlations are displayed. The data we used for the present least squares fit range from  $M_L$  4.3 to 5.9. The yellow band shown in the figure represents the spread of the correlation laws calibrated by Gasperini et al. (2013), using general orthogonal regressions (GORs), with an Italian dataset spanning over different periods of time, from 1981 to 2010.

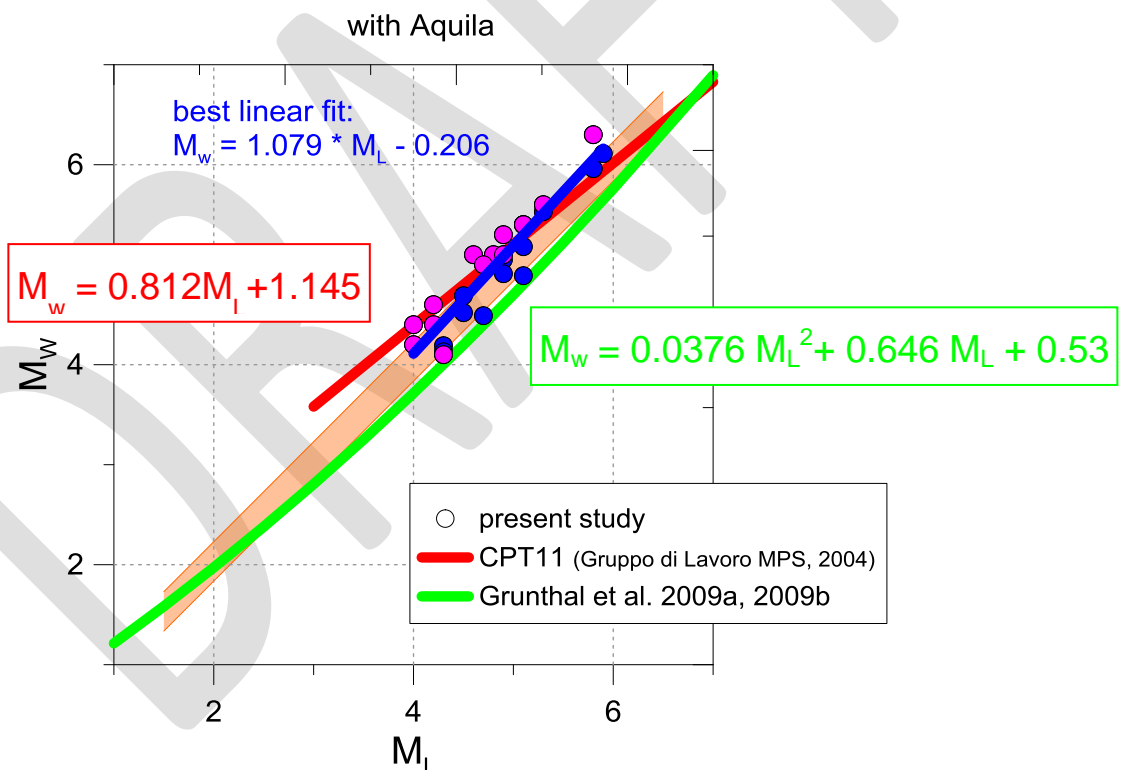



Figure 2 –  $M_L$  versus  $M_w$  for the Po Plain collected database (blue dots), using Quick Regional Moment Tensors solutions (QRMT) from Pondrelli et al. (2010) for moment-magnitude estimation. A linear fit (blue line) was used to fit the data. Other  $M_L$  -  $M_w$  correlation laws are plotted for comparison. Note that the blue dots include: the 2012 Emilia sequence, the 25.01.2012, 17.07.2011, 23.12.2008 and 15.10.1996, the magenta dots include events from l'Aquila 2009 sequence. The orange band shows the range of the correction laws proposed by Gasperini et al. (2013) for the Italian data.

	<p>Research and Development Programme on Seismic Ground Motion</p> <p>CONFIDENTIAL</p> <p><i>Restricted to SIGMA scientific partners and members of the consortium, please do not pass around</i></p>	<p>Ref : SIGMA-2013-D4-94 Version : 01</p> <p>Date : October 2013 Page :</p>
--	---	--

Note that the sample size of the database we assembled to test  $M_L$ - $M_w$  relationship is actually of 27 events. However, we did not intend to formulate a custom made conversion relationship, but to gain a feeling of the goodness of the conversion relationship we are actually relying on (the one adopted in the official CPTI11 catalogue, red line in the following plot). The LS fit we find (blue line in the plot of Figure 2) is very close to the basic result of the study of Gasperini et al. (2013), which establishes, for Italian earthquakes, an  $M_L$ : $M_w$  scaling close to 1:1, with an average offset of 0.2.

The above findings show that the  $M_L$  -  $M_w$  correlation used in previous Phase I (red line in previous figures) is not suited for events with  $M_w < 4.5$ , because of clear overestimation of  $M_w$ . For  $M_w > 4.5$ , the same conversion is closer to our least square fit and to other most recently published correlations.

For this reason we decided to update our working catalogue (now up to August 8<sup>th</sup> 2013), keeping only events from  $M_w = 4.5$ . In this way, the use of a conversion is no longer needed. This is because most of the  $M_w \geq 4.5$  events come directly from the CPTI11 catalogue (updated to 2006), while  $M_w$  values of more recent events  $\geq 4.5$  derive from the cited database of moment tensor solutions.

Since these findings apply for all SSZs, computation of updated G-R parameters for new hazard results has been carried out with  $M_w$  min 4.5 (instead of 2.5, as in Phase I), and without introducing magnitude conversion.

Other two reasons support this low cut of  $M_w$ : coherence with the SHARE project (where  $M_{w, \min}$  4.3-4.5 was used in G-R computations) and the fact that 4.5 is the threshold for earthquake induced damage of engineering interest.

### 3.1. Updating of working catalogue

The “old”, i.e. Phase I, catalogue was updated by searching in ISIDE database (<http://iside.rm.ingv.it/>) all events from February 2012 (last date in old catalogue) up to August 2013, and adding them. Note that the ISIDE database is nowadays the most updated Italian catalogue, providing revised information about the very recent seismicity, as soon as it is available. ISIDE lists  $M_L$  values, while the corresponding  $M_w$  values were found in moment tensor solutions in <http://www.bo.ingv.it/RCMT/>, see Pondrelli et al. (2011). Only mainshocks with  $M_w \geq 4.5$  have been retained at the end. Figure 3 shows with red stars the main events available for the updating of the old working catalogue (the SSZ shown are the ones defined in Phase I work, to which we refer for reference). Two events pertain to SSZ 915, while the others pertain to the two SSZs that mainly control the seismic hazard at the selected sites, that is 911 and 912+913+914; all these SSZs were used in the following tests.



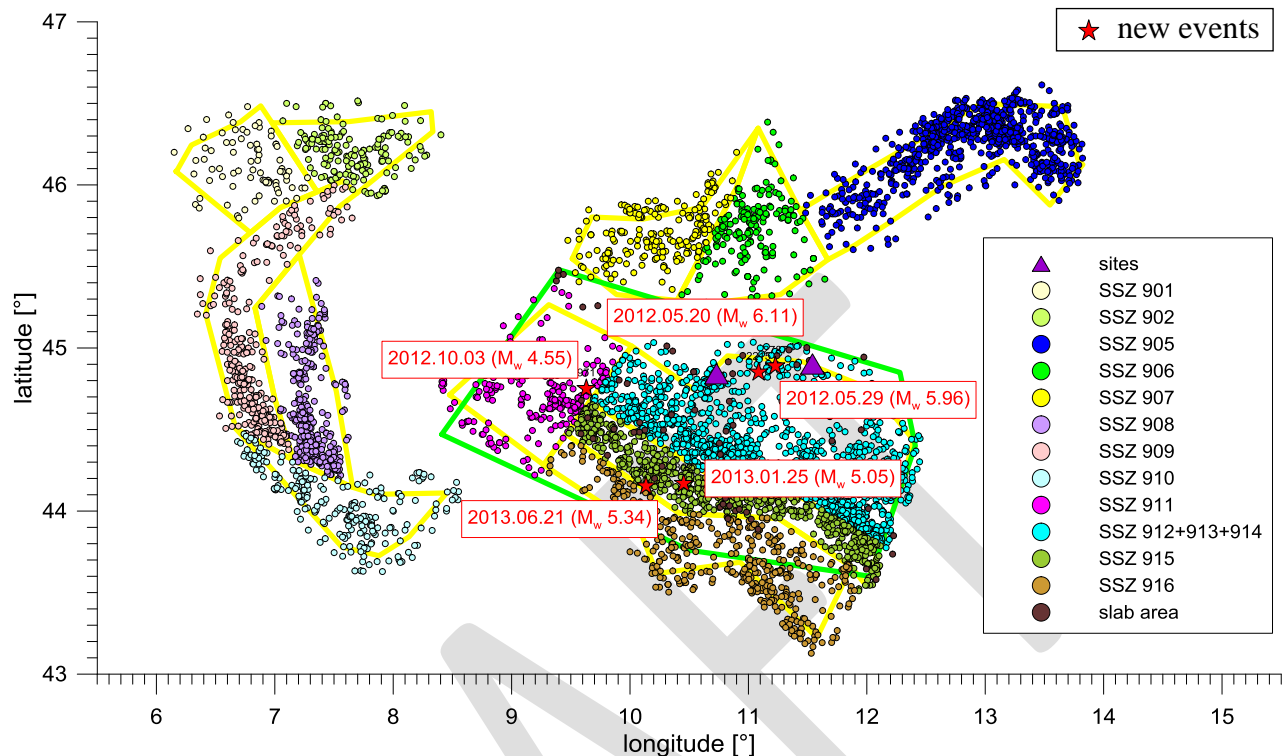


Figure 3 – Events subsets of Phase I, working catalogue associated to adopted SSZ (yellow polygons). The green polygon is the surface projection of the sinking slab. Red stars show the events added in the updating of the catalogue.

### 3.2. Updating of GR parameters

The computation of GR parameters has relied on the same completeness periods defined in Sigma Phase I work, and on the same procedures (the maximum likelihood method) but starting from a minimum value  $M_{min} = 4.5$ , against 2.5 in Phase I. As shown in Figure 4, Figure 5 and Figure 6, results change as a different  $M_{min}$  value is considered, or as the catalogue is updated, for all SSZs. One may note from the following figures that by the changes just introduced better frequency – magnitude fits are obtained. Starting from lower minimum magnitudes, as in Phase I, would have likely required a bilinear fit to appropriately adjust predictions to observations.

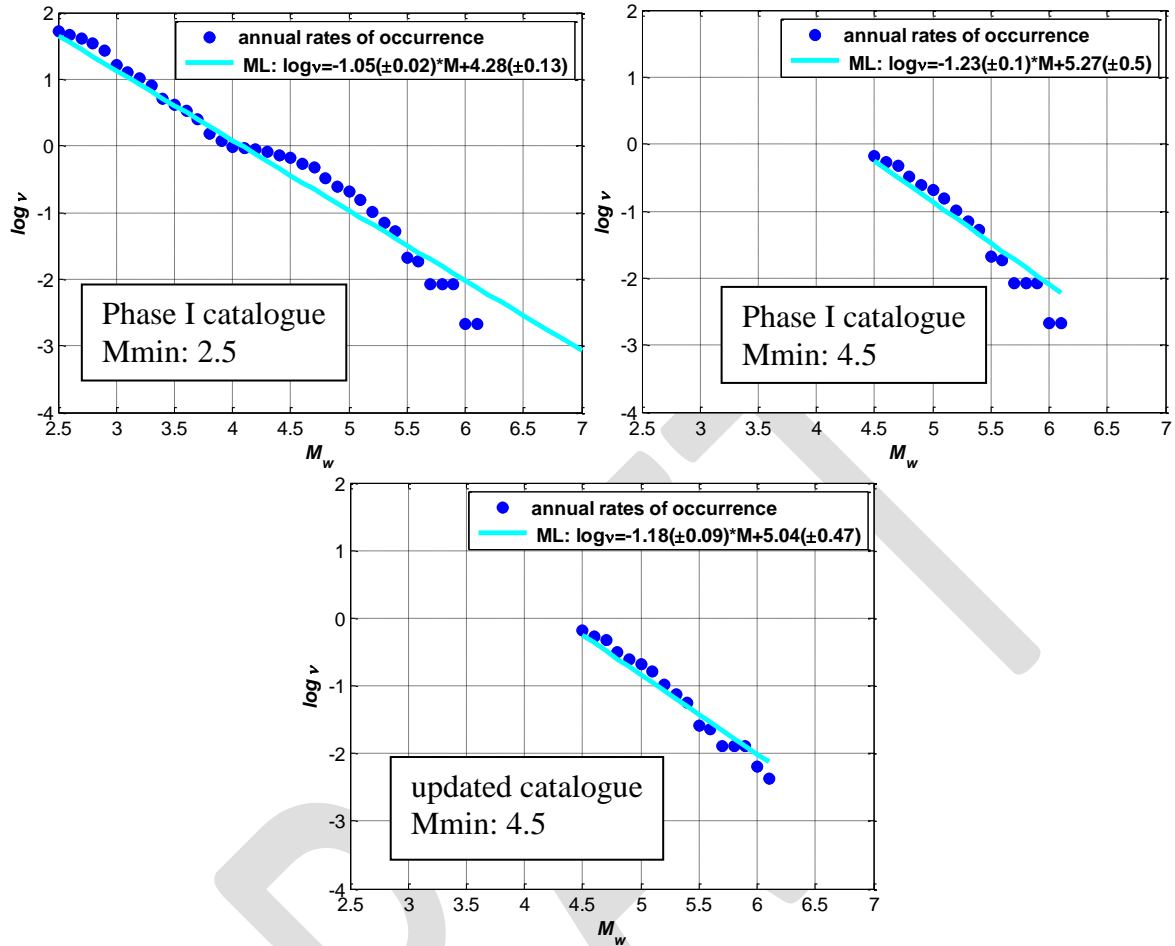


Figure 4 – SSZ 912+913+914, maximum likelihood (ML) estimation of G-R parameters. Top left: Phase I catalogue,  $M_{min}$  2.5. Top right: Phase I catalogue,  $M_{min}$  4.5. Bottom: updated catalogue,  $M_{min}$  4.5.

CONFIDENTIAL

Restricted to SIGMA scientific partners and members of the consortium,  
please do not pass around

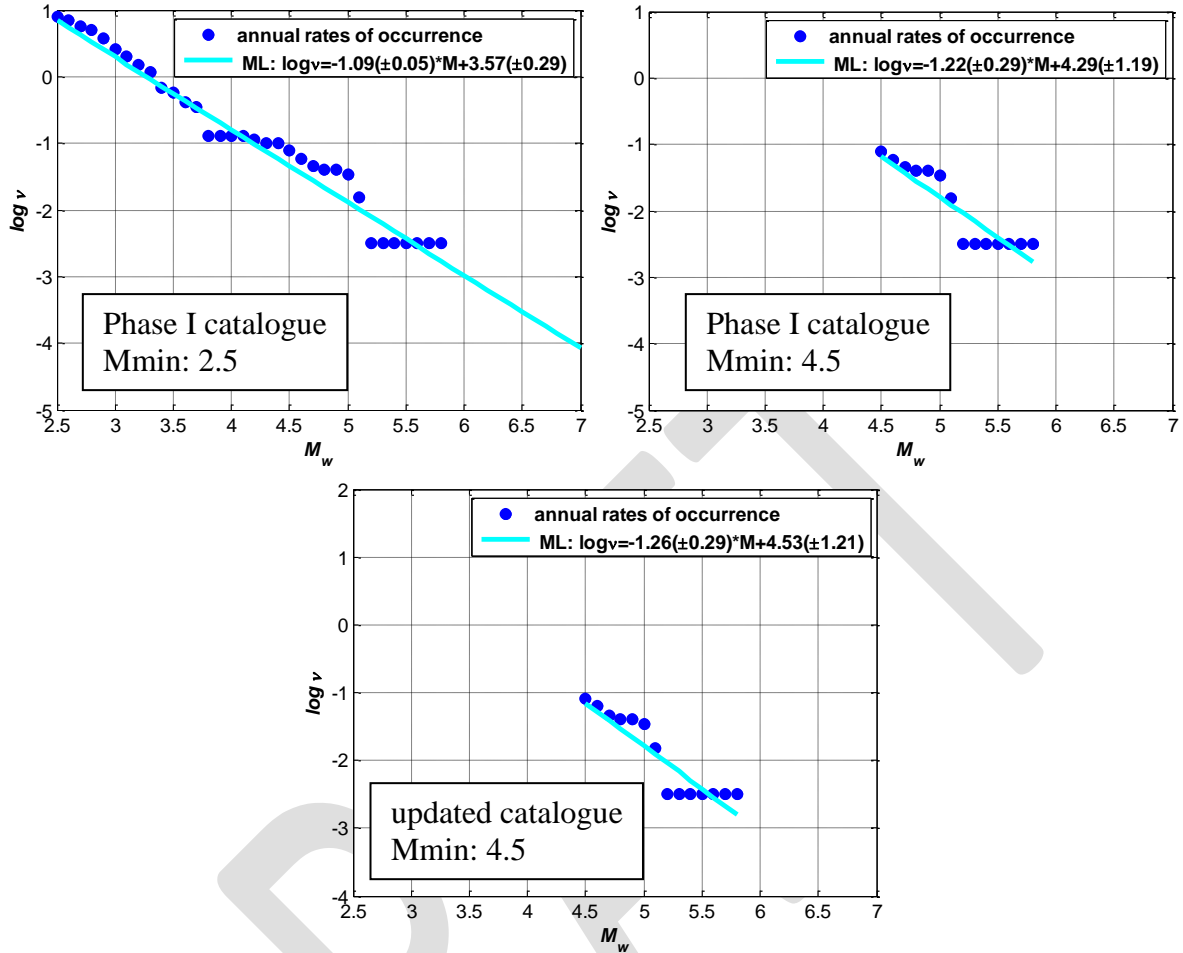


Figure 5 – Same as Figure 4, for SSZ 911

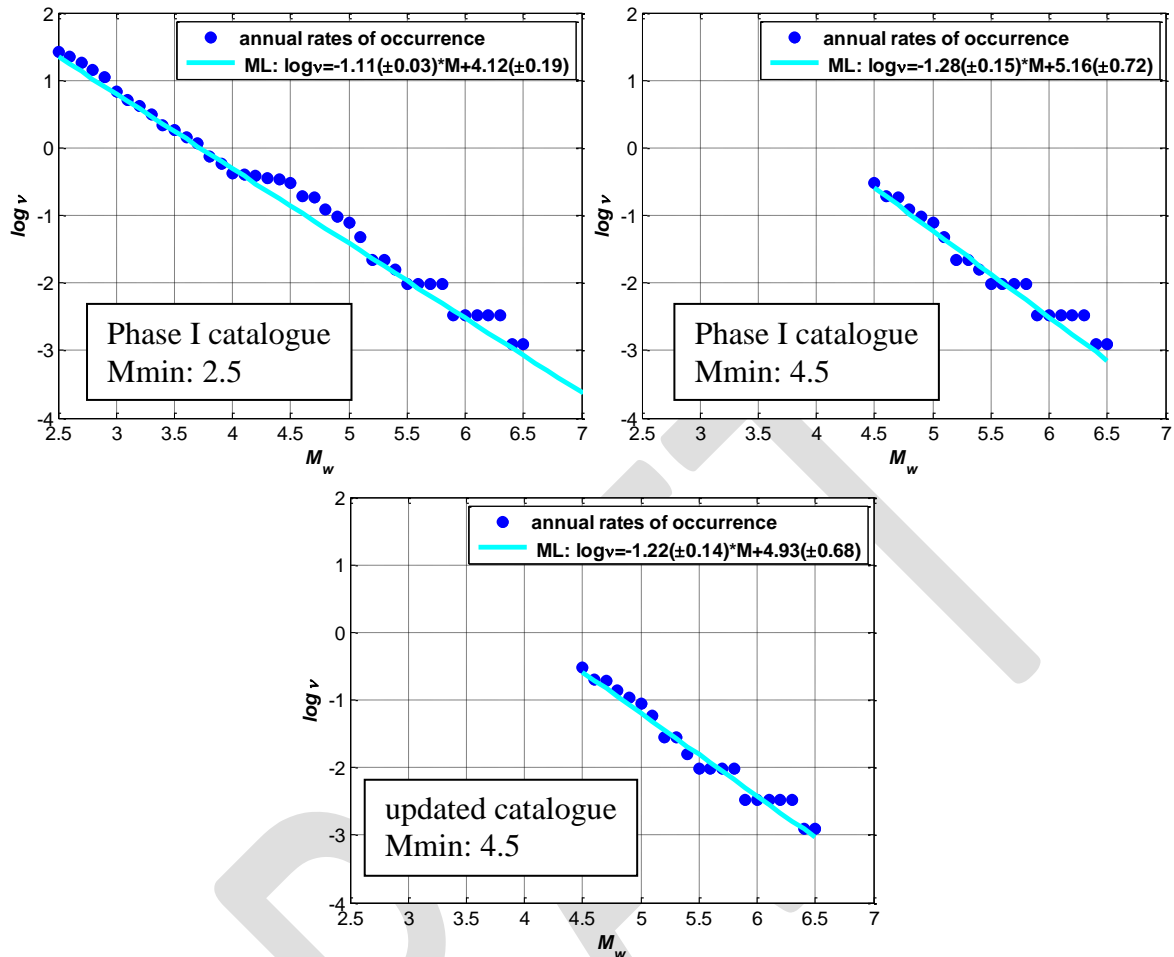



Figure 6 – Same as Figure 4, for SSZ 915.

Note that reducing the range of  $M_w$  values, the G-R parameters as well as their uncertainty increase as expected. As regards the  $b$  values, they increase by about 15% for the SSZ just shown (and about 11% for all SSZ, averaged). We decided to accept these changes, in view of the fact that their influence on SH results, as illustrated in the next Section, is moderate, leading to slightly more conservative results. We recall here that in the computational code CRISIS2008 the  $b$  values are input with their estimated variability.

Table 1 lists the updated values for all considered SSZ (see Phase I deliverable for references, and Figure 7 for a sketch of the SSZ model).


$M_{max}$  values have been kept unchanged, while the  $M_{min}$  value, as said, has been increased to 4.5. Note that, depending on the “robustness” of the specific catalogue (i.e. number of events) each SSZ suffers a different change in  $b$  value. Some SSZ see a decrease of  $b$  (such as the ‘slab’), while some other a considerable increase (such as SSZ 916). However, the main

	Research and Development Programme on Seismic Ground Motion	<b>Ref : SIGMA-2013-D4-94</b> <b>Version : 01</b>
	<b>CONFIDENTIAL</b> <i>Restricted to SIGMA scientific partners and members of the consortium,          please do not pass around</i>	<b>Date : October 2013</b> <b>Page :</b>

changes affect those SSZ having only a minor influence on the hazard at the selected sites. Appendix A shows GR estimates for all SSZ.

Table 1 - G-R parameters used in the SH analyses in terms of b values (with corresponding errors  $\sigma(b)$ ) and total occurrence rates, associated to each SSZ. Last column indicates the percentage of total rate assigned to SSZs at different depths.

SSZ	b	$\sigma(b)$	$M_{max}$	$M_{max}$ uncertainty	Total ann. Rate $\lambda_{M \geq 4.5}$	Depth (km)	%
901	0.84910	0.26670	6.5	0.4	0.0434	10	100
902	0.65230	0.16230	6.5	0.4	0.0916	10	100
905	1.03150	0.08620	-	-	0.4197 (total)	-	-
			5.0	0.3	0.08394	4	20
			5.8	0.3	0.25183	6	60
			6.7	0.3	0.08394	10	20
906	1.28550	0.24650	-	-	0.0904 (total)	-	-
			5.8	0.3	0.02711	6	30
			6.7	0.3	0.04519	9	50
			6.7	0.3	0.01808	15	20
907	1.16270	0.19810	-	-	0.1254 (total)	-	-
			5.0	0.3	0.02509	4	20
			5.8	0.3	0.02509	6	20
			6.7	0.3	0.03763	9	30
			6.7	0.3	0.01254	13	10
			6.7	0.3	0.01254	17	10
			6.7	0.3	0.01254	20	10
908	1.34290	0.26780	6.5	0.4	0.09069	10	100
909	1.32020	0.24970	6.5	0.4	0.10074	10	100
910	1.35830	0.23040	6.6	0.3	0.11042	10	100
911	1.26420	0.28620	-	-	0.0701 (total)	-	-
			5.8	0.5	0.02103	6	30
			6.5	0.5	0.02805	9	40
			6.5	0.5	0.02103	25	30
912+913+914	1.17580	0.09420	-	-	0.5642 (total)	-	-
			5.8	0.5	0.11283	6	20
			6.5	0.5	0.22566	9	40
			6.5	0.5	0.22566	25	40
915	1.22480	0.14410	-	-	0.2601 (total)	-	-
			5.8	0.3	0.07804	6	30
			7.4	0.3	0.13007	9	50
			7.4	0.3	0.02601	16	10
			7.4	0.3	0.02601	21	10
916	1.65730	0.24710	-	-	0.1694 (total)	-	-
			5.8	0.3	0.05084	6	30
			7.4	0.3	0.10167	9	60
			7.4	0.3	0.01695	18	10
slab	0.67060	0.29850	6.5	0.5	0.02766	-	-

	<p style="text-align: center;">Research and Development Programme on Seismic Ground Motion</p> <p style="text-align: center;">CONFIDENTIAL</p> <p style="text-align: center;"><i>Restricted to SIGMA scientific partners and members of the consortium, please do not pass around</i></p>	<p>Ref : SIGMA-2013-D4-94 Version : 01</p> <p>Date : October 2013 Page :</p>
--	---	--

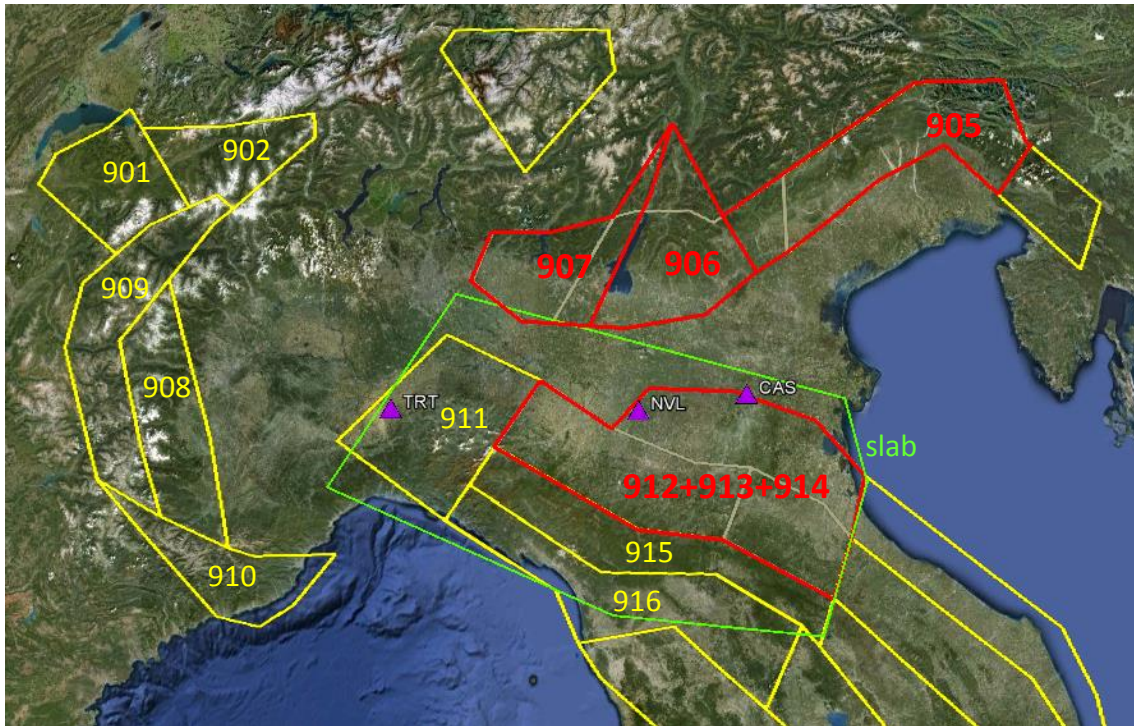


Figure 7 – Layout of the SSZ model adopted in Phase I work (all SSZ with printed number). In red: geometry of modified SSZs, in yellow: original ZS9 model. Purple triangles show location of sites of interest. In green, the deep subduction plane introduced in Phase I study.

### 3.3. Comparing old and new G-R parameters

In this section we are analysing the variability in exceedance curves resulting from the Phase I and the present estimations of G-R parameters. We are looking at exceedance curves and UH spectra from Phase I AS model, for the single LT branch 2 (GMPE as specified in the following). The computations were run for the CAS and NVL sites, on ground type C, making use of all the relevant SSZs, the “coarse” depth distribution of Phase I, and soft SSZ boundaries.

In Figure 8, Figure 9, Figure 10 and Figure 11, the results for the following two cases are compared:

- 1) old (Phase I) G-R parameters a, b (estimated starting from Mw 2.5), with  $M_{min} = 4.0$ . (blue curves);
- 2) new a,b (computed with updated catalogue starting from Mw 4.5), with  $M_{min} = 4.5$ . (green curves);

The computational code is the same as in previous Phase I work: the CRISIS2008 program.



The ITA13 (Pacor et al., 2013) GMPE was associated to SSZs with prevailing thrust mechanisms and ITA10 (Bindi et al., 2011) to those with normal and strike-slip mechanisms (as suggested in Pacor et al., 2013), keeping Zhao et al. (2006) GMPE fixed for the ‘slab’ source zone (as explained in Phase I). As shown, the analyses with the new parameters are slightly more conservative at short periods (0.1-0.5 s): UH spectra peak amplitudes (at 0.15 s) increase by about 19%.

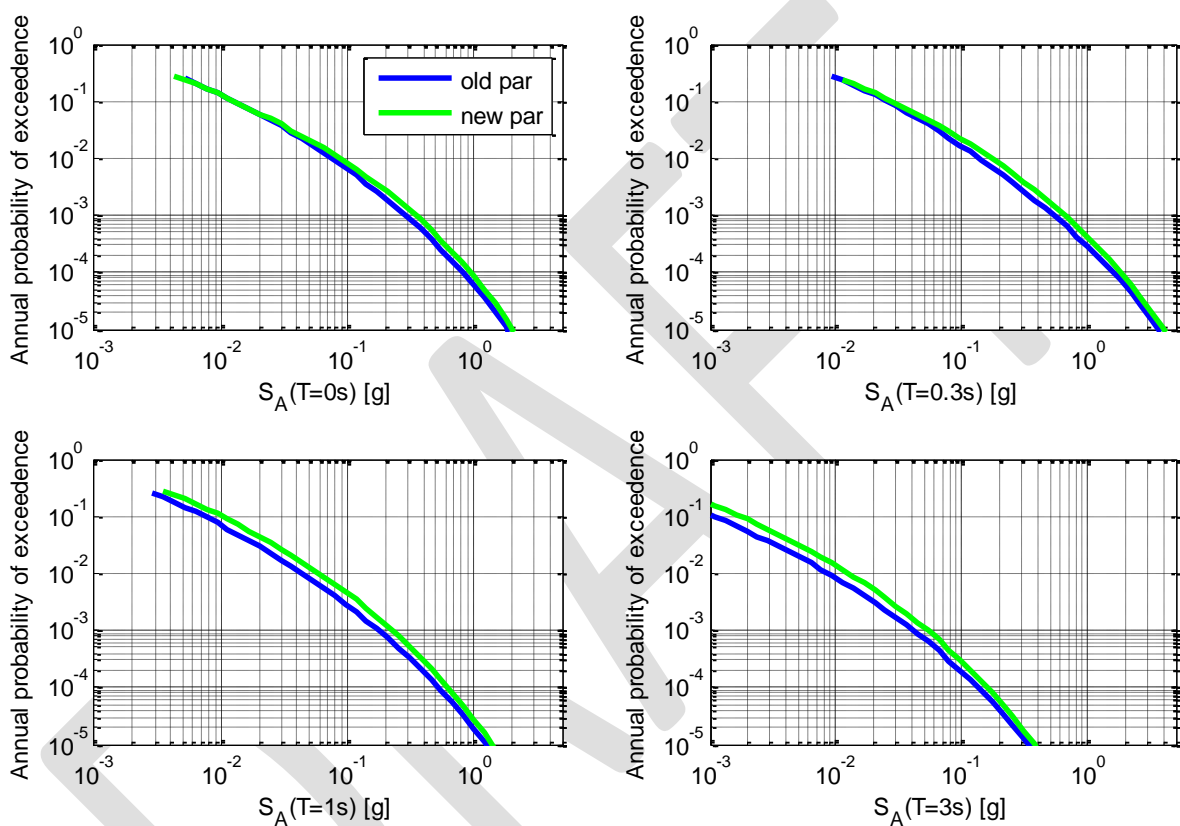


Figure 8 – NVL site. Exceedance rate curves of acceleration response spectrum ordinates at 0.05 damping for different vibration periods.

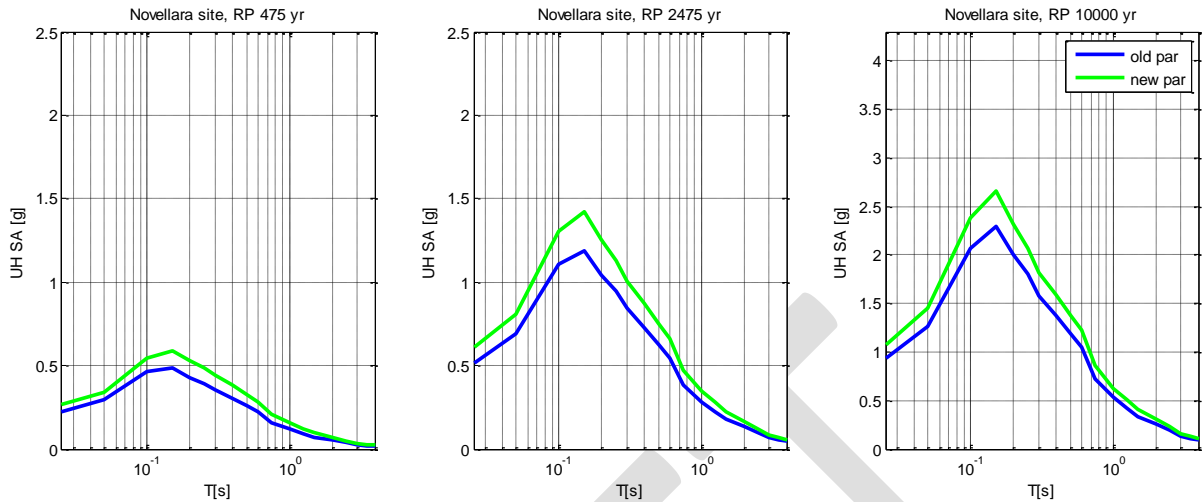


Figure 9 – NVL site. Uniform Hazard acceleration Spectra at indicated RPs.

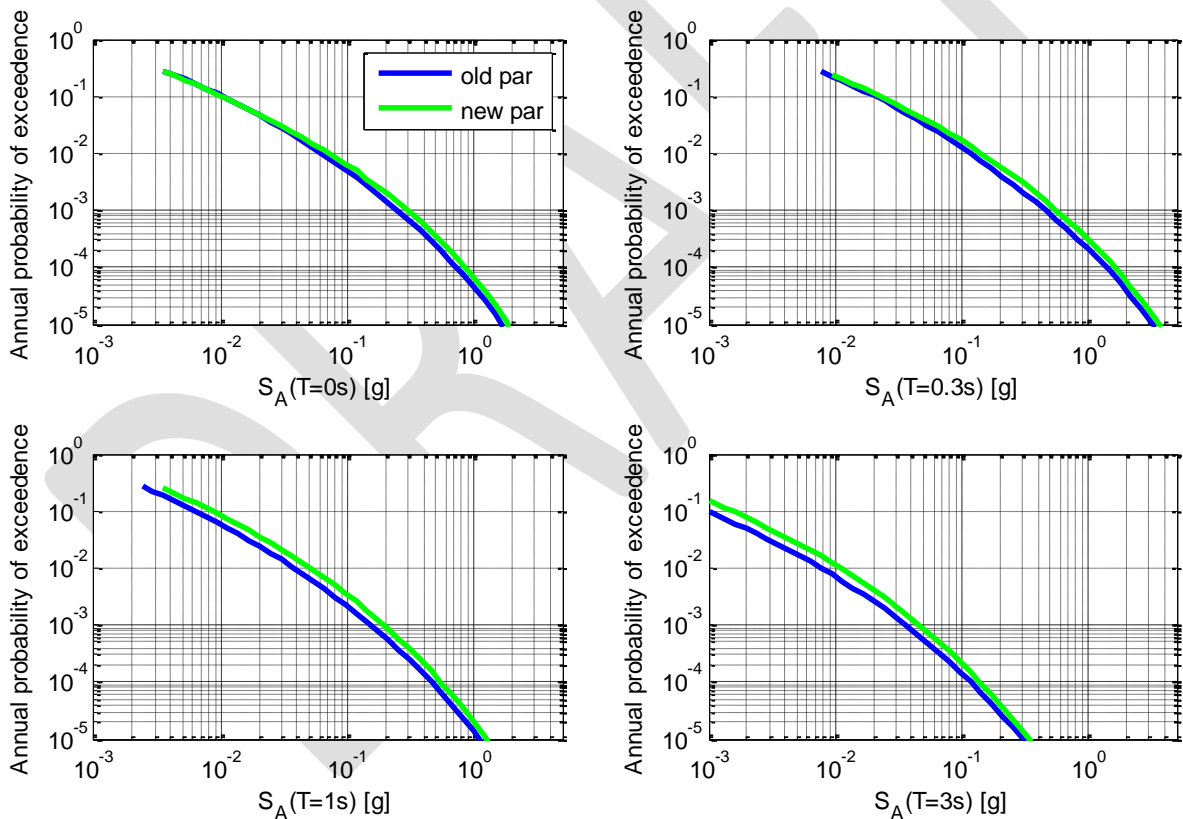


Figure 10 – CAS site. Exceedance rate curves of acceleration response spectrum ordinates at 0.05 damping for different vibration periods.



CONFIDENTIAL

*Restricted to SIGMA scientific partners and members of the consortium,  
please do not pass around*

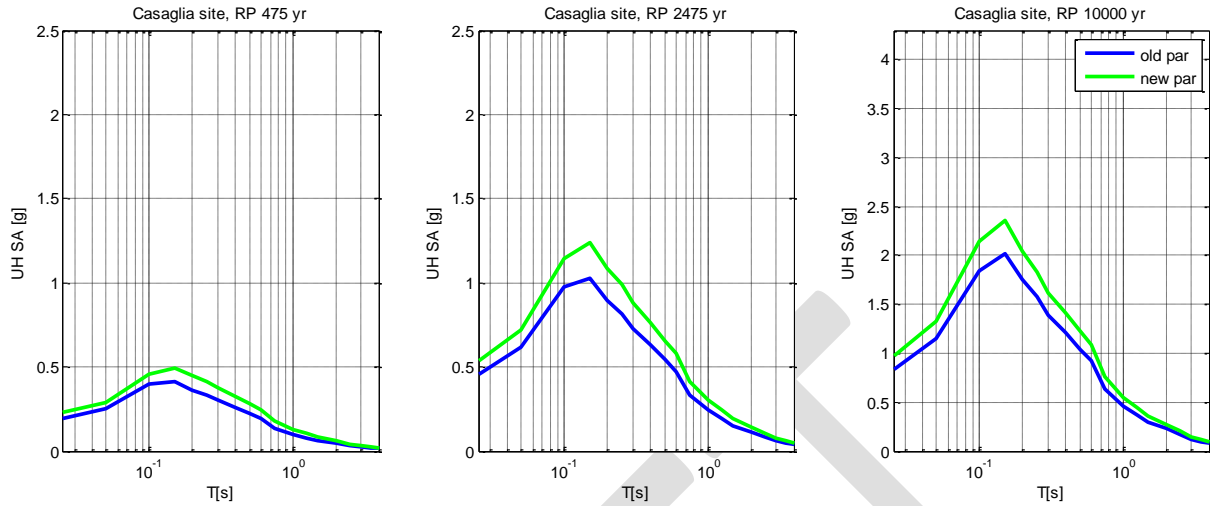



Figure 11 – CAS site. Uniform Hazard acceleration Spectra at indicated RPs.

DRAFT


	<p>Research and Development Programme on Seismic Ground Motion</p> <p>CONFIDENTIAL</p> <p><i>Restricted to SIGMA scientific partners and members of the consortium, please do not pass around</i></p>	<p>Ref : SIGMA-2013-D4-94 Version : 01</p> <p>Date : October 2013 Page :</p>
--	---	--

## 4. Updating of GMPEs

Concerning GMPEs selection, a significant updating is introduced with respect to Phase I, by which we intend to use:

- 1) the updated version of Bindi et al. 2011, developed for Sigma (Pacor et al., 2013), derived from the 2012 Po Plain data and other Northern Italy data, for C ground type sites inside the Plain, and reverse focal mechanism, combined with the original Bindi et al. 2011, for the other ground types and focal mechanisms;
- 2) in replacement of Cauzzi and Faccioli (2008) GMPE, the GMPE by Faccioli et al. (2010), in an improved version published only recently (Faccioli and Chen, 2012);
- 3) the modified version of the Boore and Atkinson (2008) GMPE, as published in Atkinson and Boore (2011).

These GMPEs are retained in accordance with the SHARE project general criteria (Delavaud et al. 2012) for active shallow crustal regions (ASCR). Thus, Chiou and Youngs (2008) is replaced with Bindi et al. (ITA13 version), because the latter uses, as already noted, a very rich regional, entirely Italian, database. Also, the Akkar and Bommer (2010) GMPE, recommended by SHARE, has been replaced with the most recent Atkinson and Boore (2011), because of its better performance, in terms of ranking analysis, as shown in Pacor et al. (2012). As to Faccioli et al. (2010, FEA10 modified) it avoids the problems that may be generated for shallow sources by the lack of saturation in Cauzzi and Faccioli (2008) when the focal distance tends to zero.

	<p>Research and Development Programme on Seismic Ground Motion</p> <p>CONFIDENTIAL</p> <p><i>Restricted to SIGMA scientific partners and members of the consortium, please do not pass around</i></p>	<p>Ref : SIGMA-2013-D4-94 Version : 01</p> <p>Date : October 2013 Page :</p>
--	---	--

## 5. The single station sigma approach

For all GMPEs, the so called ‘non-ergodic’ (or “single station sigma”) version is introduced in the logic tree, in addition to the standard (ergodic) use, by modifying the GMPE predictions through site specific correction factors ( $\delta S2S$ ) and replacing the GMPE’s sigma with the single station sigma ( $\sigma_{ss,s}$ ), see Rodríguez Marek et al. (2011) for the meaning of the symbols. As shown in Chen and Faccioli (2013), the  $\delta S2S$  factors may in first approximation be considered as an intrinsic characteristic of the site and, as such, should be roughly independent from the GMPE used to calculate them. Likewise, the  $\sigma_{ss,s}$  values seem to be even less affected by the choice of the specific GMPE introduced for the correction, but these indications need further verification.

### 5.1. Method of ground motion residual analysis

Following Rodríguez Marek et al. (2011), a general form of a ground motion prediction model can be written as:

$$Y_{es} = \mu_{es} + \delta W_{es} + \delta B_e \quad (1)$$


where  $Y_{es}$  is the base 10 logarithm of the observed ground motion parameter, and  $\mu_{es}$  is the median ground motion (log value) predicted by a GMPE.  $\delta B_e$  and  $\delta W_{es}$  are the corresponding ground motion residuals (or *variability*), which represent between-event and within-event residuals, respectively.

The between-event (also called inter-event) residual,  $\delta B_e$ , represents the average shift of the observed ground motion in an individual earthquake,  $e$ , from the median predicted by a GMPE.  $\delta B_e$  can be estimated as follows. For an individual earthquake  $e$ , let there be  $NS$  stations recording the event. Then, the average misfit between observations and predictions for earthquake  $e$ , using a GMPE, is:

$$\delta B_e = \frac{1}{NS} \sum_{s=1}^{NS} (Y_{es} - \mu_{es}) \quad (2)$$

The within-event (also called intra-event) residual,  $\delta W_{es}$ , is the misfit between an individual observation at station  $s$  from the earthquake-specific median prediction, which is defined as the median prediction  $\mu_{es}$  of the model plus the between-event term  $\delta B_e$  for earthquake  $e$ . Thus  $\delta W_{es}$  also represents the difference between an individual observation (*i.e.*,  $Y_{es}$ ) and the event-corrected median estimate, *i. e.*

$$\delta W_{es} = Y_{es} - (\mu_{es} + \delta B_e) \quad (3)$$

	<p>Research and Development Programme on Seismic Ground Motion</p> <p>CONFIDENTIAL</p> <p><i>Restricted to SIGMA scientific partners and members of the consortium, please do not pass around</i></p>	<p>Ref : SIGMA-2013-D4-94 Version : 01</p> <p>Date : October 2013 Page :</p>
--	---	--

If  $NE_s$  earthquake events are recorded at station  $s$ , the within-event residuals computed from a GMPE for that station are used to define the average site correction term, which is

$$\delta S2S_s = \frac{1}{NE_s} \sum_{e=1}^{NE_s} \delta W_{es} \quad (4)$$

$\delta S2S_s$  is a random variable that represents the average within-event residual at station  $s$  and is referred to as the *site term*. For a given station, it takes a deterministic value. Assuming no bias in the records obtained at each station,  $\delta S2S_s$  has zero mean and variance  $\phi_{s2s}^2$ . The latter quantifies the component of site-to-site variability which is not explained by GMPEs.

At station  $s$ , the between-event and within-event residuals,  $\delta B_e$  and  $\delta W_{es}$ , are assumed to be normally distributed random variables with respective variances  $\tau^2$  and  $\phi_{ss,s}^2$ . The single-station event-corrected standard deviation (the so-called event-corrected *sigma*) of the within-event residuals is defined as

$$\phi_{ss,s} = \sqrt{\frac{\sum_{e=1}^{NE_s} (\delta W_{es} - \delta S2S_s)^2}{NE_s - 1}} \quad (5)$$

Then if  $\delta B_e$  and  $\delta W_{es}$  are mutually independent for station  $s$ , the standard deviation of the total residuals at station  $s$  is given by,

$$\sigma_{ss,s} = \sqrt{\phi_{ss,s}^2 + \tau^2} \quad (6)$$

## 5.2. Non ergodic use of GMPEs in hazard analyses

As said, the main ingredients of a single-station sigma approach to the ground motion hazard estimation are the two coefficients  $\delta S2S$  and  $\sigma_{ss,s}$ , computed as explained in 5.1. These coefficients may be used to modify the predictions by a GMPE, in a very simple way. The standard error of estimate,  $\sigma_{logY}$ , of the GMPE is replaced with the  $\sigma_{ss,s}$  value, while the site correction term modifies the GMPE median prediction ( $\mu_{GMPE}(T)$ ) as follows:

$$\mu_{corrected}(T) = \mu_{GMPE}(T) \cdot 10^{\delta S2Ss(T)} \quad (7)$$

### 5.3. Adopted correction coefficients

The  $\delta S_{2S}$  and  $\sigma_{ss,s}$  values used in our analyses have been borrowed from Pacor et al. (2013) analyses with the ITA13 GMPE and the Po Plain database, which collects data from the stations shown for the most part in Figure 12.

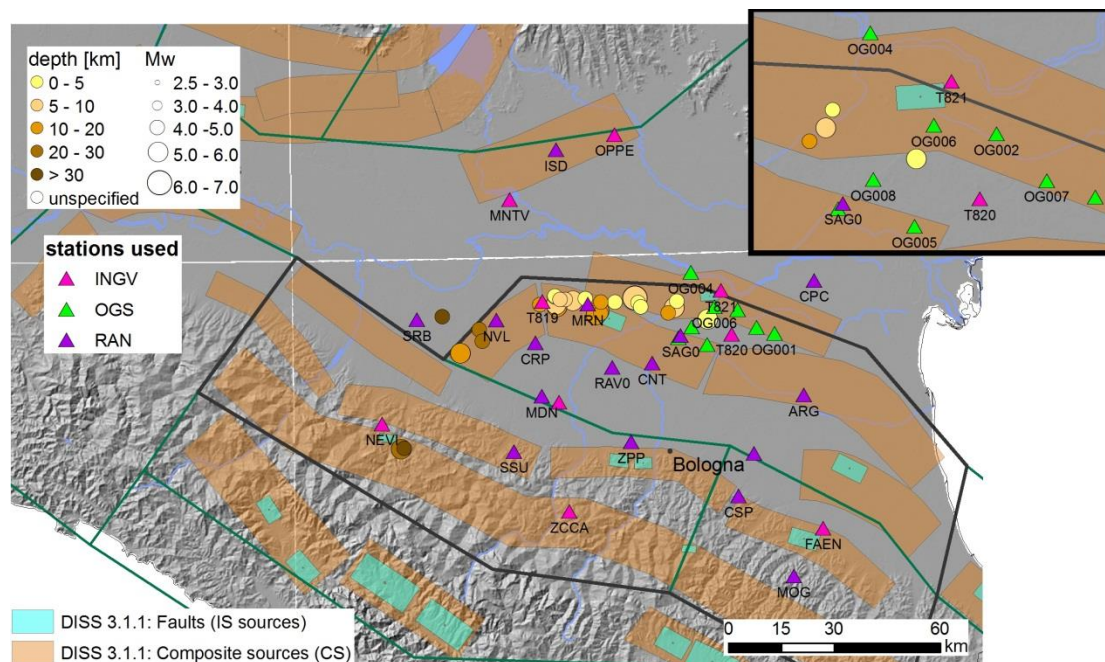


Figure 12 – Geological map of the stations and earthquake events used in single station sigma analysis for Po Plain area. Note NVL station and T821 (=CAS) station.

Figure 13 and Figure 14 show single station sigmas  $\sigma_{ss,s}$  (left panels) and site terms,  $\delta S_{2S}$  (right panels), for CAS and NVL respectively. 14 acceleration records have been used for CAS site, and 11 for NVL. We recall here that site terms represents the site-to-site variability within a site class, e. g. Eurocode 8 ground type C, that cannot be explained by the GMPE. Note that both stations have a negative site correction factor, significantly lower for CAS (about -0.4) rather than NVL (about -0.1). Moreover, the single site sigma for CAS are significantly smaller than the sigma of most of the GMPEs, and comparable to the sigma of AB11. For NVL the  $\sigma_{ss,s}$  values are significantly higher than GMPEs ones (notably AB11 one);  $\sigma_{ss,s}$  remains comparable to the other GMPEs only for periods lower than 0.7 s.

These differences will have a strong influence on the PSHA results. In particular, in the case of CAS, the reduction of sigma will combine with a negative site correction factor, leading to a large decrease of the UH spectral ordinates. On the contrary, NVL will exhibit a different behaviour, enhancing predicted spectral ordinates when  $\sigma_{ss,s}$  is larger than GMPEs ones. As

pointed out by Rodríguez-Marek et al. (2011) on Kik-net station data, in Japan, “*there is significant variability across stations; and, in some cases, the value of single-station standard deviations are higher than their ergodic counterpart*”.

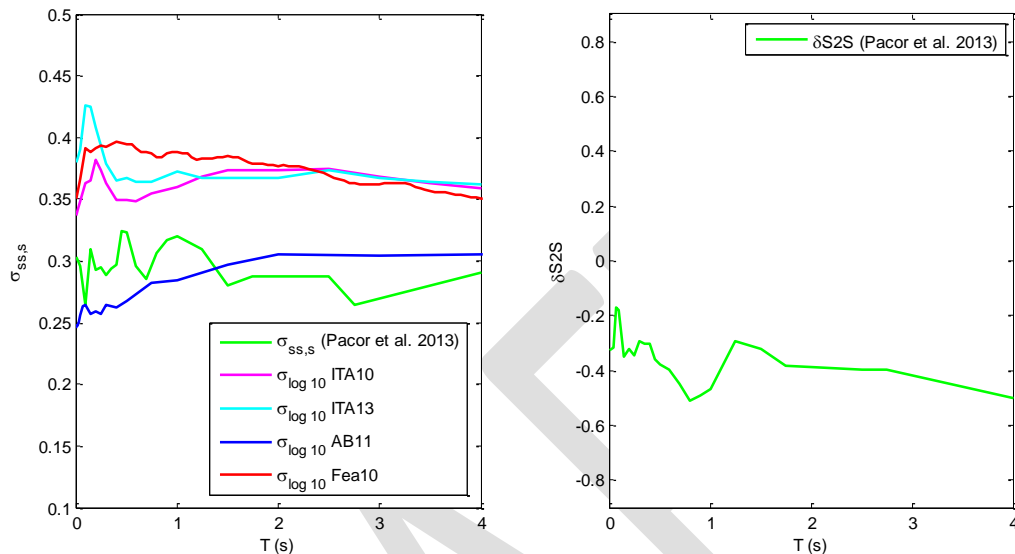


Figure 13 – Results of the residual analysis of the response spectrum ordinates at CAS site. The rhs displays the site correction factor  $\delta S2S$ , while the lhs shows the site-single station sigma ( $\sigma_{ss,s}$ ). The total standard deviation of the GMPEs used in logic tree computations are also shown for comparison (i.e.: Bindi et al. (2011) and its 2013 modified version, Atkinson & Boore 2011 and Faccioli et al. 2010 modified version).

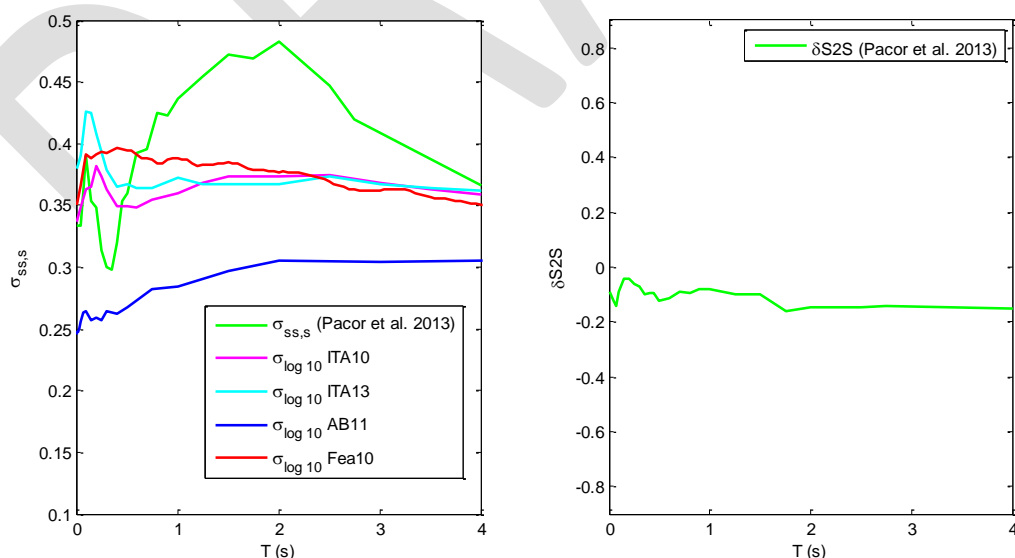


Figure 14 –Same as Figure 13, for NVL site.



Concerning site correction coefficients for rock type analyses (shown in Figure 15), we used Pacor et al. (2013) values from the available ground type A accelerometer stations closest to the Po Plain area, all located in the Apennines, that is ZCCA, SSU and NEVI. Mean values from these three stations (in thick black lines) have been used to correct GMPEs for non-ergodic SHAs. Worth noting is that the AB11 sigma value is quite close to the mean  $\sigma_{ss,s}$  curve for the rock stations, which is lower than the Fea10 and Ita13 sigmas. Concerning the site correction coefficient, none of these sites could be said to be totally free from local amplification (or de-amplification) with respect to the standard category A ground type, as it should be for a reference bedrock site.

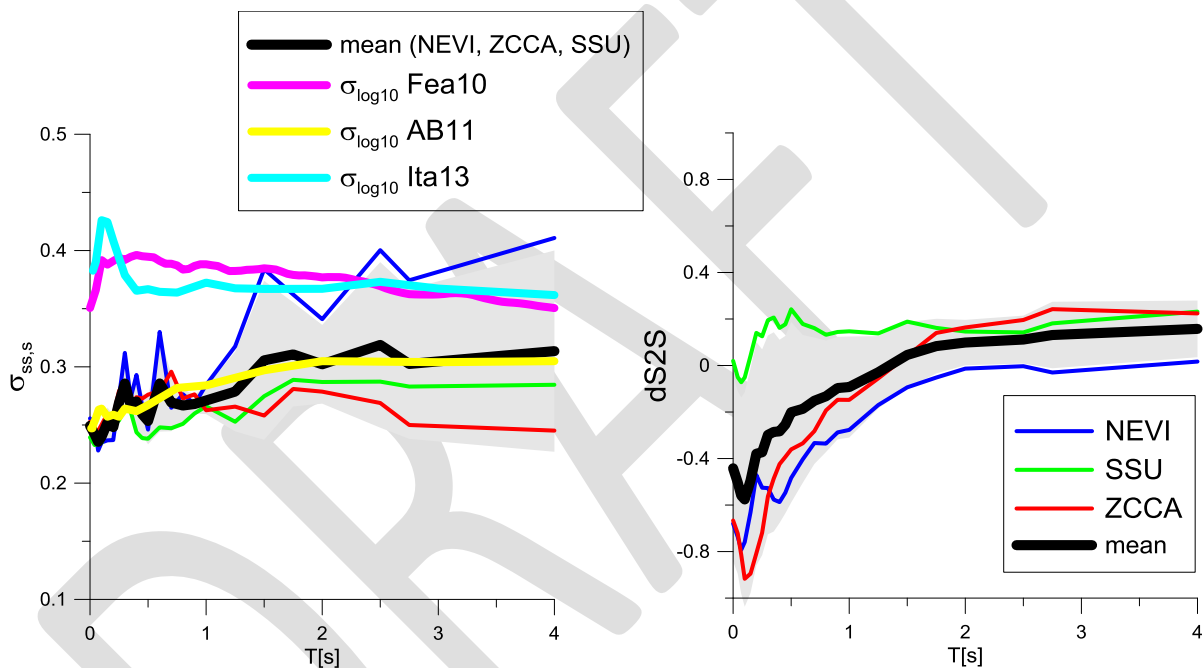


Figure 15 –Results of the residual analysis at ground type A accelerometric stations NEVI, ZCCA and SSU (with mean value in thick black line). The rhs displays the site correction factor  $\delta S2S$ , while the lhs the site-single station sigma ( $\sigma_{ss,s}$ ). The total standard deviation of the GMPEs adopted in logic tree computations are also shown for comparison (i.e.: Bindi et al. and its 2013 modified version, Atkinson & Boore 2011 and Faccioli et al. 2010 modified version).

#### 5.4. Comparing non-ergodic and ergodic hazard estimation

The next figures illustrate a first comparison among the results obtained using a simple AS description of the earthquake sources, ground category C characteristics, and the selected GMPEs in both their ‘ergodic’ and non-ergodic’ use, in terms of exceedance curves and UHS spectra, for the CAS and NVL sites.

While the amplitude reduction in the CAS non-ergodic spectra is substantial for all GMPEs. for NVL a significant reduction is evident for only two GMPEs: ITA13 (Bindi et al.) and FEA10 (Faccioli et al. 2010, modified). For AB11, non-ergodic single site sigma values significantly exceed the GMPE standard deviation for all periods (see Figure 14), causing non-ergodic hazard curves to be higher than ergodic ones.

Figure 17 shows the UH spectra of CAS, computed with the Fea10 GMPE, for rock (ground type A) conditions. These spectra will be used in the sequel of the work (Sect. 9), to test different approaches in accounting for site effects in PSHA.

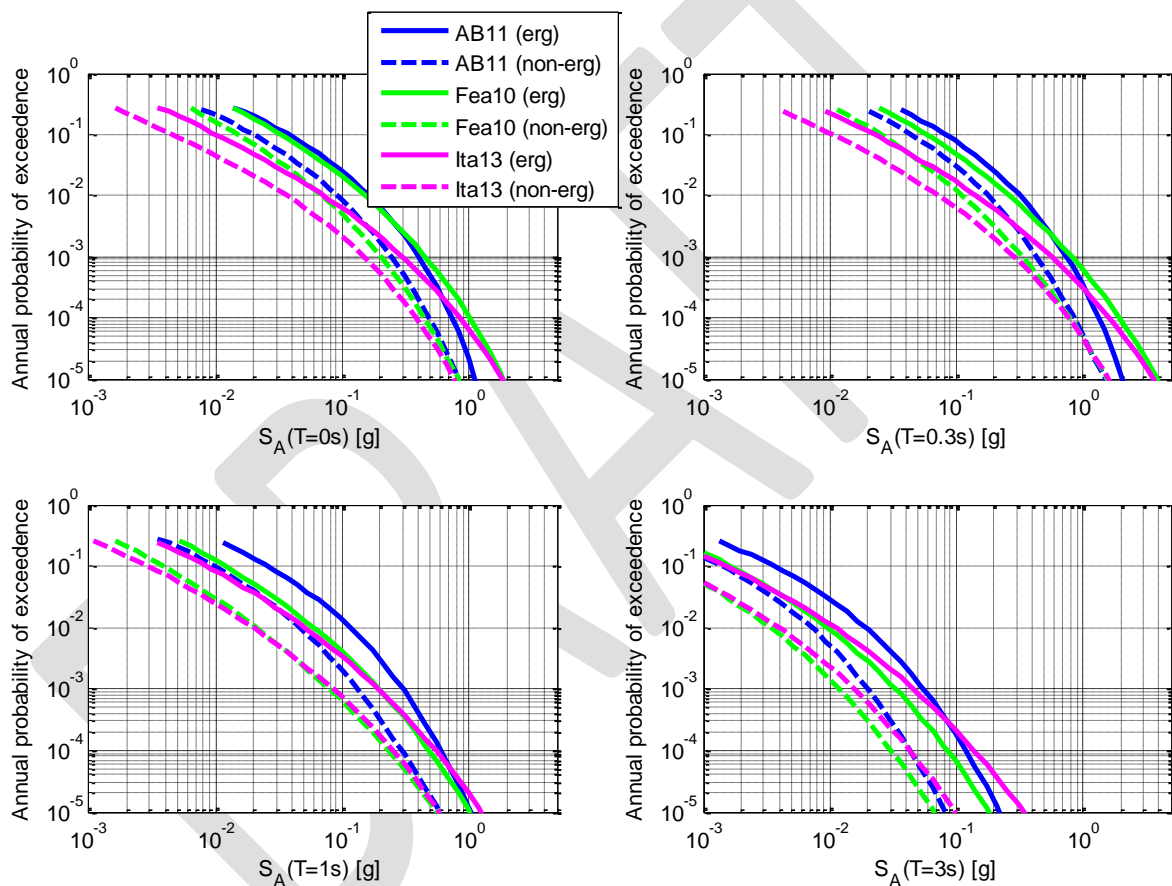


Figure 16 –CAS site. Exceedance rate curves of acceleration response spectrum ordinates at 0.05 damping for different vibration periods. Ergodic and non-ergodic use of GMPEs..



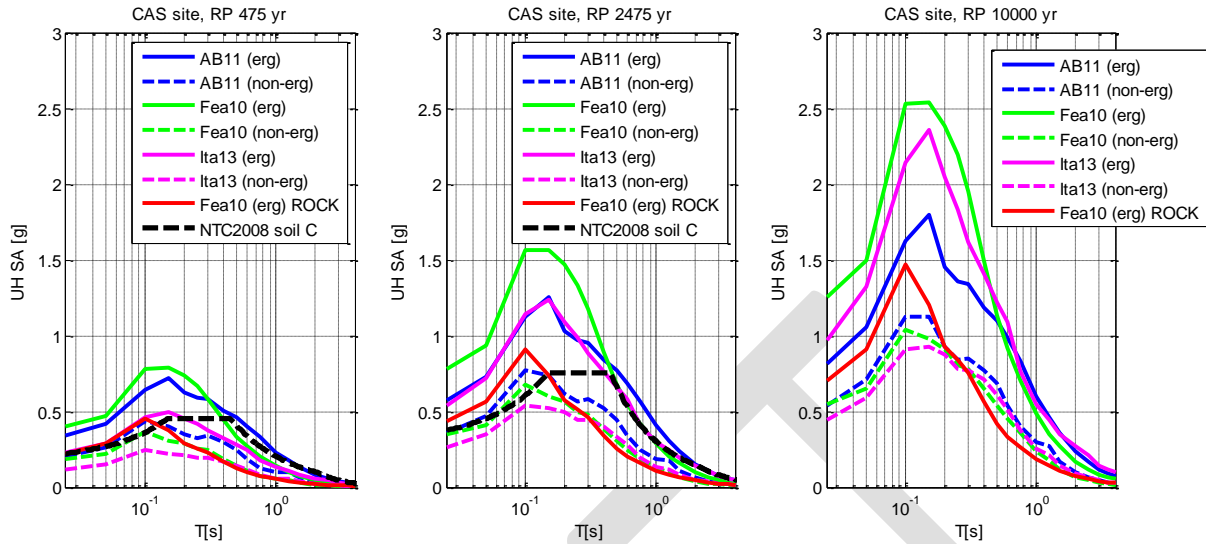


Figure 17 –CAS site. Uniform Hazard acceleration Spectra at return periods of 475, 2475 and 10000 years. NTC 2008 spectra are also shown for comparison (dashed curves). Ergodic and non-ergodic use of GMPEs. Results from ground type A and Fea10 GMPE are also shown.

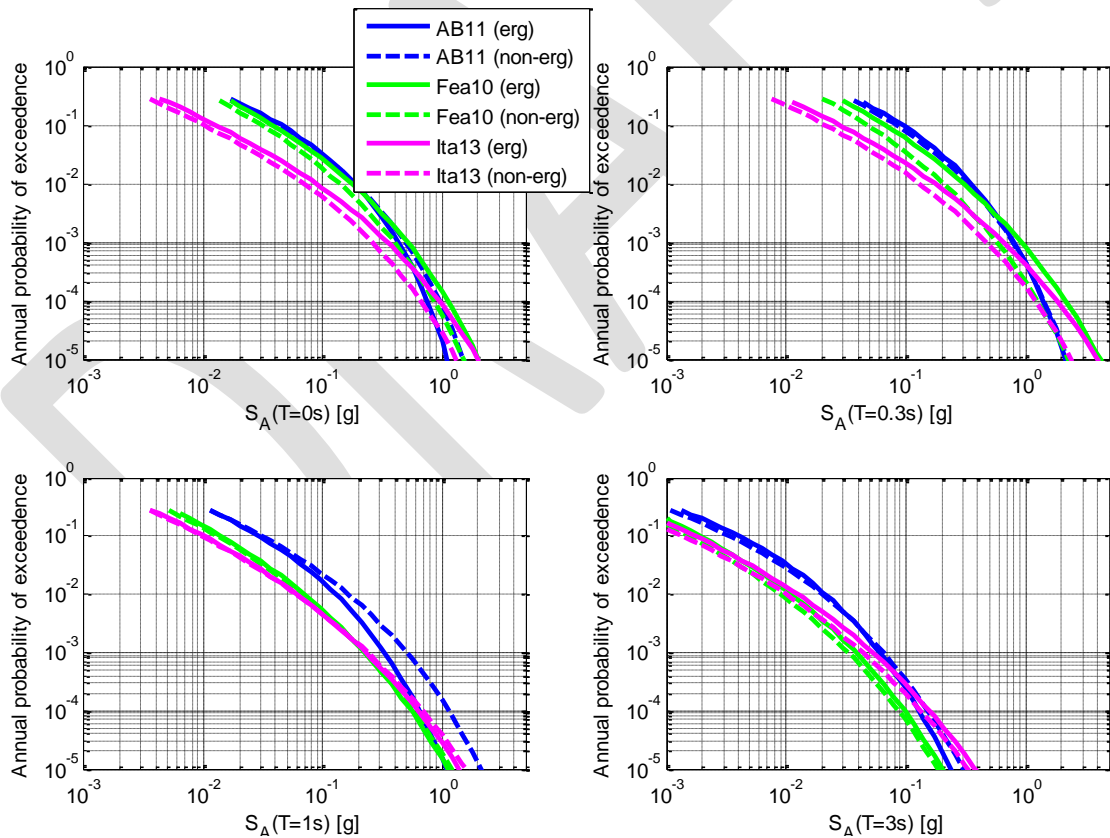


Figure 18 –NVL site. Exceedance rate curves of acceleration response spectrum ordinates at 0.05 damping for different vibration periods. Ergodic and non-ergodic use of GMPEs..

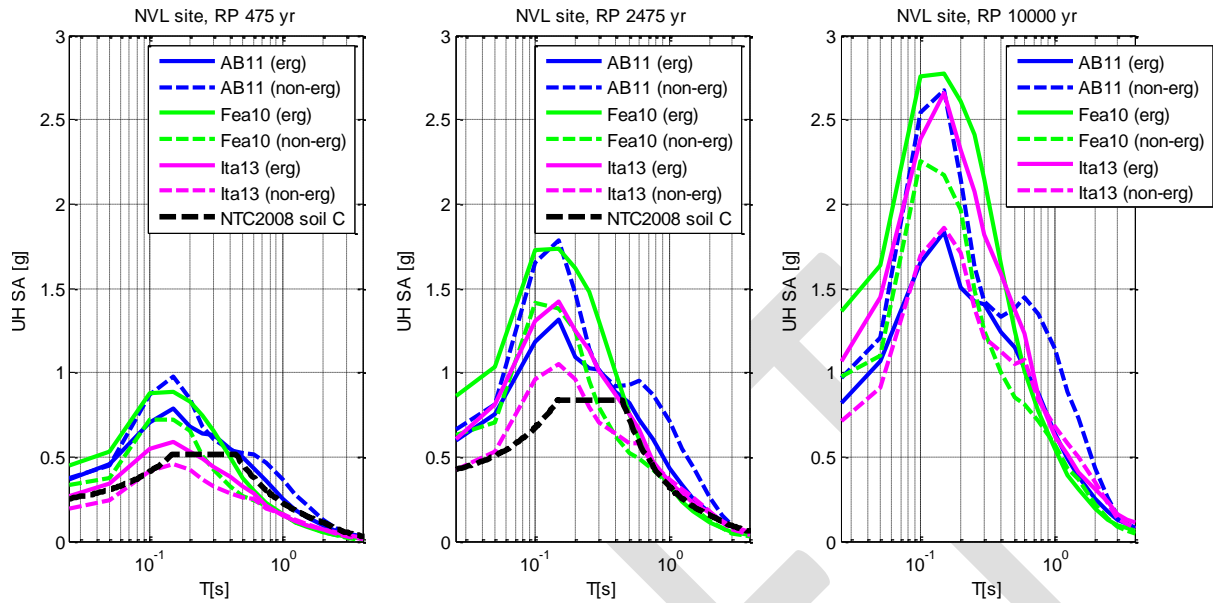



Figure 19 –NVL site. Uniform Hazard acceleration Spectra at return periods of 475, 2475 and 10000 years. NTC 2008 spectra are also shown for comparison (dashed curves), where available. Ergodic and non-ergodic use of GMPEs.

	<p>Research and Development Programme on Seismic Ground Motion</p> <p>CONFIDENTIAL</p> <p><i>Restricted to SIGMA scientific partners and members of the consortium, please do not pass around</i></p>	<p>Ref : SIGMA-2013-D4-94 Version : 01</p> <p>Date : October 2013 Page :</p>
--	---	--

## **6. Model-based description: faults + background**

Within this model we considered a fault representation of the earthquake sources coupled with a lower level background (BG) seismicity. The BG is accounted for through ASs, limited to a maximum magnitude of 5.4 (residual magnitude not covered by the fault description). The fault sources have been borrowed from the Italian Database of Individual Seismogenic Sources (DISS model, version 3; Basili et al. 2008 and 2009; DISS working group 2010, <http://diss.rm.ingv.it>).

For purposes of comparison and independent validation of the adopted modelling of FS, we also show results obtained from a different, hybrid approach to SHA, in which deterministically computed ground motion are introduced in the SHA code, in replacement of the values empirically predicted through GMPEs. For this purpose, we performed full time domain simulations of fault rupture and propagation in a 1D Earth crustal structure, using the Exsim code (Motazedian and Atkinson 2005).

The results of the two approaches are found to be quite consistent.

### **6.1. DISS database of fault sources**

The DISS database is a large repository of geological, tectonic and active-fault data for Italy and the surrounding areas that has been compiled based on field work and literature studies on fault data (Basili et al. 2008). DISS stores two main categories of parameterized fault sources: individual seismogenic sources (ISS) and composite seismogenic sources (CSS), both of which are considered able to release earthquakes of Mw 5.5 or larger. In most cases, the ISSs represent the preferred source solutions of well-known large earthquakes of the past that might have ruptured the fault from end to end (i.e., a fault segment). Thus, historical and pre-historical earthquakes, and occasionally potential seismic gaps, are associated with individual large faults identified and parameterized by geological and geophysical methods.

In recognition of the inherent difficulties in identifying all possible fault segments in the Italian geologic/geomorphic record, in 2005 the DISS was extended to include Composite Seismogenic Source (CSS), a source category that expands the territorial coverage and the completeness, and hence the capabilities of the database. A CSS is essentially an inferred structure based on regional surface and subsurface geological data that are used to identify and map a complete fault system. In contrast to an ISS, the termination of a CSS may either represent an identified fault limit or a significant structural change. This implies that any CSS may span an unspecified number of potential individual ruptures, and may in principle be able to generate earthquakes of any size, up to an assigned maximum magnitude. The maximum

magnitude assigned to a CSS may either be the magnitude of its largest child ISS, or the magnitude of the largest historical earthquake associated with this CSS, or a default  $M_w=5.5$  if none of the above apply. As a matter of fact, to balance the unavoidable uncertainties and its main scopes, DISS considers only sources with a potential for  $M_w$  5.5 or larger. Although relaxing the fault-segment boundaries prevents the straightforward use of empirical relationships based on fault length, it dramatically increases the ability to map fault sources in areas in which active fault information is scarce but main fault trends can be traced based on the general tectonic framework. All CSS are mapped following identical criteria of scale and accuracy, and are characterized by geometrical (strike, dip, depth) and kinematic (rake, slip rate, maximum magnitude) parametric descriptors (Basili et al. 2009). Other data on the seismogenic sources in Italy were recently published by the DISS Working Group (2010).

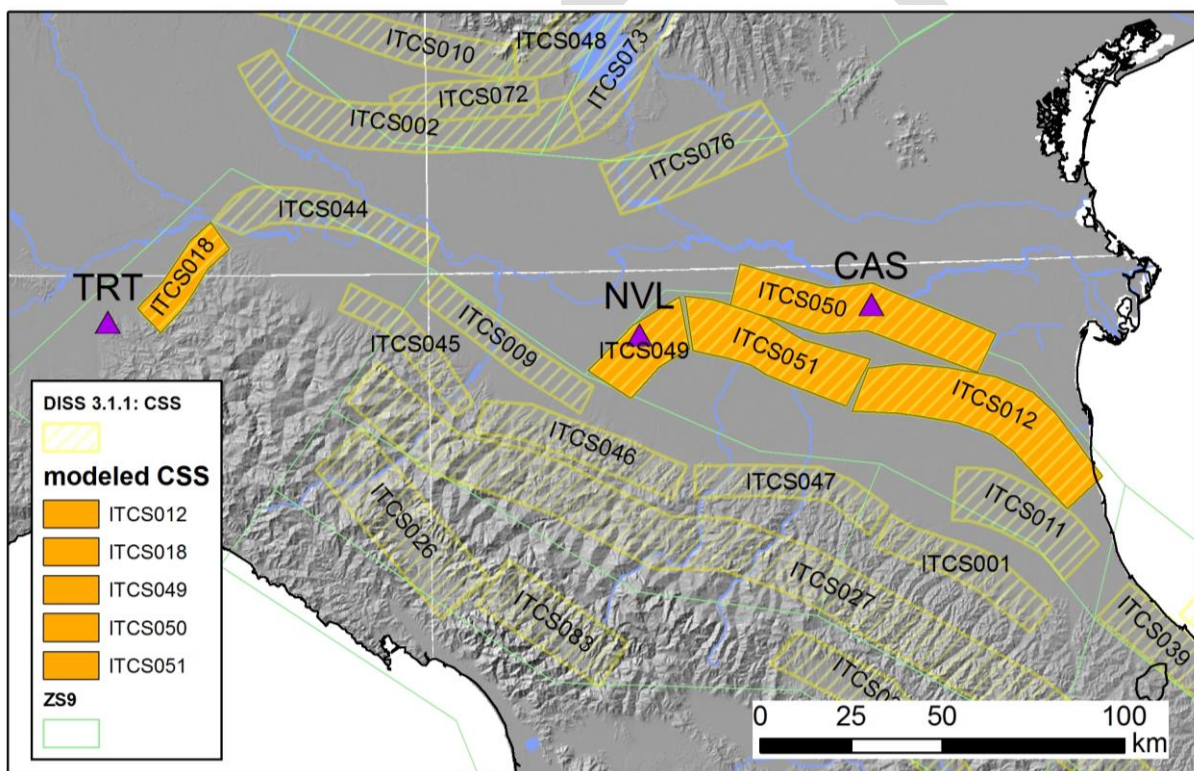



Figure 20 – Representation of seismogenic sources available in DISS3 database in the region of interest, limited to the composite fault sources (CSS), shown in pink. Purple triangles show sites location.

We have used the latest version of the database (DISS3.1.1) and its very recent reviews by Burrato et al. (2012, 2013, SIGMA deliverables) as the starting point for our ground-shaking calculations (Figure 20), considering those Composite faults (CSS) that mainly control the seismic hazard at the sites of interest: ITCS018, for TRT, and ITCS049-ITCS050-ITCS051



	<p>Research and Development Programme on Seismic Ground Motion</p> <p>CONFIDENTIAL</p> <p><i>Restricted to SIGMA scientific partners and members of the consortium, please do not pass around</i></p>	<p>Ref : SIGMA-2013-D4-94 Version : 01</p> <p>Date : October 2013 Page :</p>
--	---	--

and ITCS012 for NVL and CAS. Only faults giving a significant contribution (peak response spectrum accelerations > about 0.03g) to seismic hazard were retained. Appropriate tests were made in order to validate these assumptions.

For the Po Plain, based on the strong earthquake sequence of May – June 2012, an important update of CSSs is about to be introduced in DISS database, as anticipated in the last SC meeting (SC meeting n. 5, June 5-7 2013, Paris, oral presentation by P. Burrato). As shown in Figure 21, a new CSS will be introduced in-between sources ITCS050 and ITCS051: the 20 May CSS.

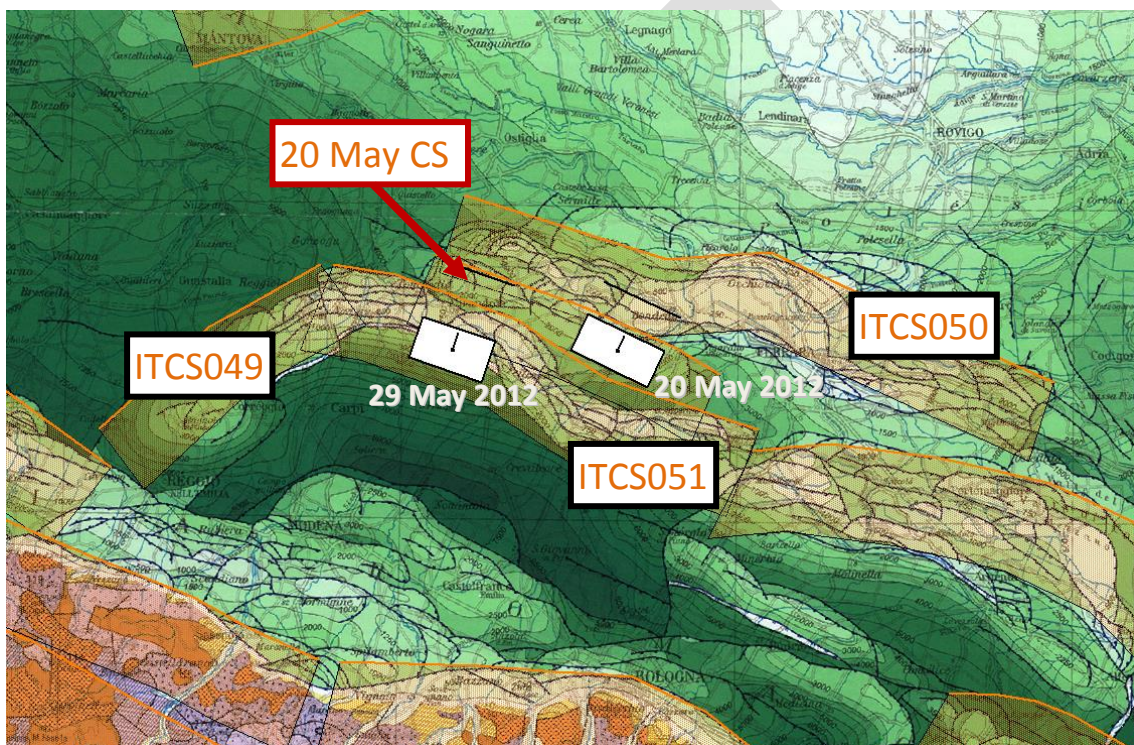


Figure 21 – CSS sources of Po Plain region, from the presentation of P. Burrato, SC meeting n. 5, June 5-7 2013, Paris.

As a final remark on the modelling of CSS, the essential features to be considered are recalled in Figure 22. Concerning the spatial arrangement and mutual orientation of the potential characteristic earthquake sources, both a parallel or a dipping pattern may be assumed, the former being generally more conservative, albeit not consistent with the layout shown in the figure.

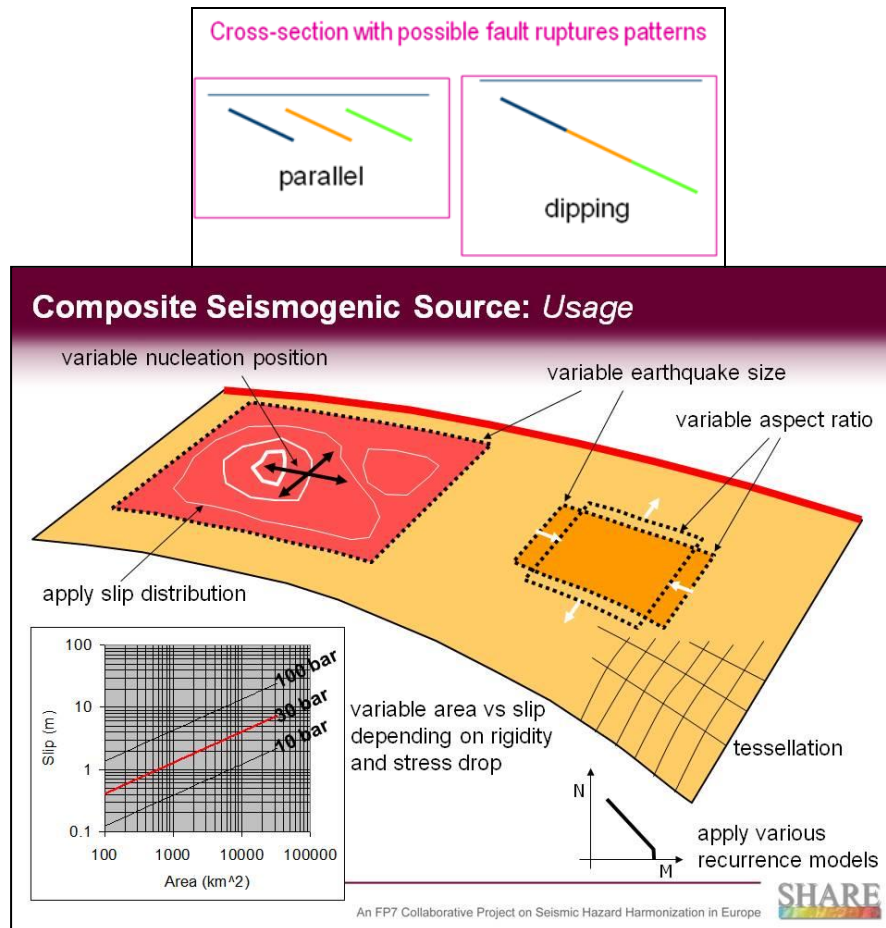


Figure 22 – CSS usage, from the presentation of P. Burrato, SC meeting n. 5, June 5-7 2013, Paris.

## 6.2. Background seismic activity

The background seismicity has been accounted for with the single area source polygon enclosed within the thick black lines shown in Figure 23. This area has been chosen in order to cover the low seismicity ( $M_w$  4.5 - 5.4) not accounted for by fault modelling. Its boundaries enclose two of the background areas defined in the SHARE project ([www.share-eu.org](http://www.share-eu.org)), within in the fault source – background model branch of their logic tree of hazard analysis.



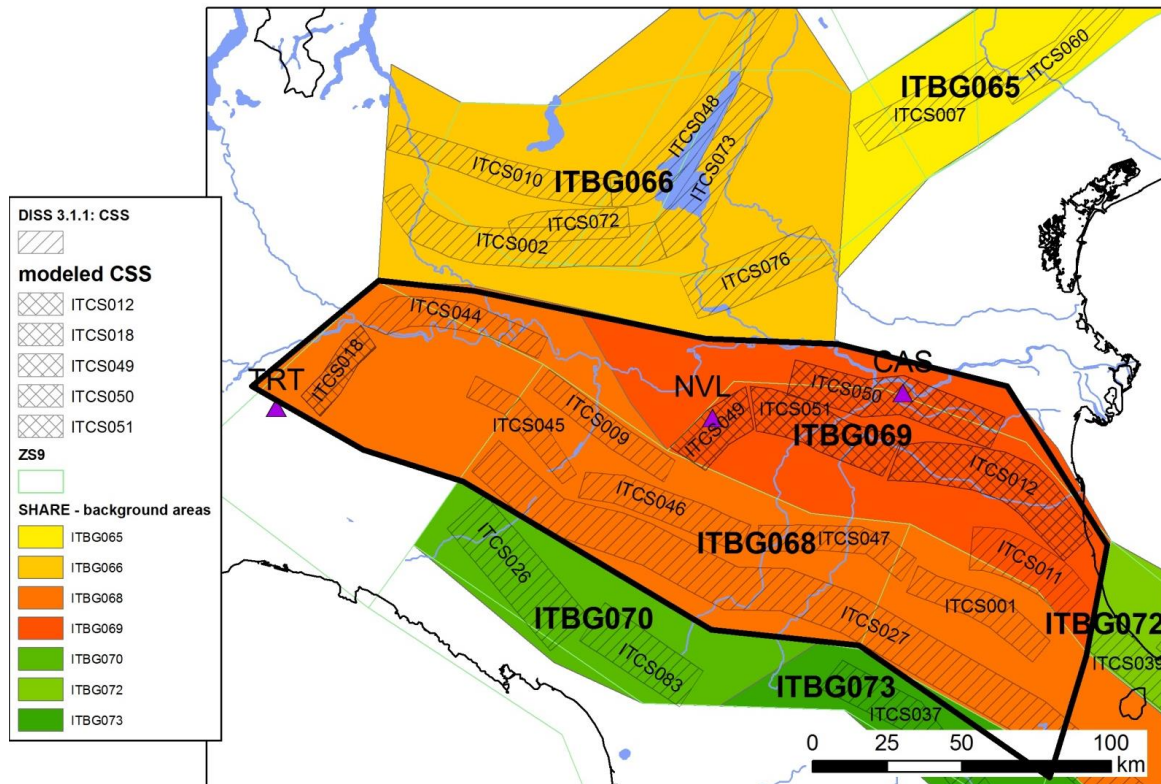


Figure 23 – Area source (within the black thick polygon) used in modelling the background seismicity. SHARE background areas are also shown with different colours, together with DISS composite sources. Purple triangles show studied sites.

The G-R parameters for this area have been computed as shown before, selecting events from the updated catalogue, starting from a minimum value of 4.5 up to a maximum of 5.4 (158 events in all) and relying on the same completeness periods defined in Sigma Phase I. Figure 24 shows results of estimation of GR parameters, Table 2 shows parameters used in hazard computations. Note that a bilinear GR fitting was used, to follow more closely the occurrence rates of this area, avoiding an artificial overestimation of rates at the higher magnitudes.

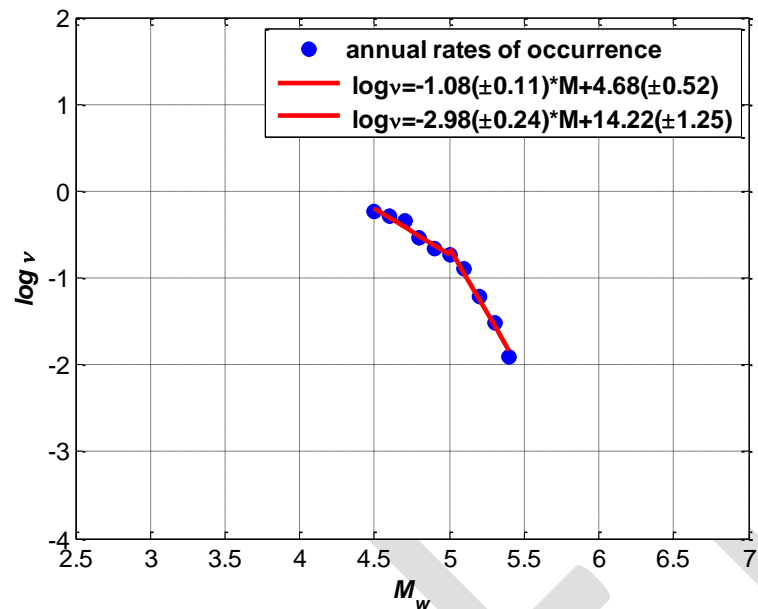


Figure 24 – Estimation of G-R parameters, for background area.

Table 2 – G-R parameters used in the SH analyses in terms of  $b$  values (with corresponding errors  $\sigma(b)$ ) and total occurrence rates, for background (BG) area source.

SSZ	$b$	$\sigma(b)$	$M_{\max}$	$M_{\max}$ uncertainty	Total ann. Rate $\lambda_{M \geq M_{\min}}$	Depth (km)
BG 1	1.08	0.11	5	0.3	0.63907	10
BG 2	2.98	0.24	5.4	0.3	0.10283	10

Figure 25 and Figure 26 show hazard computations for the BG contribution, for NVL and CAS, considering the three selected GMPEs, for unspecified mechanism. For the Bindi et al. GMPE, the 2011 version was used for the unspecified mechanism, as suggested by the authors, instead of its latest 2013 version (2013).



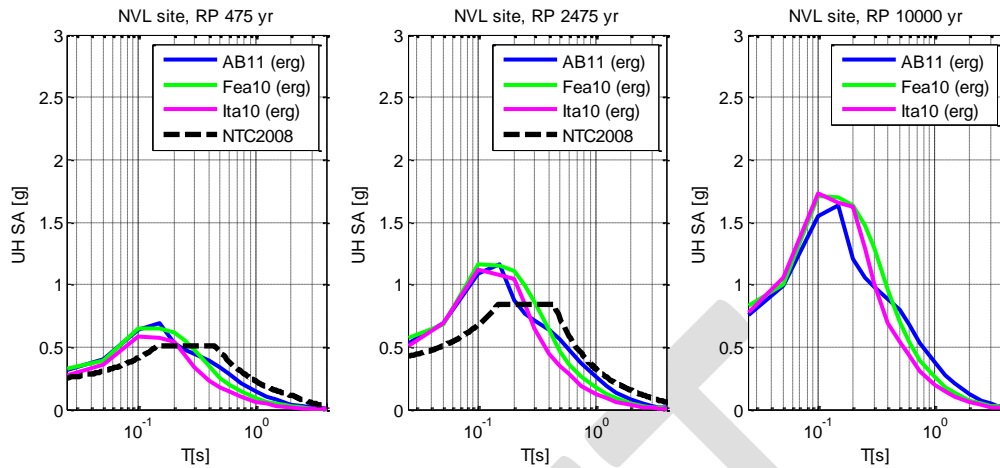


Figure 25 – NVL site, BG contribution. Uniform Hazard acceleration Spectra at indicated RPs. NTC2008 spectra are shown for comparison.

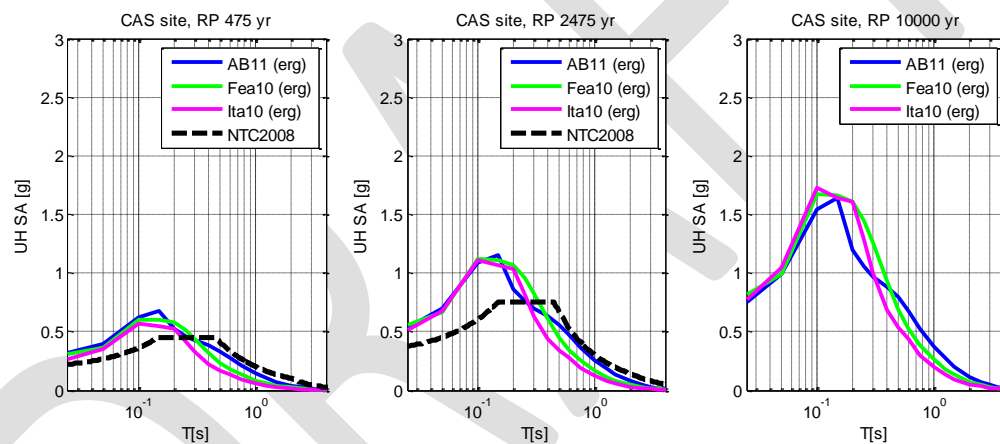



Figure 26 – Same as Figure 25, for CAS site.

### 6.3. Faults

CSS sources were first modelled through the SH computational tool (CRISIS2008) as area sources whose earthquake occurrence is assumed to follow a Poisson process, and using the characteristic earthquake model.

CRISIS assumes that, within an extended source, seismic activity is evenly distributed by unit area (area sources). In order to correctly implement this modelling assumption, CRISIS performs a spatial integration by subdividing the original sources into sub-sources. CRISIS assigns to a single point all the activity associated to the sub-source, and then the spatial integration adopts a summation form. In this work, this scheme has been adopted for the modelling of CSS. Rupture areas for distance computation are assumed to be circular, centred

	<p>Research and Development Programme on Seismic Ground Motion</p> <p>CONFIDENTIAL</p> <p><i>Restricted to SIGMA scientific partners and members of the consortium, please do not pass around</i></p>	<p>Ref : SIGMA-2013-D4-94 Version : 01</p> <p>Date : October 2013 Page :</p>
--	---	--

in the centroid of the source subdivisions (and with radius depending on magnitude in a way specified by the user). Note this filling of CSS with the characteristic earthquake structure is actually imperfect, since it allows overlapping of rupture areas, and trespassing of CSS boundaries. This is particularly important in the vicinity of the area source boundary, where hazard estimation may be slightly overestimated.

We recall here that the characteristic events have a magnitude distribution that differs from the exponential one (as for earthquake occurrence rates described by the Gutenberg – Richter relationship), as shown in Figure 27. In the model implemented in CRISIS2008 a truncated normal distribution is assumed for the magnitude of the characteristic earthquake.

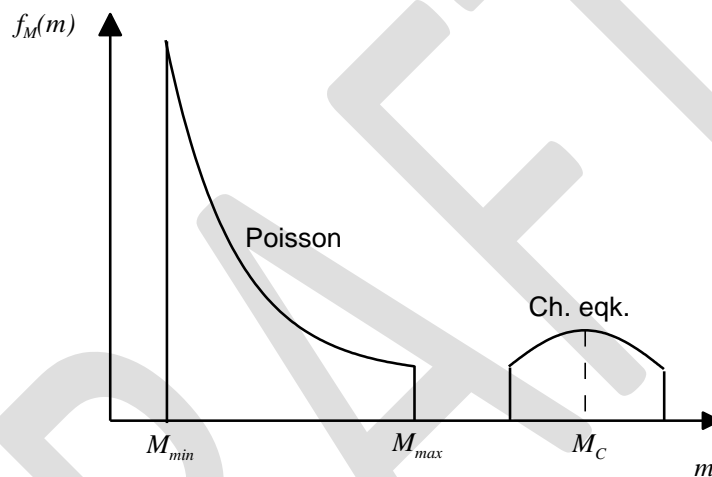



Figure 27 – Representation of the truncated exponential magnitude probability density function  $f_M(m)$  for the Poisson process and the Characteristic (Ch) earthquake process of expected magnitude  $M_C$ :  $M_{min}$  and  $M_{max}$  are the bounds of the Gutenberg–Richter relationship.

Moreover, CRISIS allows a slip-predictable behaviour in time that is modelled assuming, after Jara and Rosenblueth (1988), that the expected value of the magnitude of the characteristic earthquake ( $E(M)$ ) grows with the time elapsed since the last characteristic event,  $T_{00}$ , in the following fashion :

$$E(M) = M_{min} + F \ln(T_{00})$$

By assuming  $F=0$ , the process becomes time-independent.

The main parameters used to model composite sources are: characteristic magnitude ( $M_C$ ) and recurrence time (RT). The recurrence time refer to the estimated recurrence intervals (or inter-event time) between similar-sized, maximum expected earthquakes on the individual source. The mean recurrence time and its variability are the basic ingredients to compute the earthquake probability of occurrence, as show in next Section 6.4.

	Research and Development Programme on Seismic Ground Motion	<b>Ref : SIGMA-2013-D4-94</b> <b>Version : 01</b>
	<b>CONFIDENTIAL</b> <i>Restricted to SIGMA scientific partners and members of the consortium,          please do not pass around</i>	<b>Date : October 2013</b> <b>Page :</b>

A completely different approach will be used to validate results of CSS modelling as shown hereafter.

#### 6.4. Recurrence time

The “ideal” situation for a given fault segment would obviously be to carry a long list of associated earthquakes with clear neo-tectonic markers, so that statistics could be derived directly from observations. The actual observations of multiple, characteristic events on the same fault segment in Italy are definitely few, mostly represented by recent active sources in Central Apennines. Therefore, the value of RT has to be estimated by a combination of fault parameters. A widely used practice invokes the criterion of the “segment seismic moment conservation”, proposed by Field et al. (1999), by which:

$$RT = \frac{1}{Char\_Rate} = \frac{10^{(1.5M+9.05)}}{\mu VLW}$$

where the numerator is the seismic moment associated to the characteristic earthquake, and the denominator the annual moment rate. More specifically, *RT* is the mean recurrence time in years, *Char\_Rate* is the annual mean rate of occurrence, *M* is the characteristic magnitude,  $\mu$  is the shear modulus of the crustal rocks in  $N/m^2$ , *V* is the long-term slip rate on the fault in m per year, and *L* and *W* are the geometrical parameters of the fault, in m. The coefficients 1.5 and 9.05, proposed by Hanks and Kanamori (1979) in the relationship to derive the seismic moment (in  $N \cdot m$ ) from magnitude, formally they refer to  $M_S$ , but we can assume they are equivalent to  $M_W$ , considering the magnitude range of interest (Peruzza et al., 2008).

Table 3 summarizes the relevant parameter values used to model composite sources, in particular, characteristic magnitude (*Mc*) and recurrence time (*RT*). *Mc* was borrowed from the DISS database, while *RT* was estimated for each fault as explained. Fault length (*L*) and width (*W*) has been estimated after Wells and Coppersmith (1994), for specific reverse mechanisms. Slip rates are mean values taken from Burrato et al. (2013).

Table 3 – Composite faults from DISS3 used in the PSHA analysis, *Mc* is the characteristic magnitude and *RT* is the recurrence time. Depth is average between the smallest and largest depth of the CSS.

CSS	Mc	L [m]	W [m]	Depth [km]	slip rate [m/yr]	RT [years]	Annual probability
ITCS050	6	11482	7079	4.5	0.00042	939	0.001065
ITCS051	6	11482	7079	6.5	0.00099	398	0.00251
ITCS049	6	11482	7079	6.5	0.00053	744	0.001344
ITCS012	5.6	6730	4853	5	0.00044	561	0.001784
ITCS018	5.5	5888	4416	5	0.0003	731	0.001368

## 6.5. Comparing AS modeling versus FS+BG

Figure 28, Figure 29 and Figure 30 compare results of faults and area source modeling, using the different GMPEs, in their ergodic mode. UH spectra, for ground type C (CAS and NVL) and B (TRT), are shown with the respective code spectra. Results are for the most part closely comparable, for all return periods and for all sites. For NVL and CAS results with FS+BG modeling show higher amplitudes, in particular for 10 000 yr RT, unlike TRT site where the AS approach predominates. This was expected since the hazard at that site is affected by the proximity of a single CSS (ITCS018), while NVL and CAS are very near to more than one CSS (see Figure 20). Only results with the Fea10 GMPE, for TRT site, tend to increase hazard from FS+BG modeling, but this is due to the background, whose contribution is enhanced by the use of that GMPE (see Figure 34). Note how with AB11 GMPE results are quite similar for all approaches, for sites NVL and CAS.

Figure 31, Figure 32, Figure 33 and Figure 34 show contributions of BG with respect to AS and FS+BG modeling, with two GMPEs: Fea10 and AB11. Note how the contribution of BG to local seismic hazard changes with the site and with the GMPE used. For TRT site, The BG plays always a significant role as expected.

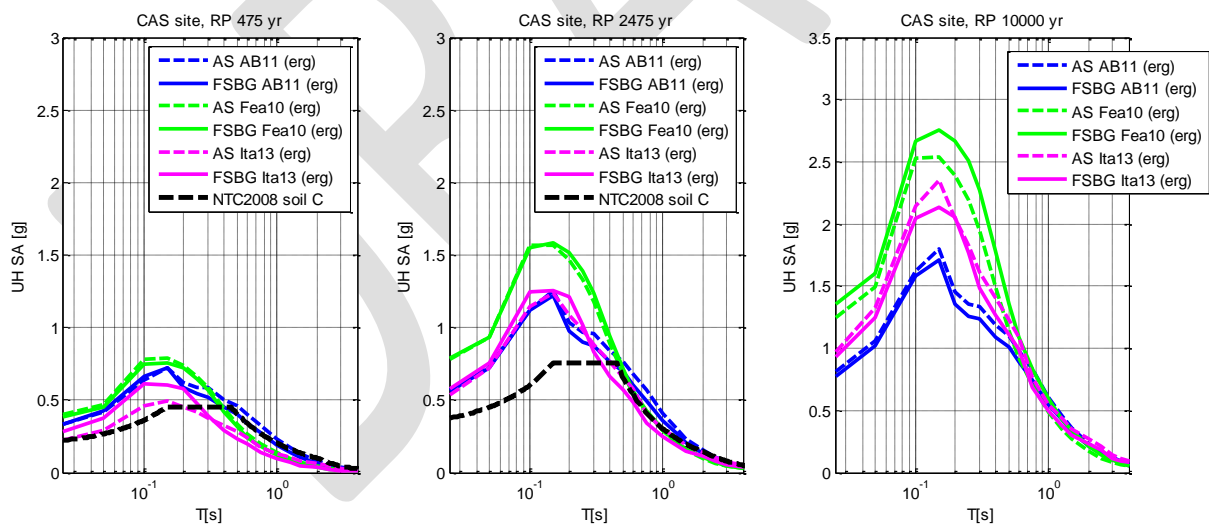


Figure 28 –CAS site. Uniform Hazard acceleration Spectra at return periods of 475, 2475 and 10000 years with respective NTC2008 code. AS versus FS+BG modelling, with different GMPEs.

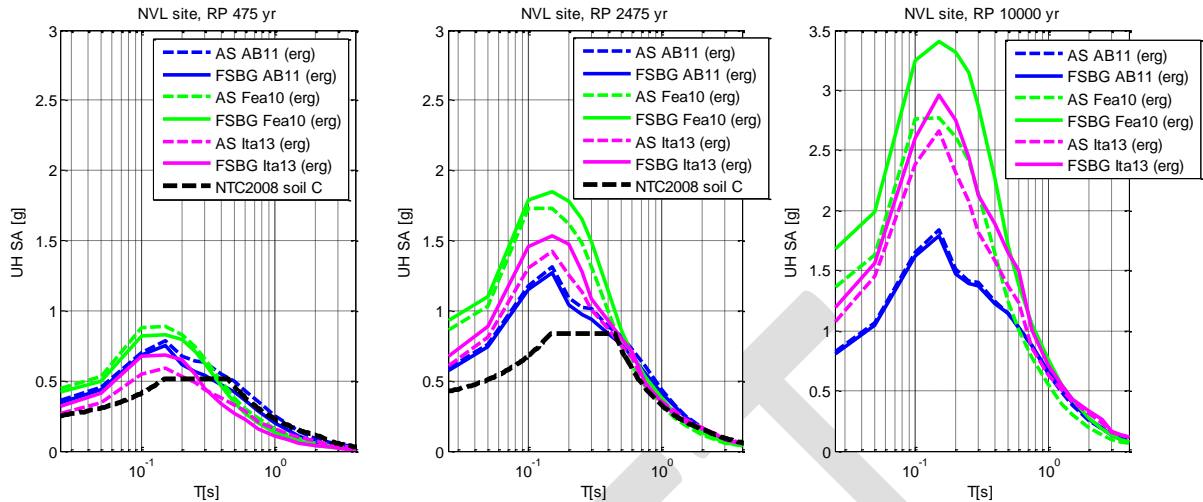


Figure 29 – NVL site. Uniform Hazard acceleration Spectra at return periods of 475, 2475 and 10000 years with respective NTC2008 code. AS versus FS+BG modelling, with different GMPEs.

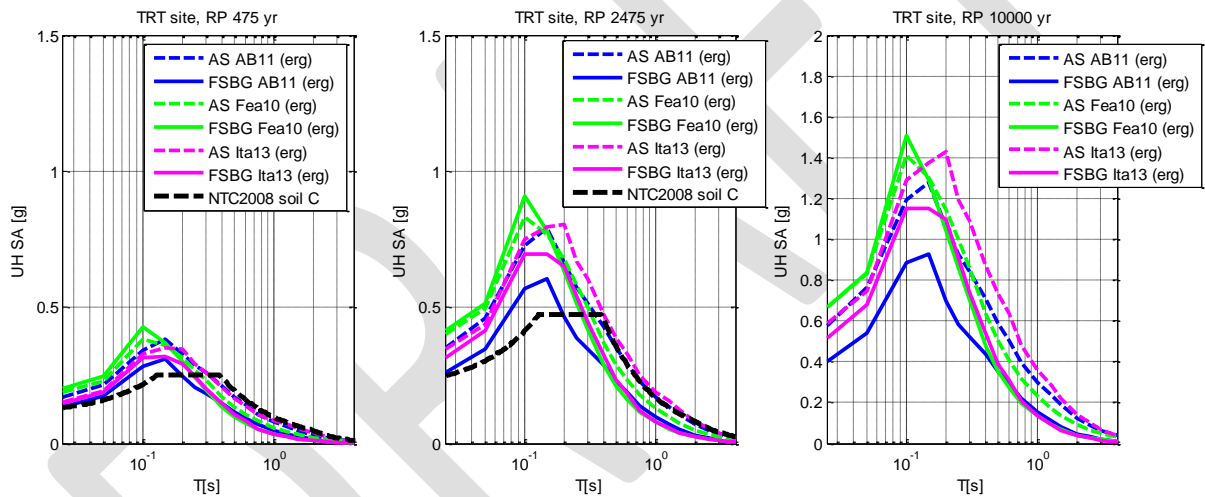


Figure 30 – TRT site. Uniform Hazard acceleration Spectra at return periods of 475, 2475 and 10000 years with respective NTC2008 code. AS versus FS+BG modelling, with different GMPEs.

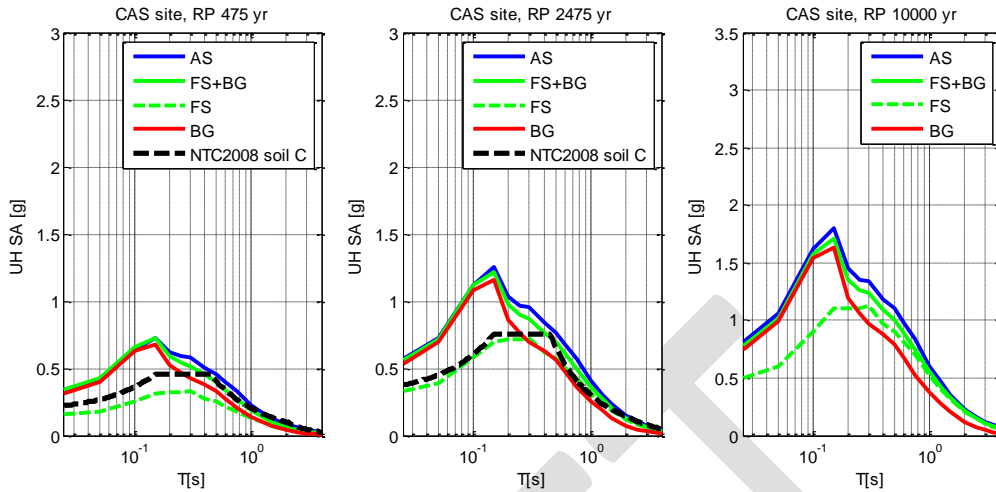


Figure 31 –CAS site. AB11 GMPE. UH acceleration Spectra at return periods of 475, 2475 and 10000 years with respective NTC2008 code. AS, FS+BG, FS and only BG modelling.

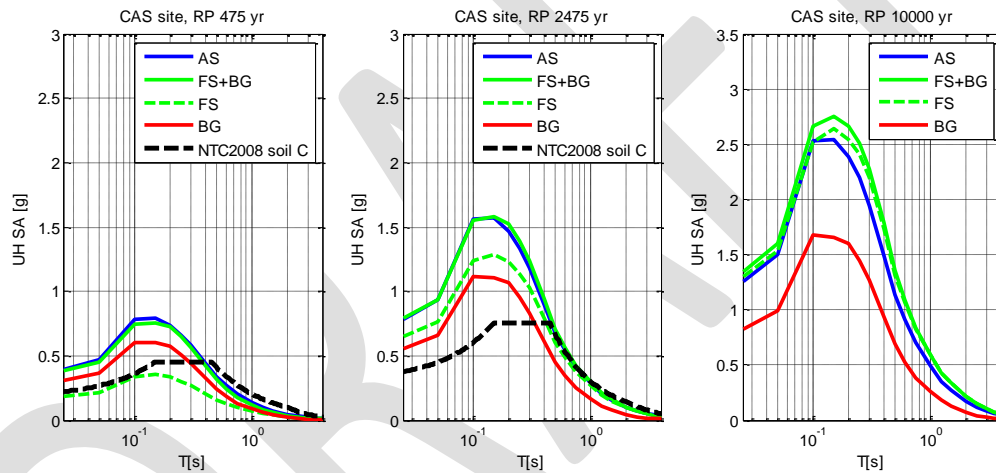


Figure 32 –CAS site. Fea10 GMPE. UH acceleration Spectra at return periods of 475, 2475 and 10000 years with respective NTC2008 code. AS, FS+BG, FS and only BG modelling.

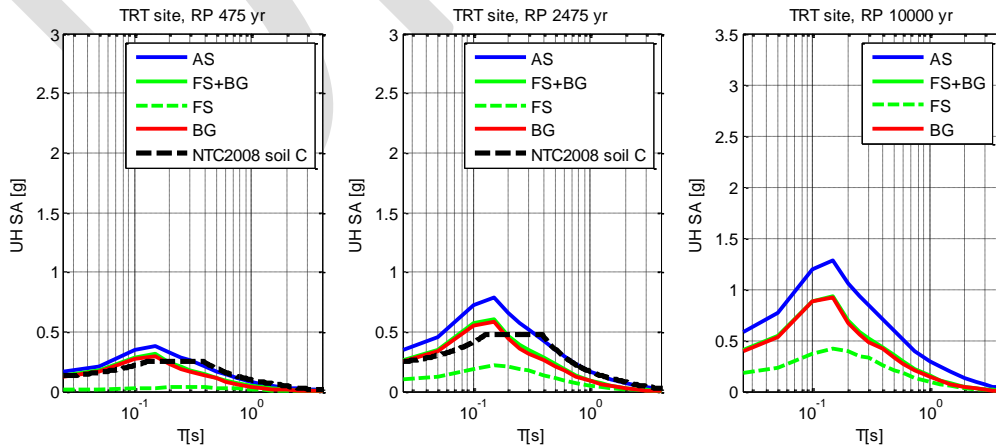


Figure 33 –TRT site. AB11 GMPE. UH acceleration Spectra at return periods of 475, 2475 and 10000 years with respective NTC2008 code. AS, FS+BG, FS and only BG modelling.



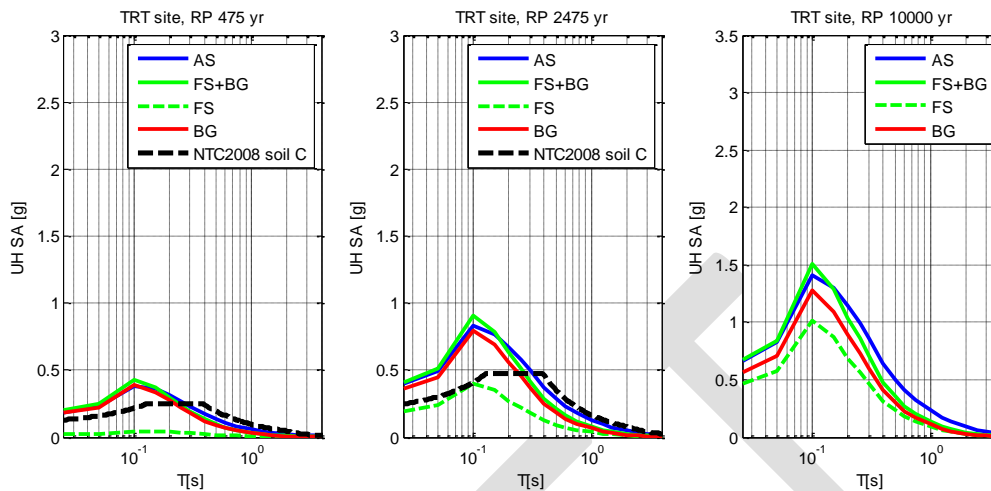


Figure 34 –TRT site. Fea10 GMPE. UH acceleration Spectra at return periods of 475, 2475 and 10000 years with respective NTC2008 code. AS, FS+BG, FS and only BG modelling.


## 6.6. Modelling faults with an alternative approach

As a matter of comparison and validation of the adopted modeling of faults sources, with special regard for near field locations, we implemented a very recent novel approach for probabilistic seismic hazard analyses, in which deterministically computed ground motion is introduced, in replacement of the empirically predicted values of GMPEs.

This approach, thoroughly discussed in Villani et al. (2012) and Villani (2010), to which we refer for details, was first proposed by Convertito et al. (2006), who used a predominantly far field approximation for generating the deterministic ground motions. Moreover within the SCEC's CyberShake Project (Graves et al., 2011) 3D simulations and finite fault rupture descriptions in the low frequency range have been used to compute seismic hazard analyses in Southern California.

As a matter of fact, databases of most ground motion prediction equations (GMPEs) tend to be insufficiently constrained at short distances and data may only partially account for the rupture process, wave propagation and 3D complex configurations (Somerville et al., 1997). These characteristics can play a critical role when the sites at interest are located at source-to-site distances comparable with the fault dimension, where few records of strong ground motion are available.

That's why an appealing alternative to the use of the GMPEs is represented by the injection in PSHA of the results of numerical simulations of the source and wave propagation into the SHA, exploiting the capabilities of CRISIS2008 code. Results of the numerical simulations

	<p>Research and Development Programme on Seismic Ground Motion</p> <p>CONFIDENTIAL</p> <p><i>Restricted to SIGMA scientific partners and members of the consortium, please do not pass around</i></p>	<p>Ref : SIGMA-2013-D4-94 Version : 01</p> <p>Date : October 2013 Page :</p>
--	---	--

for selected earthquake scenarios are introduced as input in the SHA as "non-standard" or "generalized" description of attenuation.

### 6.6.1. Generalized description of ground motion attenuation (GAF)

The method relies on the generation of a fairly large set of numerical source and wave propagation simulations (with appropriate source parameter variations) at each site of interest (in our case: modeling of representative faults and simulations at selected sites), aimed at establishing realistic envelopes for near-source ground motion levels. Results are then used in SHA in the form of a grid of median values and associated dispersion measures and then used to compute, as a function of position, the first two moments of the ground motion parameter (intensity measure) for each spectral ordinate considered in the analysis. These two moments become the main ingredients for the computation of the probability of exceeding a certain level of ground motion at a site, given the occurrence of a specific event (of magnitude  $m_i$ ) on the considered  $k$  source (at distance  $r_k$ ):  $P(Y > y | m_i, r_k)$ .

Note that when this term is computed through the use of numerical simulations, the predicted variability in the ground motion at a given site directly includes the 3D path and rupture characteristics specific and unique to the studied site for a specified rupture (Graves et al., 2011). Hence, when the sigma is computed over different results of simulations of a specified earthquake scenario, at a particular site, such sigma really represents the variability of the ground motion amplitudes expected at a single site over many earthquake cycles on a given fault.

Crucial for exploiting the foregoing approach is the ability of the PSHA tool used to handle occurrence probabilities according to the full probability theory formalism, instead of occurrence rates. This was implemented in the code CRISIS2008 (Ordaz et al. 2013) by computing the probability that the ground motion parameter (Y) exceeds a certain threshold  $y$  at a site in the following  $T_j$  years in the form


$$P(Y \geq y | T_j) = 1 - \prod_{k=1}^{N_k} \prod_{i=1}^{N_m} \left( \sum_{s=0}^{N_s} P_k(s, m_i, T_j) [1 - P(Y > y | m_i, r_k)]^s \right)$$

where  $P_k(s, m_i, T_j)$ , is the probability of having  $s$  events ( $s=0,1, \dots, N_s$ ) of magnitude  $m_i$  in the following  $T_j$  years at a given source  $k$ . In this formulation, the probabilities of  $s=0,1,\dots,N_s$  events in the window  $T_j$  are assumed to be mutually exclusive, such that:

$$\sum_{s=0}^{N_s} P_k(s, m_i, T_j) = 1$$

Each event that occurs on source  $k$  has probability  $P(Y > y | m_i, r_k)$  to be a special event, i.e. to cause at a site ground motion exceeding  $y$ . Moreover, the source  $k$  can generate earthquakes of different and independent magnitudes ( $m_i$  with  $i=0,1,\dots,N_m$ ). With this formulation



	<p>Research and Development Programme on Seismic Ground Motion</p> <p>CONFIDENTIAL</p> <p><i>Restricted to SIGMA scientific partners and members of the consortium, please do not pass around</i></p>	<p>Ref : SIGMA-2013-D4-94 Version : 01</p> <hr/> <p>Date : October 2013 Page :</p>
--	---	--

$P_k(s, m_i, T_j)$  can be computed with any time-independent or dependent earthquake recurrence model. Moreover, the earthquake occurrences in different sources are assumed independent from each other, as well as the possible earthquake magnitudes and seismic sources. (For a complete discussion of the aforementioned formulation see Villani, 2010).

### 6.6.2. Finite fault stochastic modeling: EXSIM code

In this work, finite-fault stochastic simulations have been carried out with the EXSIM program (Motazedian and Atkinson, 2005). Note that the PSHA formulation is general and any numerical method can be adopted in order to produce the ground shaking.

The stochastic approach typically models the ground motion, in terms of acceleration, as Gaussian noise with a spectrum that is either empirical, or based on a physical model of the earthquake source, e.g. the  $\omega^2$  spectral source model (Bouchon and Aki, 1967). Among the methods that use a stochastic representation of some or all the physical processes controlling the ground shaking, the method proposed by Boore (2003) has been adopted in this work.

The method relies on the simulation of several small earthquakes as sub-events that make up a large fault-rupture event. The fault is divided into N sub-faults, each of which is considered as a small point source, modelled by the stochastic point-source method (Boore, 1983). The authors Motazedian and Atkinson (2005) remark that at close distances from the source, stochastic methods do not adequately describe the coherent long-period pulses that may control near-fault ground motions for frequencies lower than 1 Hz while these are typically well-simulated with physically-based numerical approaches.

### 6.6.3. Approach used for hazard computations with Composite Sources (CSS)

Ground motion hazard from selected CSS in the near field of two of the sites (NVL and CAS) has been quantified following the hybrid approach outlined in the next steps. The starting point of this procedure (thoroughly discussed in Faccioli, 2012) was partially borrowed from the work of Zonno et al. (2012), where ground motion contribution from CSS on the Italian territory was computed using EXSIM program. The code was used to simulate motions from the Typical Fault (i.e. portion of the corresponding CSS that may generate the maximum credible earthquake that any individual CSS may release), that was allowed to float at regular steps along the strike of its CSS, mapping in this way all possible seismogenic contributions to ground motion. We recall here that CSS are regarded as “containers” of a characteristic type earthquake, not associated to a specific fault segment within the CSS, with  $M (=m_c)$  estimated from earthquake catalogue.

In synthesis:

1. Each CSS is partitioned into faults of equal size, consistent with the associated characteristic magnitude  $m_C$  on the basis of the Wells and Coppersmith (1994) relations, and the CSS representative focal mechanism, (see Figure 35, for modeled CSSs).
2. For a rupture on a single fault, ground motions at the sites of interest are computed with the finite-source stochastic simulation code EXSIM, after choosing a slip distribution on the fault, a distance dependence of the signal amplitude and a site soil profile, and a set of response spectra  $Y(T)$  is obtained.
3. Combining contributions from all CSS, a large ensemble of simulated spectra (all compatible with the characteristic magnitude  $m_C$ ) is thus made available at each site, from which the first two statistical moments are derived for any ordinate, and a site distribution  $F_Y[y(T)|m_C]$  is picked (e. g. lognormal or gamma, as discussed in Villani, 2010) having these two moments.
4. For each CSS involved, the probability  $P(1, m_C, T_N)$  of one characteristic earthquake occurring in the time windows  $T_N$  needs to be separately estimated;
5. Finally, in the simple case where  $m_C$  is the same for all the CSS (as herein assumed), one obtains:

$$P(Y \geq y, T_N) = [1 - F_Y(y|m_C)] \cdot P(1, m_C, T_N)$$

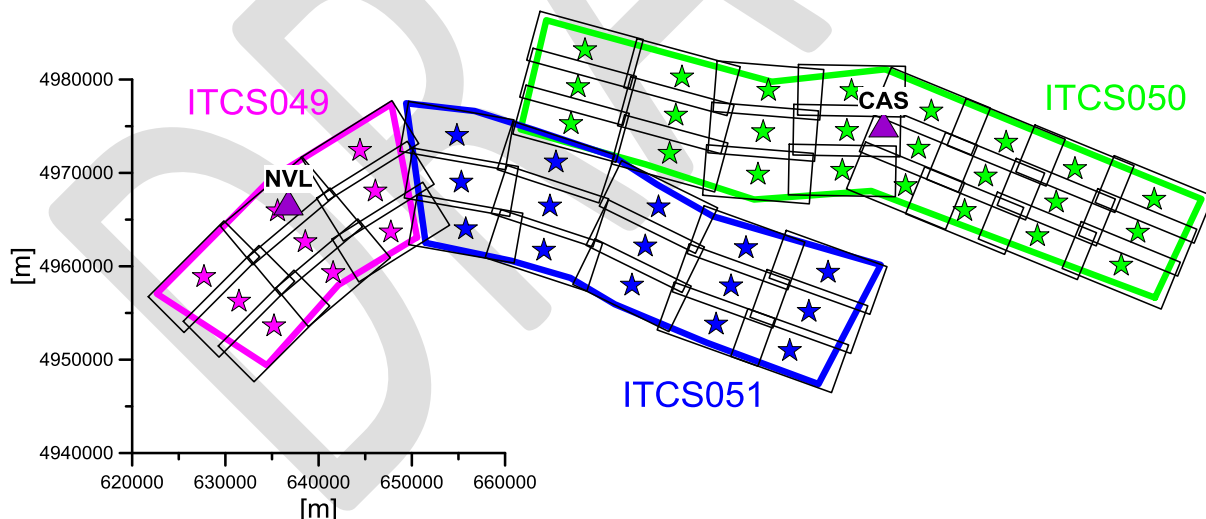



Figure 35 – Partition of CSSs ITCS049, ITCS050, ITCS051. Triangles show test sites position.

The probability  $P(1, m_C, T_N)$  has been estimated assuming a Poissonian dependence of the mean recurrence time (estimated as explained in Sect 6.4) in the observation period of interest  $T_N$ :

$$P(1, m_C, T_N) = 1 - \exp^{-T_N / RT}$$

	Research and Development Programme on Seismic Ground Motion	Ref : SIGMA-2013-D4-94 Version : 01
	CONFIDENTIAL <i>Restricted to SIGMA scientific partners and members of the consortium,          please do not pass around</i>	Date : October 2013 Page :

The adopted recurrence times are those shown in Table 3 for modeled CSS.

We included in the simulation three out of all the CSS used in the fault source logic tree branch, as shown in Figure 35: ITCS049 and ITCS050, where NVL and CAS sites are respectively located, and ITCS051, lying in between. The main parameters used in EXSIM are summarized in Table 4. Kappa value has been fixed to 0.04, while stress drop values of 50 and 30 bar were assumed. These two values have been selected after the analysis of 28 records observed during the main shock of May 29<sup>th</sup> 2012 in the epicentral area. A recent work from Castro et al. (2013), supported our choices. Path effect parameters were chosen after Zonno et al. (2012), while slip distribution on the source was taken after the slip pattern of the May 29<sup>th</sup> event (Atzori, pers. comm., and Atzori et al., 2012); random distributions were tested as well. For each subfault, 30 realizations were computed.

Table 4 - Input parameters for the EXSIM program. Note that Length and Width refer to the dimension of the faults that map the entire CSS, while the subfaults refer to the integration of the single fault.

CSS	Depth of fault top [km]	dip	rake	Mw	Length [m]	Width [m]	# of subfaults on each fault	# of simulations for each fault	# of faults
ITCS049	3	40	90	6	11482	7079	21*13	30	9
ITCS050	1	40	90	6	11482	7079	21*13	30	24
ITCS051	3	40	90	6	11482	7079	21*13	30	15

#### 6.6.4. Accounting for site response

Concerning site and crustal amplification functions used in EXSIM to quantify the contribution of local site effects at the location where ground motion is computed, two different choices have been made for NVL and CAS respectively.

For NVL site, results of a recent Italian project have been used (S2 project *Constraining Observations into Seismic Hazard*, <https://sites.google.com/site/ingvdpc2012progettos2/home>); this project aimed at quantifying the effects of local site conditions on PSHA results. For NVL, we used the consensus site profile of the project, and computed the 1D analytical site amplification function down to the crustal layers where the modeled source is located (shown in Figure 36).

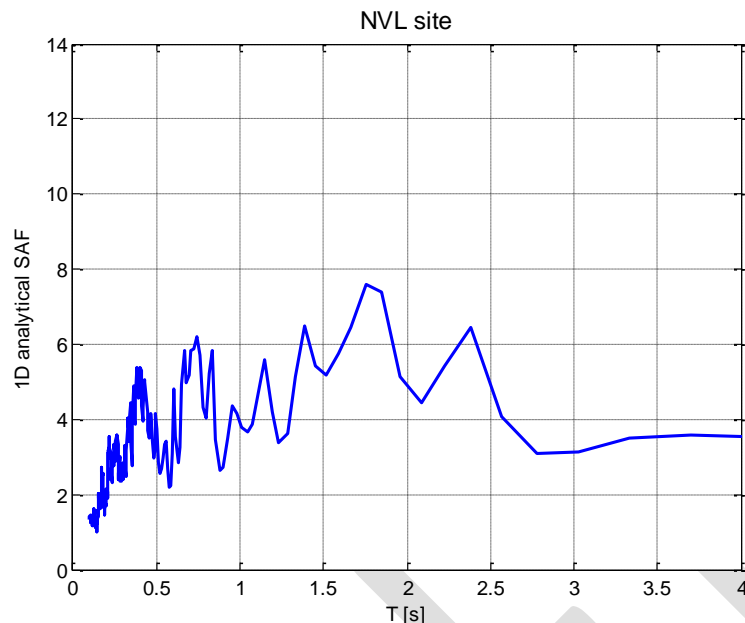


Figure 36 – NVL site. 1D analytical estimate of site amplification function to be used in EXSIM code.

For CAS, a different approach has been used, relying on the availability of observations at the site of interest, at surface and at a bedrock interface of 130 m, from the Ferrara temporary network installed by OGS and collected in the OASIS database (OGS Archive System of Instrumental Seismology, <http://oasis.crs.inogs.it>). Figure 37 show response spectral ratios from six events, with  $M_w$  ranging from 3.6 to 5.2. Note that the empirical function (from spectral ratios with respect to borehole location, red line) had to be corrected for the so called depth effect (green line), to overcome the bias of the estimation of the transfer function with reference to a standard outcrop rock site. The procedure, borrowed from Cadet et al. (2012), consists of a simple frequency-dependent curve, to be adapted for each site as a function of the first “destructive” interference frequency at depth. The procedure was empirically calibrated using the Kiknet database.

The green line of Figure 37 is the one used to account for site effects in the EXSIM code.

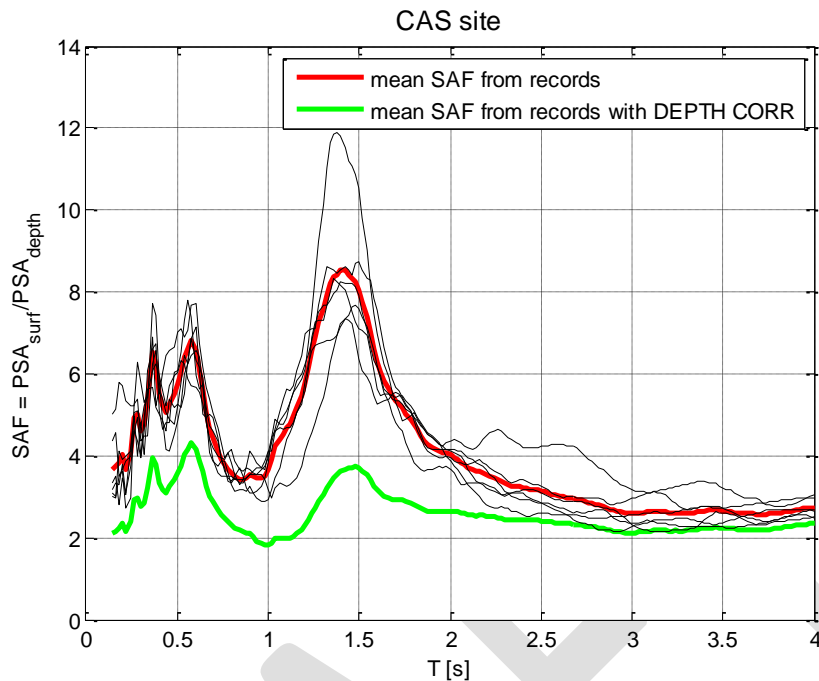


Figure 37 – CAS site. Empirical estimate of site amplification function to be used in EXSIM code. Red line is computed from record spectral ratios, green line is the corresponding average function, corrected for depth effect (after Cadet et al., 2012).

### 6.6.5. Results

In the following figures, results of hazard analyses computed with the GAF approach, in terms of uniform hazard spectra, are compared with SHA where the corresponding CSS are modeled as simple area sources with a characteristic earthquake behavior (as explained in Sect. 6.3). The CSS involved in computations are again ITCS049, ITCS050 and ITCS051, with the model parameters shown in Table 3 and Table 4. SHA computations used as attenuation models the three GMPEs selected in this phase of the work.

Comparisons are shown for a return period of 2475 years, since the probability assigned to the characteristic earthquake of the CSS intrinsically limits the resolution of the resulting exceedance curves (that saturate at exactly that level).

Results are in good agreement, notably at CAS. The intrinsic (and unavoidable) uncertainty in the stress drop matches the variability inherent in the use of traditional GMPEs. The site amplification function, more appropriately calibrated in CAS site, where an empirical estimation was possible, improves the comparison with the AS approach.

The use of the site amplification function in the GAF enhances the hazard at the site at the typical resonance frequencies of the local site response, not necessarily seen by the GMPEs.



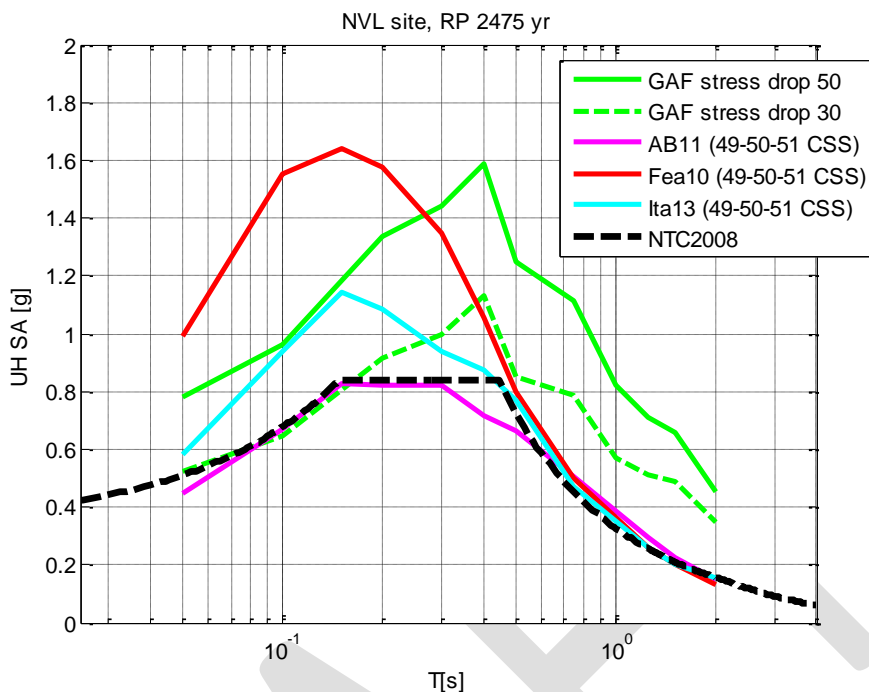


Figure 38 – NVL site. UH spectra from PSHA (ergodic) analyses with area sources with characteristic model (and selected GMPEs), and GAF approach, with different stress drop values.

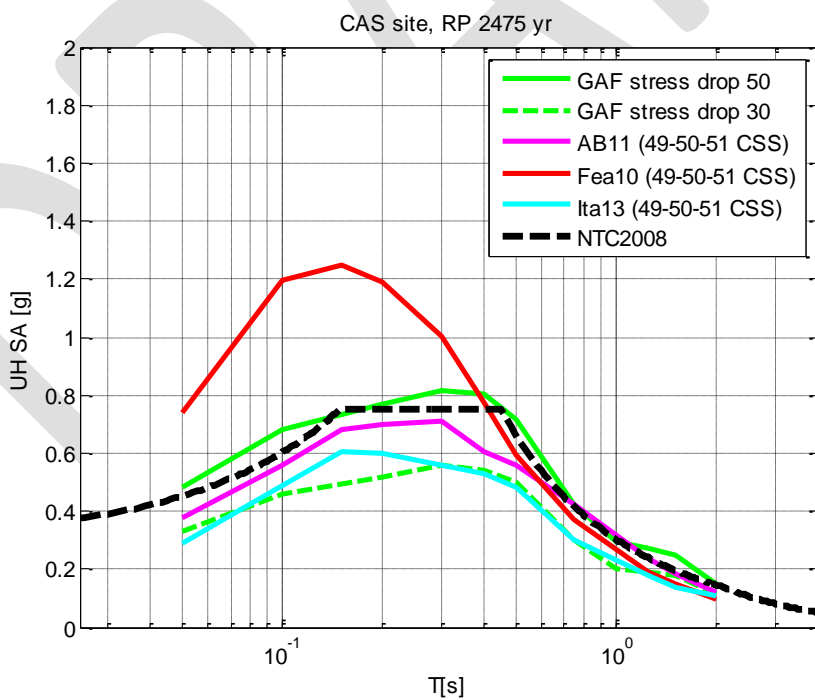


Figure 39 – CAS site. UH spectra from PSHA analyses with area sources with characteristic model (and selected GMPEs), and GAF approach, with different stress drop values.

## 7. Gridded seismicity

As in Phase I, a different representation of seismicity is used in a separate branch of the analysis, considering a gridded map of probability occurrences. One recurrence model has been selected in this stage of the work, namely: the time-independent, poissonian HAZGRID model (D2.2 of same DPC-INGV S2 project, 2007-2009; Akinci, 2010), in its latest version using CPTI11 (Rovida et al., 2011) as its reference catalogue.

All the previously introduced GMPEs were used, either for ground type C (CAS and NVL) or B (TRT), in the unspecified fault mechanism mode. For the Bindi et al. GMPE, the 2011 version was used for the unspecified mechanism, as suggested by the authors, instead of its latest 2013 version (2013).

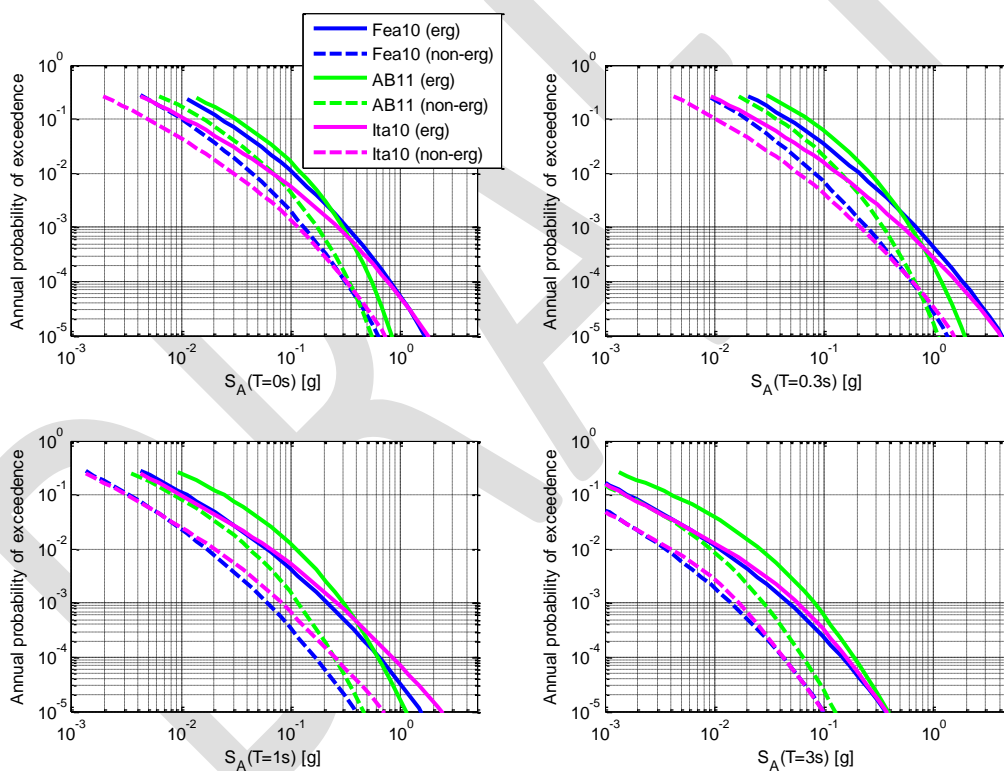


Figure 40 – CAS site. Exceedance curves for HAZGRID model with different GMPEs, corrected or not with the non-ergodic coefficients.

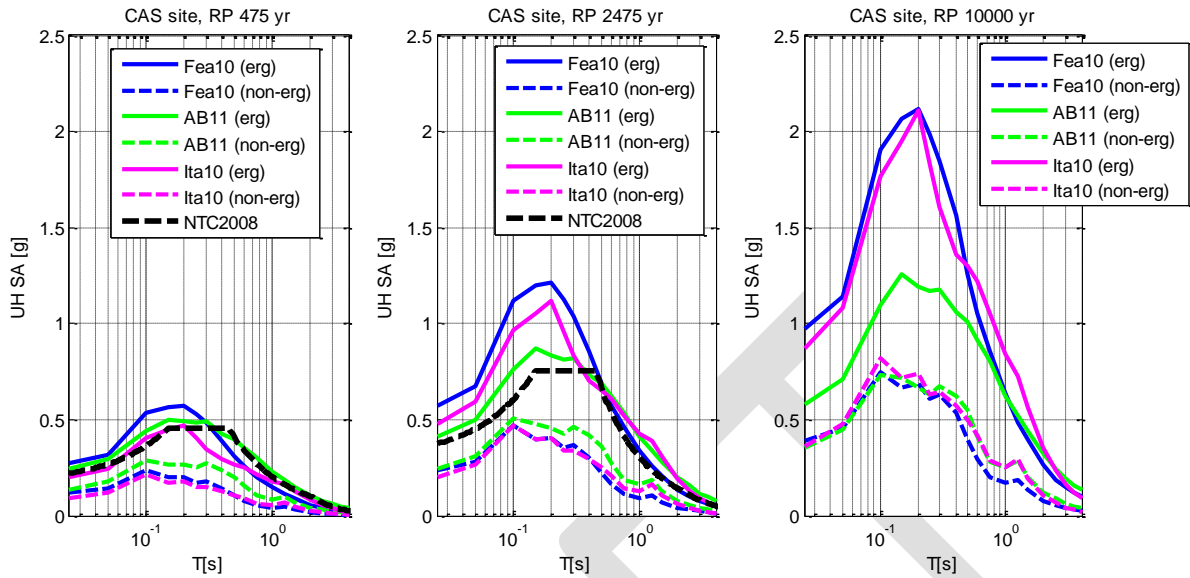


Figure 41 – CAS site. UHS for HAZGRID model with different GMPEs, corrected or not with the non-ergodic coefficients.

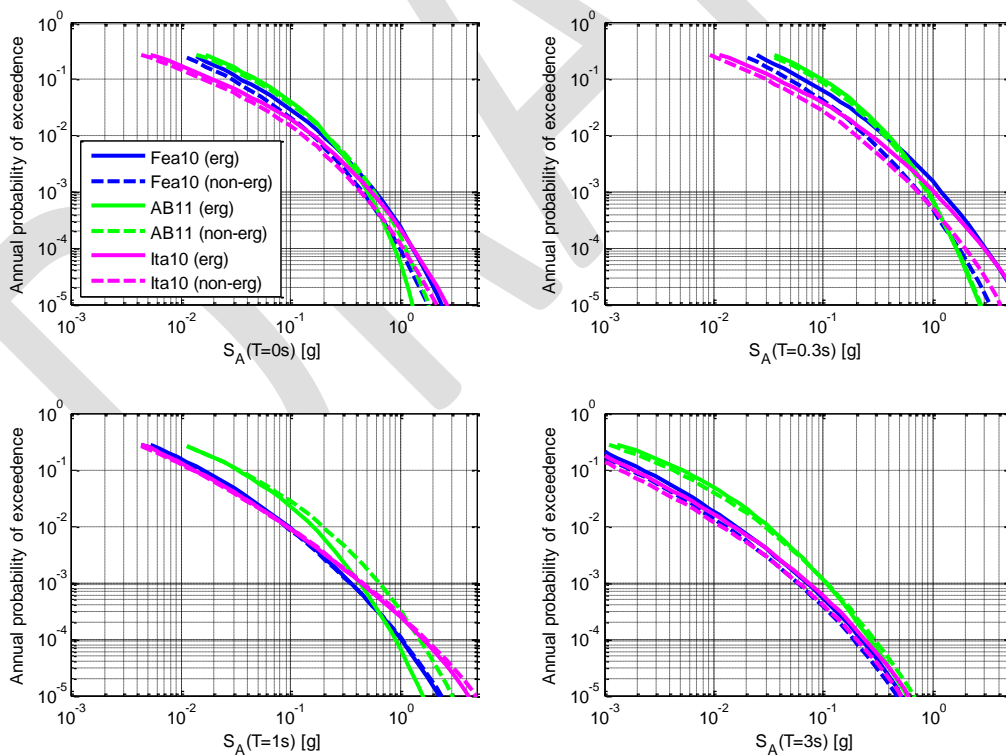


Figure 42 – NVL site. Exceedance curves for HAZGRID model with different GMPEs, corrected or not with the non-ergodic coefficients.

CONFIDENTIAL

Restricted to SIGMA scientific partners and members of the consortium,  
please do not pass around

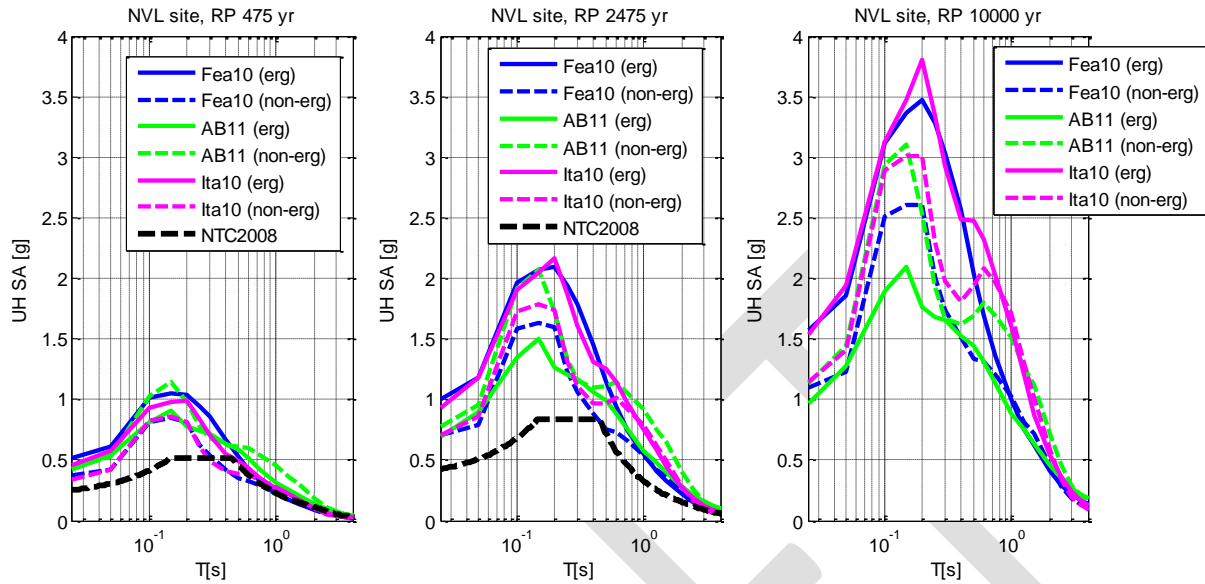



Figure 43 – NVL site. UHS for HAZGRID model with different GMPEs, corrected or not with the non-ergodic coefficients.

	<p>Research and Development Programme on Seismic Ground Motion</p> <p>CONFIDENTIAL</p> <p><i>Restricted to SIGMA scientific partners and members of the consortium, please do not pass around</i></p>	<p>Ref : SIGMA-2013-D4-94 Version : 01</p> <p>Date : October 2013 Page :</p>
--	---	--

## 8. Logic tree

Figure 44 shows the logic tree scheme adopted in Phase II work.

The ‘AS’, or SSZ, branch refers to the source model developed in Phase I, with 12 ASs (derived with some changes from ZS9) and a deeper ‘slab’ source. For the depth distribution of the ASs, we herein consider only the ‘coarse model’ defined in Phase I, having typically 3 values of effective depth, carefully chosen from depth distribution analyses of the events in the working catalogue.

Selection of GMPEs has been discussed in Sect. 4. As mentioned, for single-station (non-ergodic) analyses, the same site correction factors and single-site sigma have been used for all GMPEs. These factors have been estimated by the INGV Milano Sigma working group, by computing residuals with ITA13 GMPE, for CAS and NVL among many other sites. For the TRT site not enough records were available for a reliable analysis. Since we rely on the more sophisticated, site specific, single station analyses we assigned a higher weight to the non-ergodic branches.

Concerning GMPEs weights, as ITA13 and its earlier version ITA10 are insufficiently constrained by data at the higher magnitude levels of our analyses ( $M > 6.5$ ), we assigned a lower weight to respective branches.

As to the weights assigned to the different earthquake source model branches, we relied on the very recent results of the statistical performance of several hazard models for Italy tested vs. strong motion observations (<https://sites.google.com/site/ingvdpc2012progettos2/home>), with the highest scores gained by the same type gridded seismicity model used herein. For AS and FS+BG models, the results of separate analyses did not give us any reason to assign different weights, as shown in Sect. 6.5.

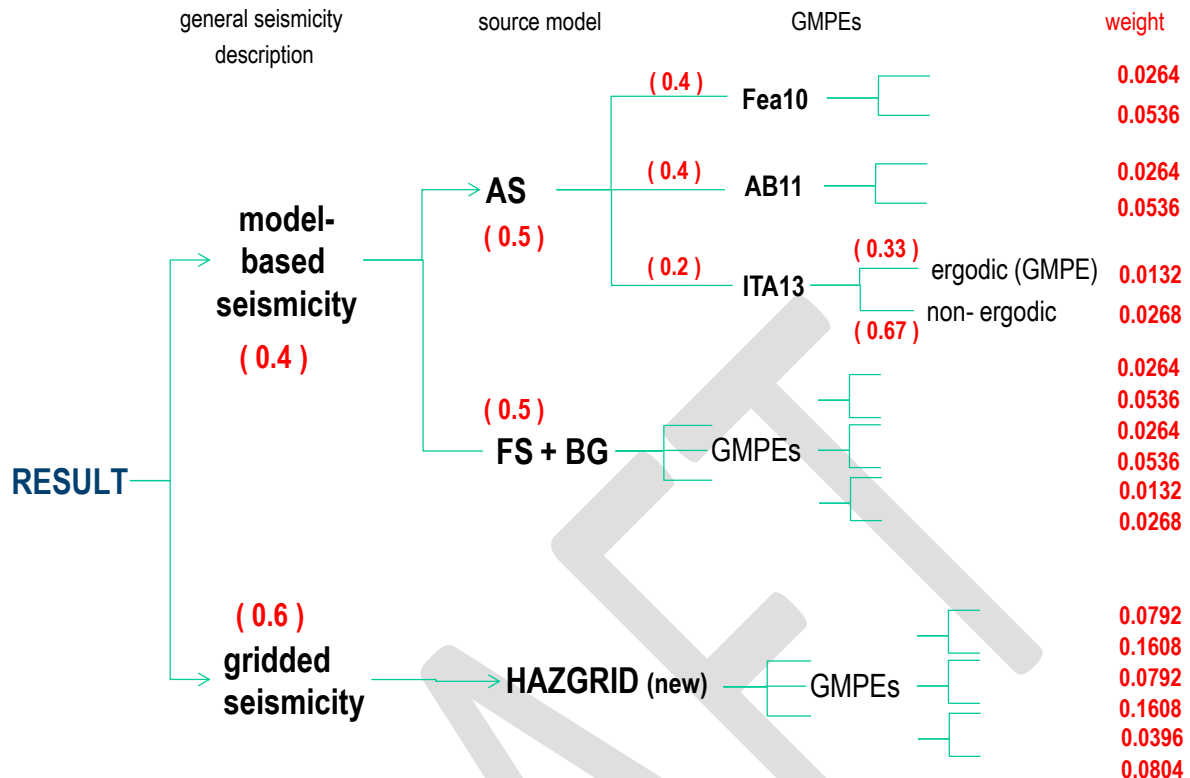



Figure 44 – Logic tree envisaged for ground types C and A. In red are the values of weights assigned in this phase to each branch. “Non-ergodic” means single-station sigma analysis.

Actually, 3 different LTs were needed to evaluate site specific hazard in Phase II:

- one LT with ground category B characteristics for the single Tortona (TRT) site, containing in the terminal branches only the ergodic options,
- a second LT with ground category C characteristics for the Novellara (NVL) site, and Casaglia (CAS = T821, named after the INGV temporary accelerometric station) site, containing in the terminal branches both the non-ergodic and the ergodic options, with their respective coefficients.
- a third LT with ground category A characteristics for all the three sites, containing in the terminal branches both the non-ergodic and the ergodic options, where the non-ergodic coefficients have been estimated from ground A stations nearest to the Po Plain area.

The LT with ground category A characteristics was also needed to introduce, in the following step, site effects in a different way, combining PSHA results on rock with site specific amplification functions whose evaluation may be empirical or analytical, as extensively explained in Deliverable D3-96 by this working group.



	<p>Research and Development Programme on Seismic Ground Motion</p> <p>CONFIDENTIAL</p> <p><i>Restricted to SIGMA scientific partners and members of the consortium, please do not pass around</i></p>	<p>Ref : SIGMA-2013-D4-94 Version : 01</p> <hr/> <p>Date : October 2013 Page :</p>
--	---	--

In the next section, we will show a first application of such approaches, using a branch of the LT on ground type A soil, for CAS site, for a return period of 2475 years.

We have also considered alternative assumptions on the weights, as follows.

- 1) Invert the weight values between ergodic and non-ergodic for NVL site, when the AB11 GMPE is used because the latter is heavily penalized in the non-ergodic case due to the fact that its sigma is substantially lower than that of the other two GMPEs. This change is not applied to the CAS site because its  $\sigma_{s,s}$  is comparable to that of the AB11 GMPE.
- 2) Invert the weight values between Fea10 and Ita13 GMPEs, based on the consideration that the C/A spectral amplification factor of the former are higher and shifted towards the low period range with respect to the latter.

It will be seen in Sect. 11, that the final logic tree results are only slightly affected by the foregoing changes.

Final results of LT computations will be actually delivered for three different return periods: 475, 2475 and 10.000 years.

Application of site specific approaches in PSHA will be performed using LT of ground type A and site amplification functions derived from a 10.000 years return period, using the AS non-ergodic branches of Fea10 and AB11. The Ita13 and Ita10 GMPEs are in fact not suited for use at such low exceedance probabilities, as already explained.

## 9. Accounting for site effects

Table 5 recalls the classes of approaches discussed in Deliverable D3-96 to account for site effects in the framework of a PSHA, considering both a “regional” (generic) and a “local” (site-specific) scale. We illustrate herein the use of these approaches, for a specific branch of our logic tree (AS, with FEA10 modified GMPE), for one site (CAS), and for one return period RP (2475 yr).

Actually, another approach may be included in the ‘Fully probabilistic’ classes, i. e. the PSHA at a site with the single station sigma application, as discussed in Sect. 5.

Table 5 - Classes of approaches to account for site effects in PSHA. SAF = site amplification function.

Hybrid probabilistic/deterministic		Fully probabilistic		
Generic site (HyG)	Site-specific (HyS)	Generic site (FpG)	Site-specific (FpS)	
PSHA at rock + SAF based on seismic norms	PSHA at rock + SAF based on 1D analyses	PSHA based on GMPE with site correction factor	PSHA at rock + convolution with SAF conditioned to rock ground motion	PSHA at site with single-station sigma applied

Figure 45 compares, for CAS, site specific PSHA results in terms of UH acceleration spectra, from the following approaches:

- the standard GMPE use (FpG approach), blue curve
- the single site sigma approach, green curve
- PSHA on ground A combined with different SAFs based on 1D analyses (HyS approach), red solid curves.

The SAF (site amplification function) has been estimated in different ways, extensively discussed in Deliverable D3-96. First, a selection of records compatible with the UH spectra on ground type A (dashed red curve in Figure 45) has been sought, then these records have been used as exposed bedrock input motion for 1D equivalent linear analyses on a specific soil profile selected for the CAS site (see also the D3-96), computing the surface ground motion on the top of the soil profile. Response spectral ratios have been then used to computed SAF at selected periods. The same set of recorded acceleration waveforms have been used in two different ways: uncorrected (‘SAF’ in the figure) and corrected (‘SAF corr’ in the figure) so as to achieve a close matching with the target spectrum.

Note from Figure 45 that the correction of the input signals for spectral matching does not affect values beyond 0.2 s, where a close agreement with the NTC2008 code is attained (in-between ergodic and non-ergodic results).

For  $T < 0.2$  s, on the other hand, the input correction slightly affects the results; in particular, the PGA value of the spectrum with the matched selection falls exactly on the rock curve. More significant, however, is that the use of both SAFs leads to decreasing the values of the site specific spectra below the bedrock values at periods  $0 < T < 0.2$  s, mostly due to non-linear effects. Also worth noting is that the non-ergodic PSHA spectrum from the GMPE (green curve) is not far from the “rock\*SAF” spectra, and hardly exceeds the input rock spectrum for  $T > 0.2$  s.

On the whole, the CAS example strongly indicates that the uncertainty associated to the soil surface spectra decreases significantly when using results from local site analyses (such as SAFs or single site coefficients and sigmas) instead of the site coefficient of the GMPEs.

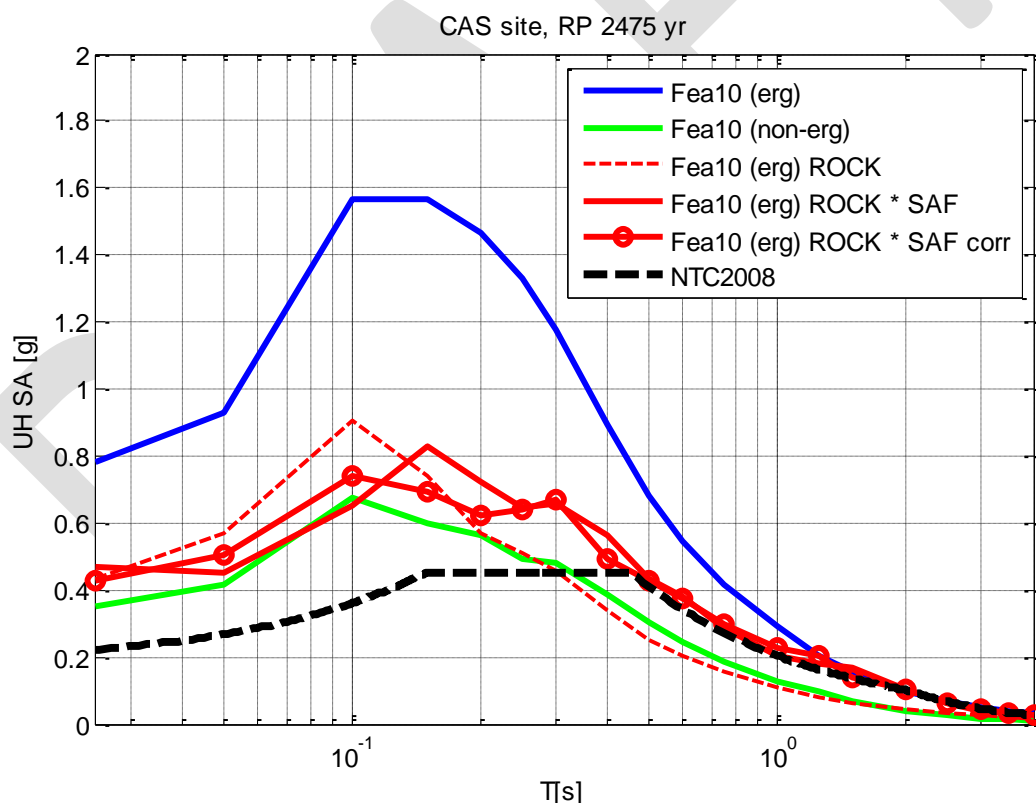


Figure 45 – CAS site. Site specific PSHA from different approaches.

## 10. Results of logic tree for ground type A

The results of the LT calculations on ground type A are displayed in Figure 46, Figure 47 and Figure 48 as percentile-level exceedance curves, and in Figure 49, Figure 50 and Figure 51 as UH spectra, with the respective Italian seismic code (NTC2008) spectra, where available.

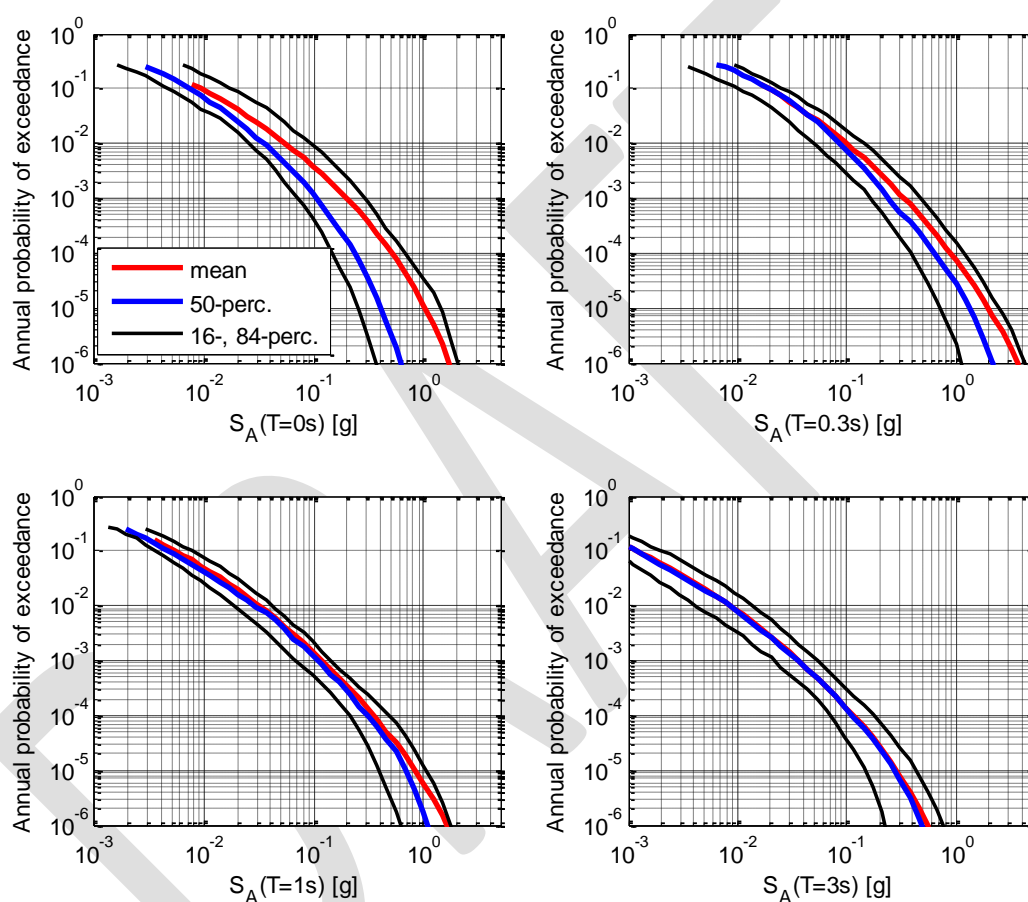


Figure 46 – NVL site, ground type A: exceedance curves of acceleration response spectrum ordinates at 0.05 damping for periods T = 0-0.3-1 and 3 s for the logic tree of Figure 44.

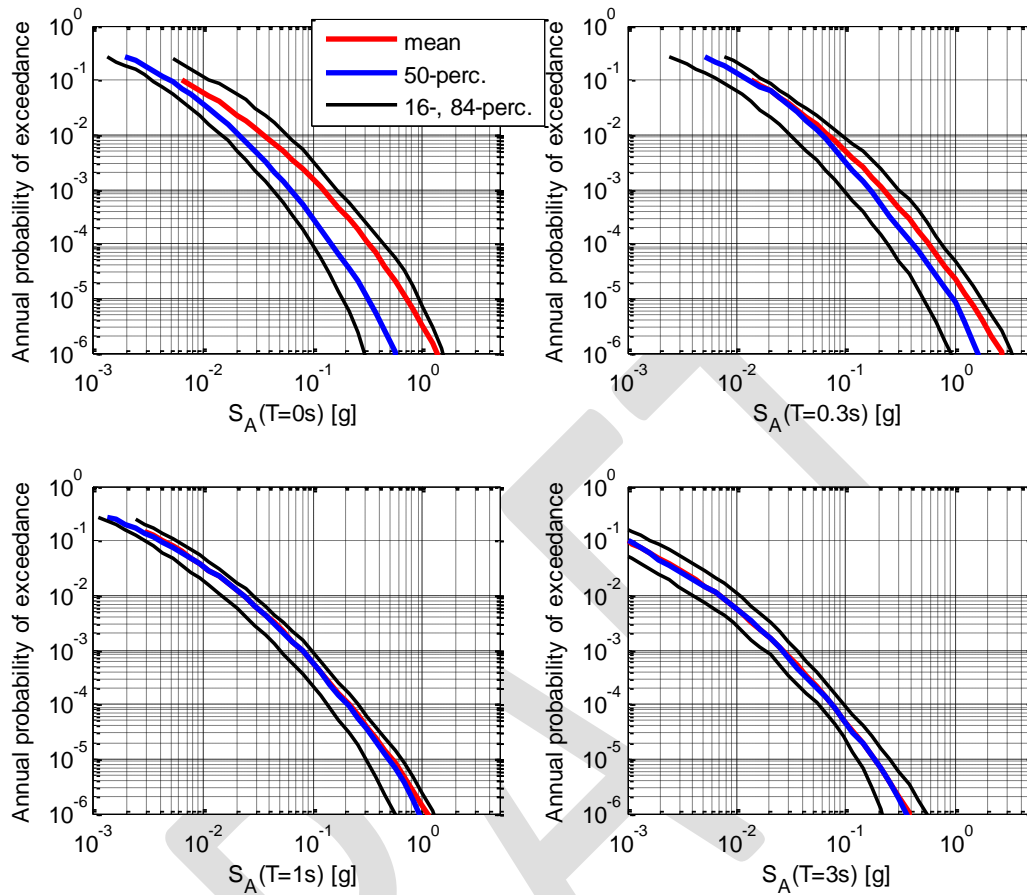


Figure 47 – CAS site, ground type A: exceedance curves of acceleration response spectrum ordinates at 0.05 damping for periods  $T = 0-0.3-1$  and  $3$  s for the logic tree of Figure 44.

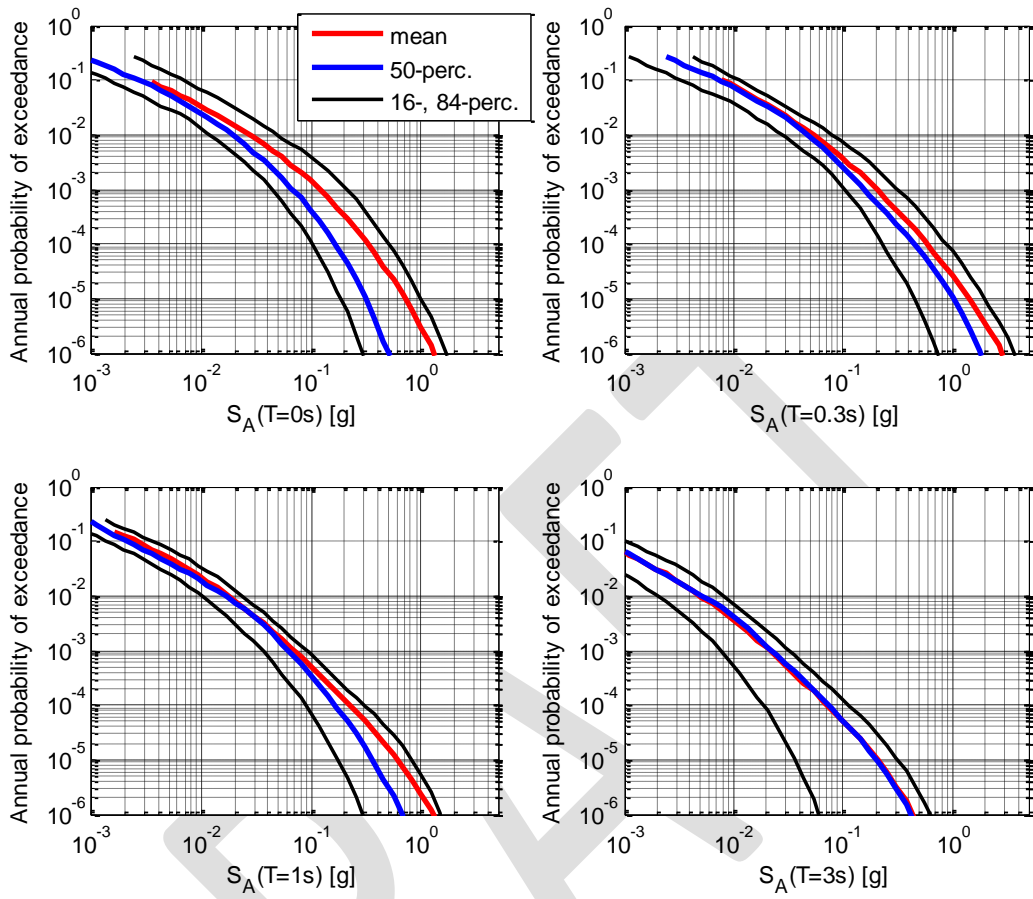


Figure 48 – TRT site, ground type A: exceedance curves of acceleration response spectrum ordinates at 0.05 damping for periods  $T = 0-0.3-1$  and  $3$  s for the logic tree of Figure 44.

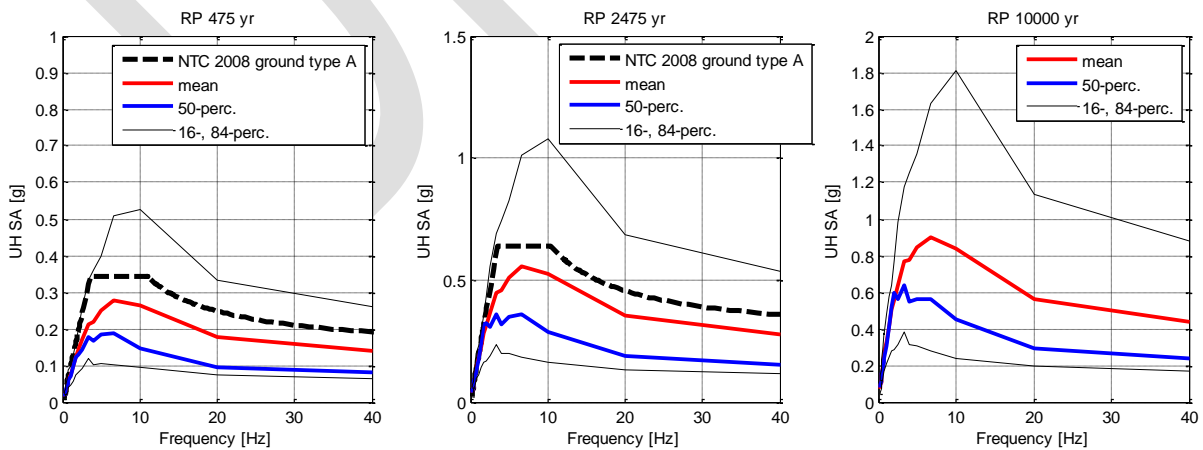


Figure 49 – NVL site (ground type A): Uniform Hazard acceleration spectra at return periods of 475, 2475 and 10000 years. NTC 2008 spectra are also shown where available.



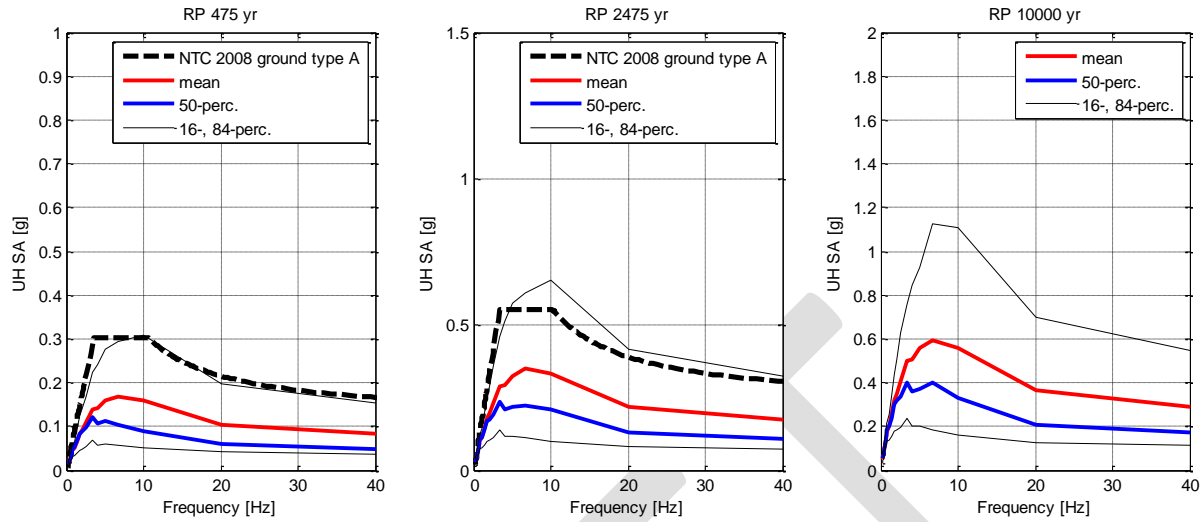


Figure 50 – CAS site (ground type A): Uniform Hazard acceleration spectra at return periods of 475, 2475 and 10000 years. NTC 2008 spectra are also shown where available.

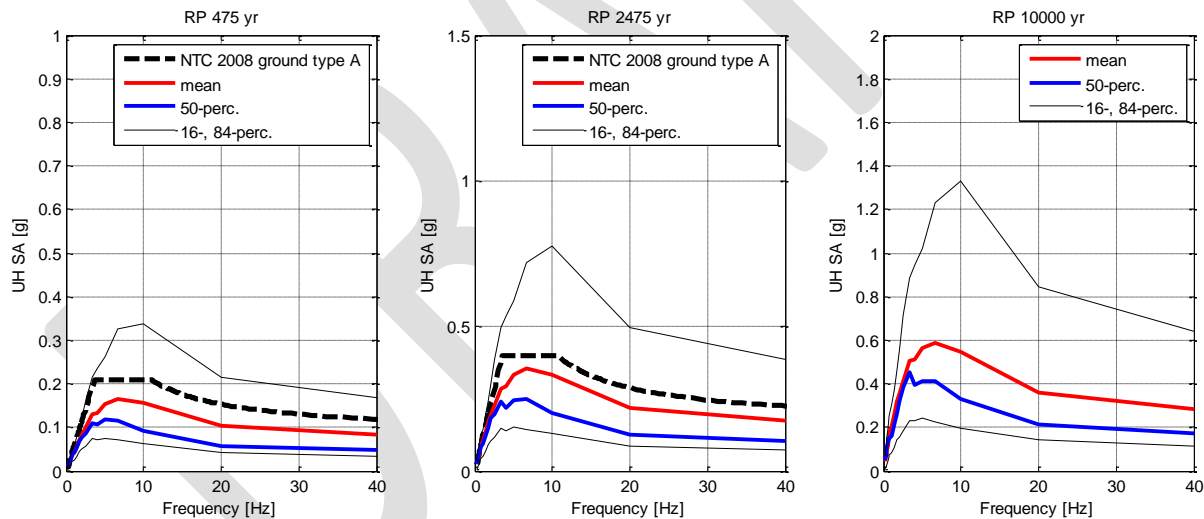


Figure 51 – TRT site (ground type A): Uniform Hazard acceleration spectra at return periods of 475, 2475 and 10000 years. NTC 2008 spectra are also shown where available.

The PSHAs on ground type A at the three sites indicate that:

- the exceedance curves exhibit a trend of decreasing variability with structural period, from 0 s (where it is generally highest) to 1.0 s, for all three sites; beyond 1 s, TRT shows an increase while the other sites do not;
- the NTC 2008 code spectra for 475 and 2475 return period lie in the 15- to 81-percentile prediction band, but always above the present mean spectrum;
- at 10 000 years RP the peak of mean spectrum reaches about 0.9 g at NVL, while it does not exceed 0.6 g at the other two sites;
- the comparison of the present results with those of Phase I shows that the latter, in terms of mean response spectra, were considerably more conservative, as shown in Figure 52, Figure 53, and Figure 54 for NVL, CAS, and TRT, for all return periods.

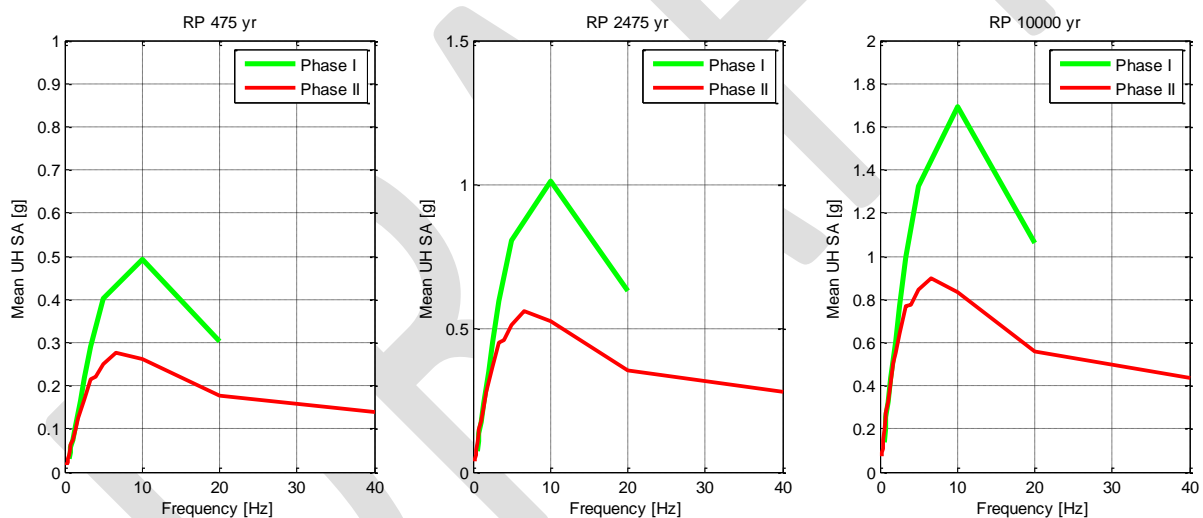


Figure 52 – NVL site. Comparison between Phase I and Phase II mean UH spectra.

CONFIDENTIAL

Restricted to SIGMA scientific partners and members of the consortium,  
please do not pass around

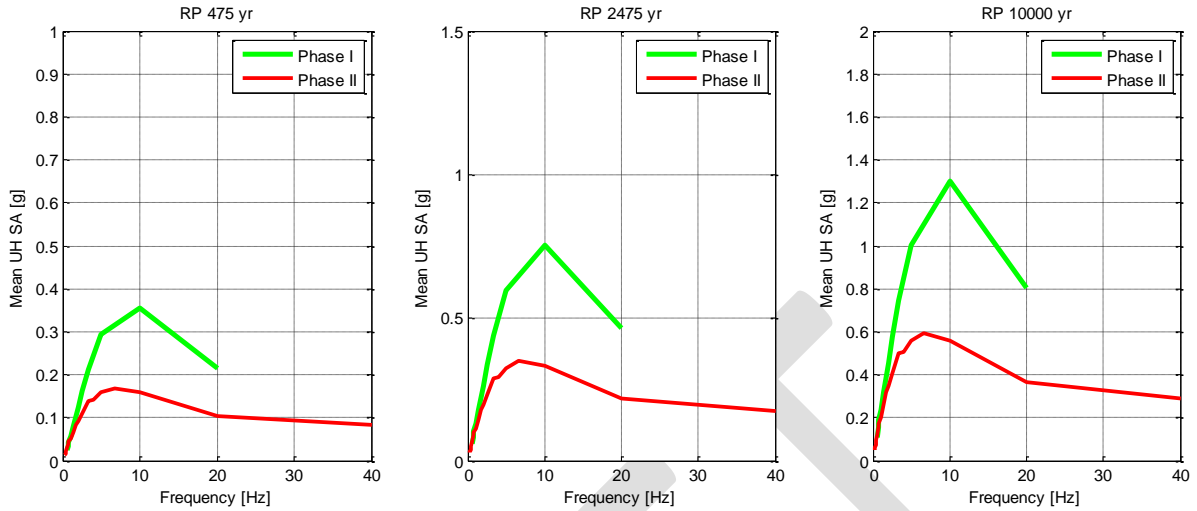


Figure 53 – CAS site. Comparison between Phase I and Phase II mean UH spectra.

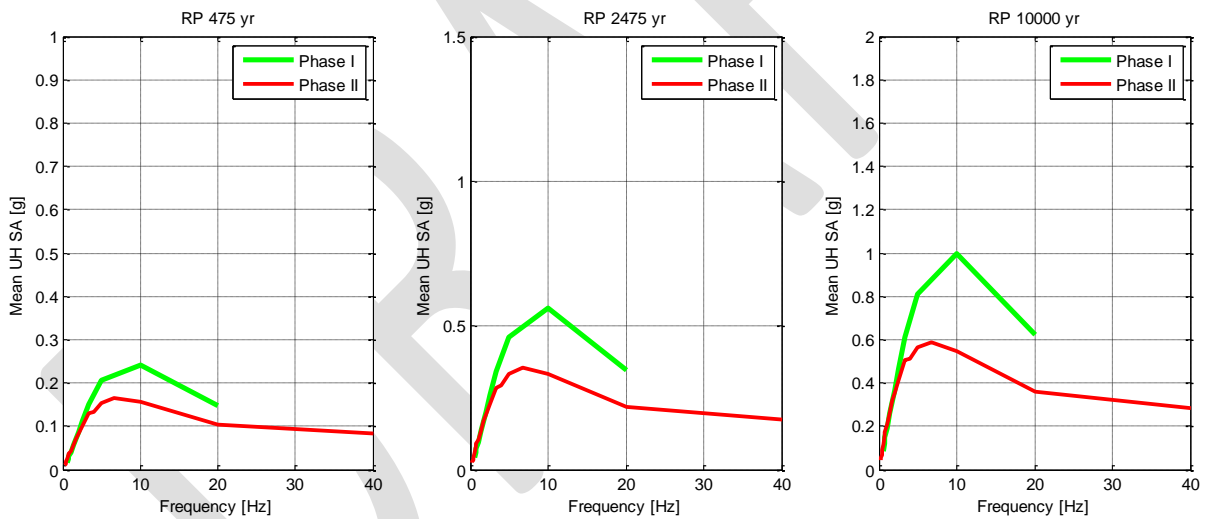


Figure 54 – TRT site. Comparison between Phase I and Phase II mean UH spectra.

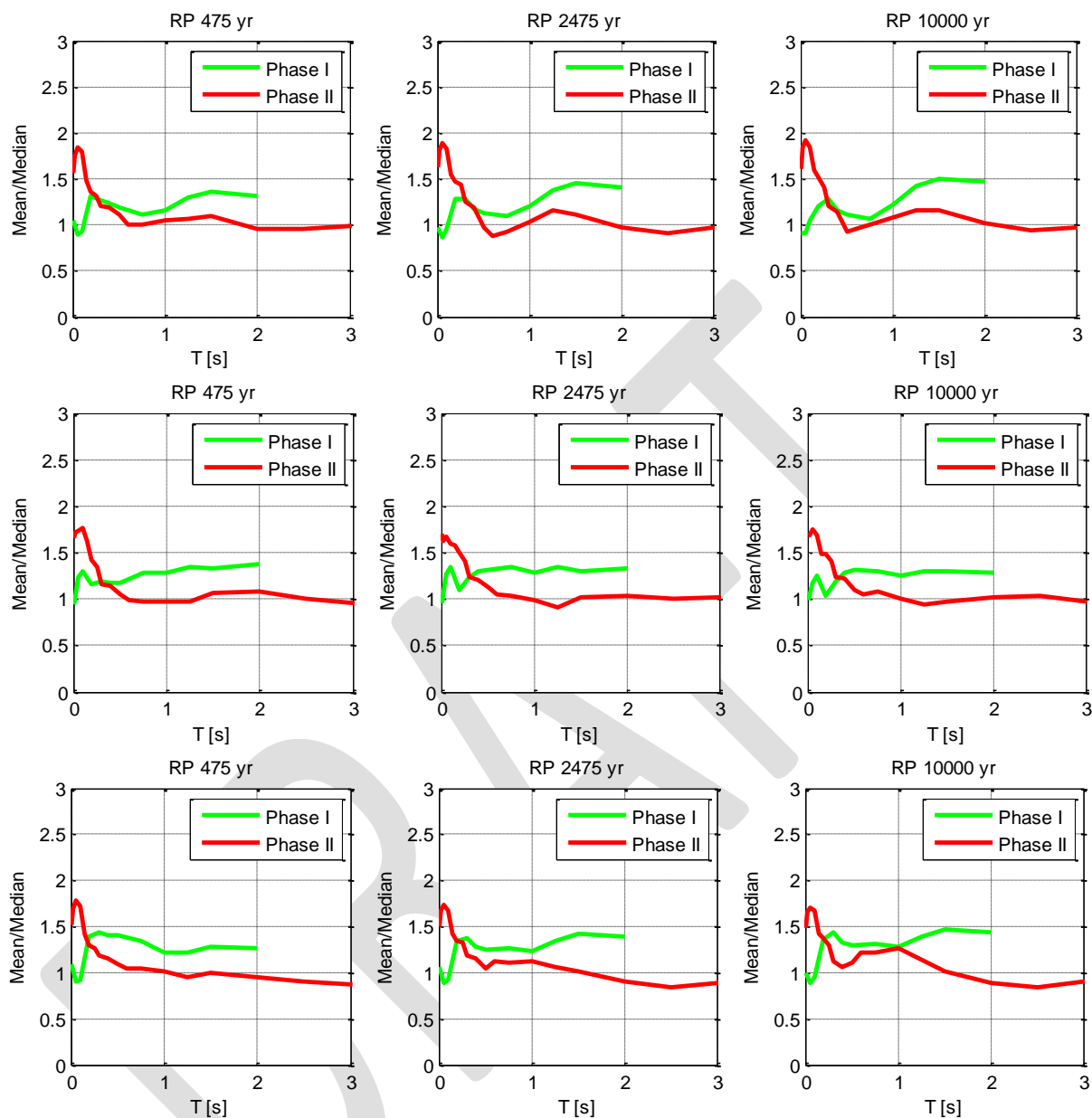



Figure 55 – Comparison between Phase I and Phase II statistical measures of LT spreads, represented by the mean/median ratios of response spectrum ordinates, for NVL (top row), CAS (middle row), and TRT (bottom row), at the three indicated return periods (RP).

As regard the variability affecting the present Phase 2 hazard estimates, a representation of it is proposed in Figure 55 and compared with that associated to the Phase I results. As a measure of such variability, we have used the mean/median ratio of the estimates of UH spectrum ordinates as a function of structural period and RP. While the significance of these results is briefly commented also in the following Conclusions, we note here that the ratio in question would equal  $\exp(\sigma_{\ln}^2/2)$  if the output of the LT branches were lognormally

	<p style="text-align: center;">Research and Development Programme on Seismic Ground Motion</p> <p style="text-align: center;">CONFIDENTIAL</p> <p style="text-align: center;"><i>Restricted to SIGMA scientific partners and members of the consortium, please do not pass around</i></p>	<p>Ref : SIGMA-2013-D4-94 Version : 01</p> <hr/> <p>Date : October 2013 Page :</p>
--	---	--

distributed: in this case the ratio would be directly related to  $\sigma_{lnY}^2$ . On the other hand, a mean/median ratio tending to one obviously indicates that the distribution becomes symmetrical and could be assimilated to a normal one.

DRAFT

## 11. Results of logic tree for ground type C and B

The results of the LT calculations for each studied site are displayed in Figure 56, Figure 57 and Figure 58 as percentile-level exceedance curves, and in Figure 59, Figure 60 and Figure 61 as UH spectra, with the respective Italian seismic code (NTC2008) spectra, where available.

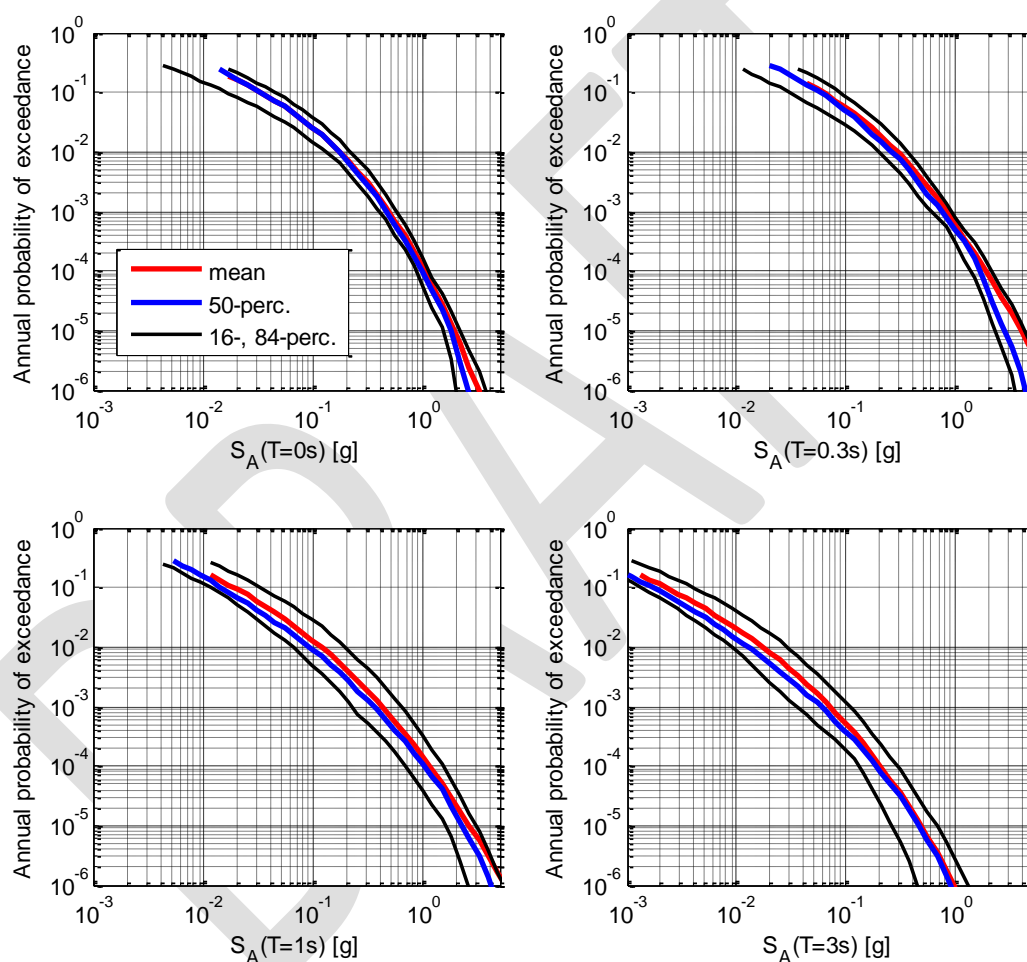


Figure 56 – NVL site, ground type C: exceedance curves of acceleration response spectrum ordinates at 0.05 damping for periods T = 0-0.3-1 and 3 s for the logic tree of Figure 44.



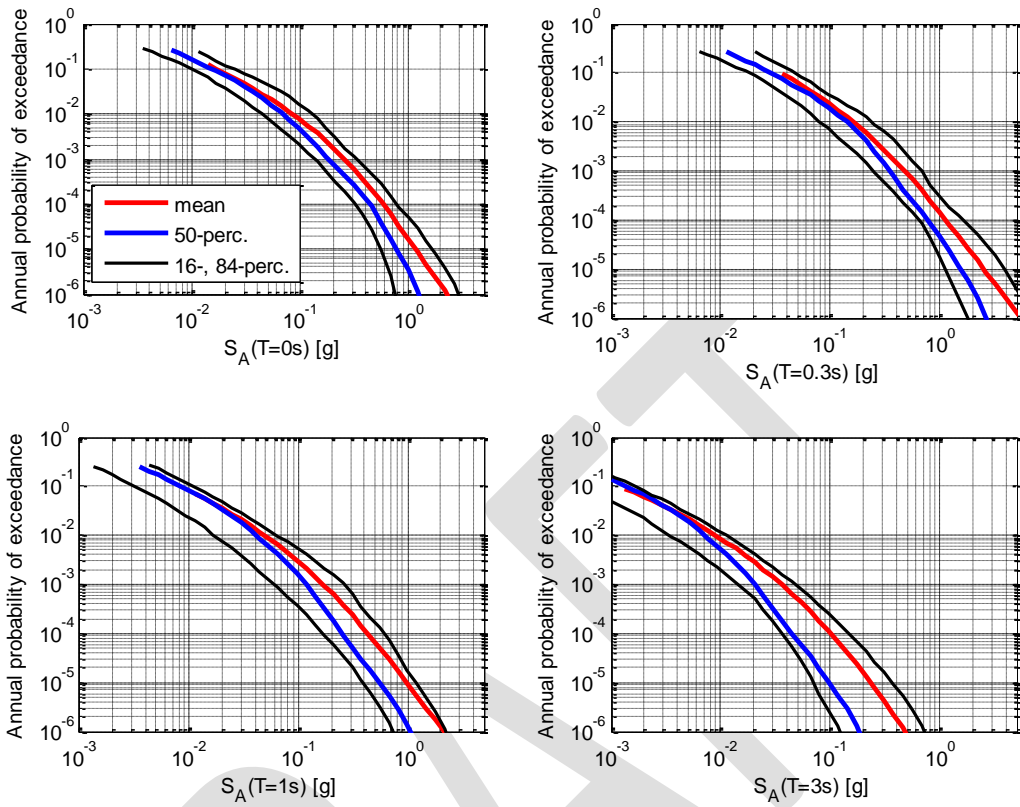


Figure 57 – CAS site, ground type C: exceedance curves of acceleration response spectrum ordinates at 0.05 damping for periods  $T = 0-0.3-1$  and  $3$  s for the logic tree of Figure 44.

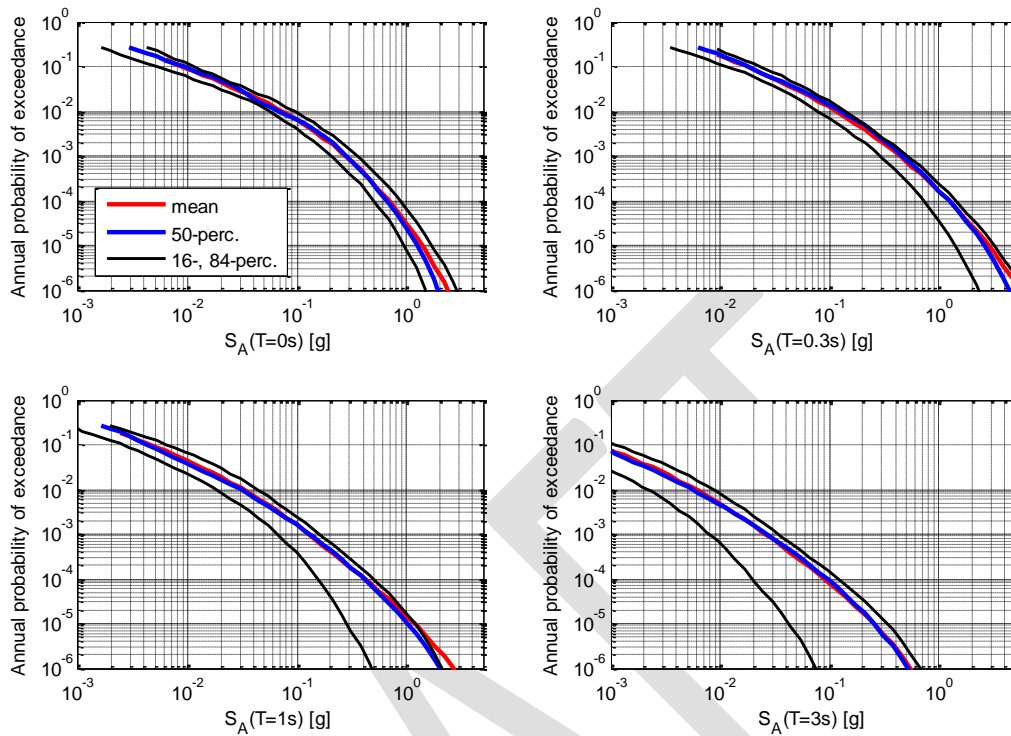


Figure 58 – TRT site, ground type B: exceedance curves of acceleration response spectrum ordinates at 0.05 damping for periods  $T = 0-0.3-1$  and  $3$  s for the logic tree of Figure 44.

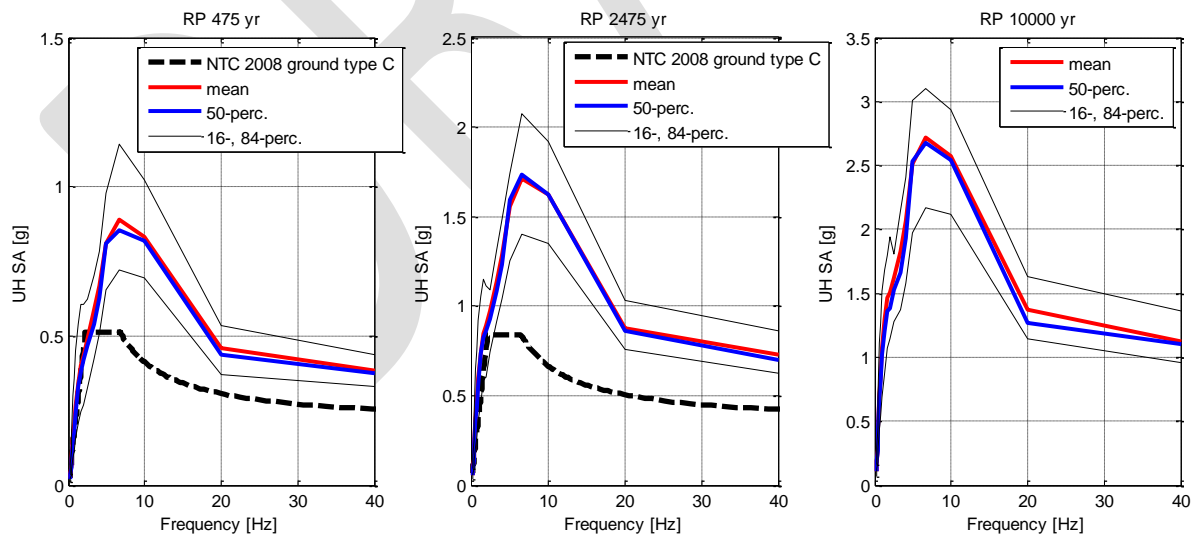


Figure 59 – NVL site (ground type C): Uniform Hazard acceleration spectra at return periods of 475, 2475 and 10000 years. NTC 2008 spectra are also shown where available.

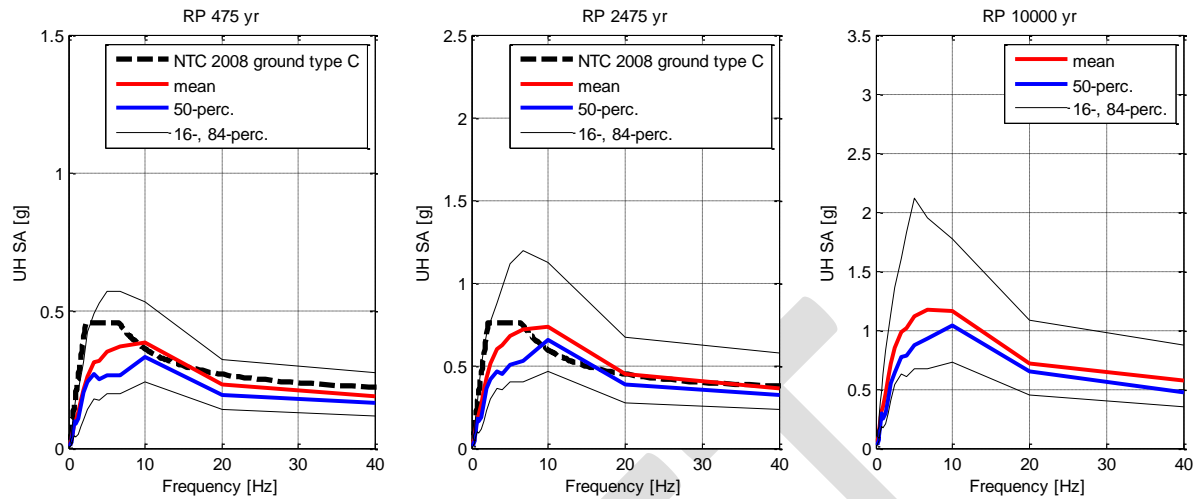


Figure 60 – CAS site (ground type C): Uniform Hazard acceleration spectra at return periods of 475, 2475 and 10000 years. NTC 2008 spectra are also shown where available.

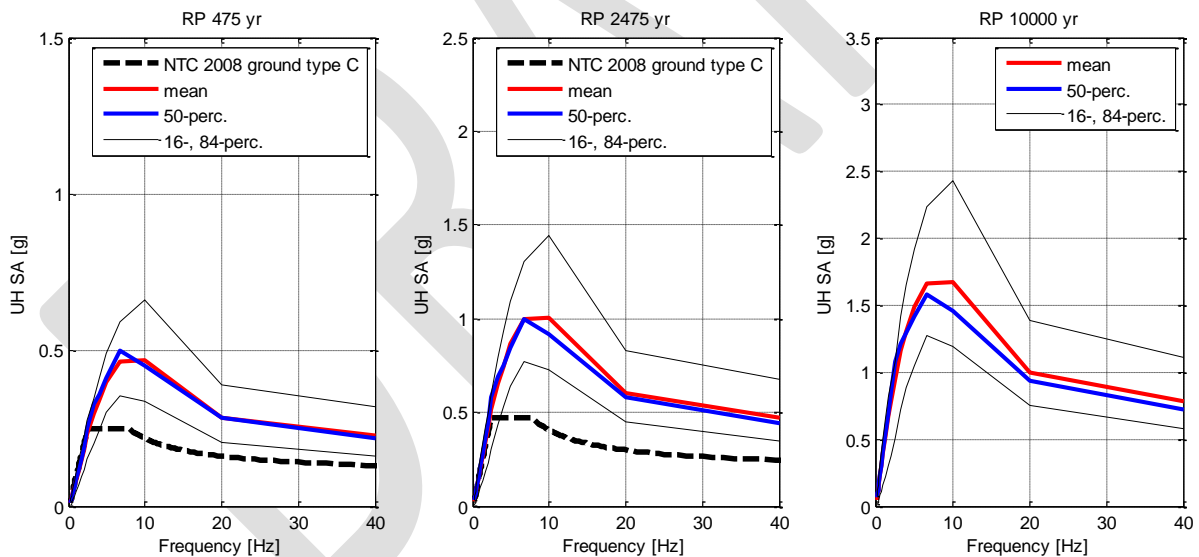


Figure 61 – TRT site (ground type B): Uniform Hazard acceleration spectra at return periods of 475, 2475 and 10000 years. NTC 2008 spectra are also shown where available.

The PSHAs on ground type C at the three sites indicate that:

- The exceedance curves exhibit a trend of increasing variability with structural period, from 0 s (where it is generally lower) to 3.0 s, for all three sites.
- The NTC 2008 code spectra for 475 and 2475 return period lie in the 15- to 81-percentile prediction band only for CAS site, for which mean values are comparable to code prescriptions; for the other two sites, results are quite above code spectra for all return periods.
- At 10 000 years RP the peak of mean spectra reaches about 2.6 g at NVL, 1.6 at TRT, and 1.2 at CAS site.
- The comparison of the present results with those of Phase I show different features depending on the site at study. For NVL, quite similar spectra are achieved, for CAS, the non-ergodic use of GMPEs decreases significantly the spectra amplitudes, while for TRT slightly more conservative spectra are achieved (shown in Figure 62, Figure 63 and Figure 64 for NVL, CAS, and TRT, respectively).

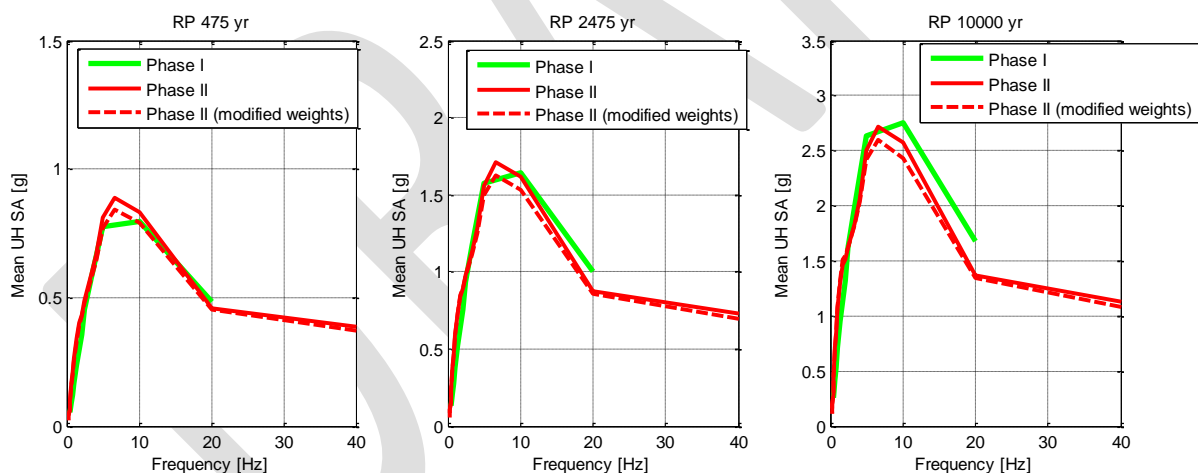


Figure 62 – NVL site. Comparison between Phase I and Phase II mean UH spectra. Shown in red dashed curves are the Phase II results obtained by introducing the two combined alternative assumptions on LT weights discussed at the end of Sect. 8.

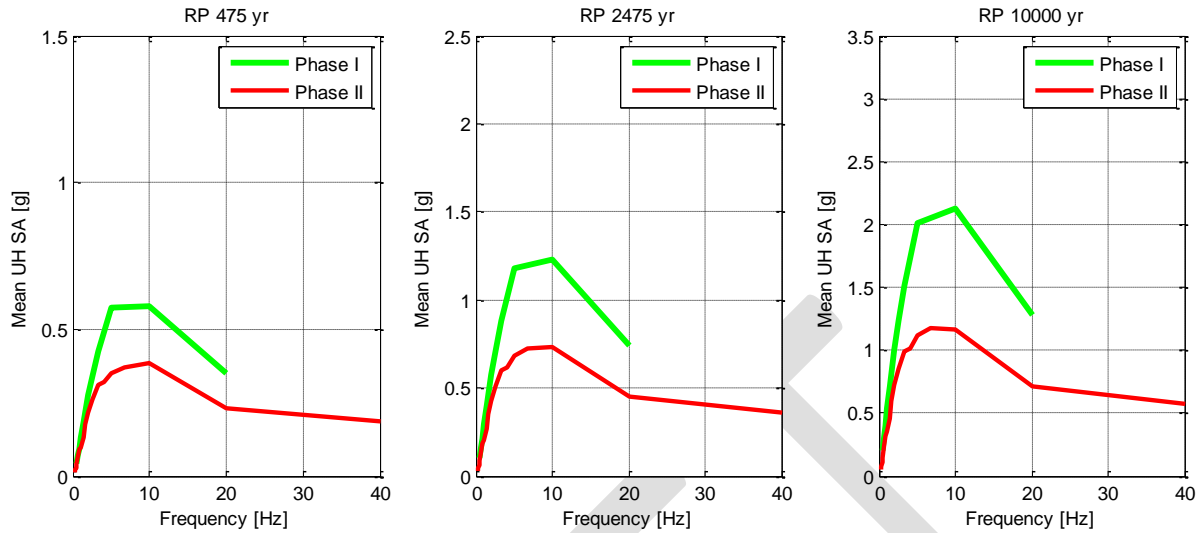


Figure 63 – CAS site. Comparison between Phase I and Phase II mean UH spectra.

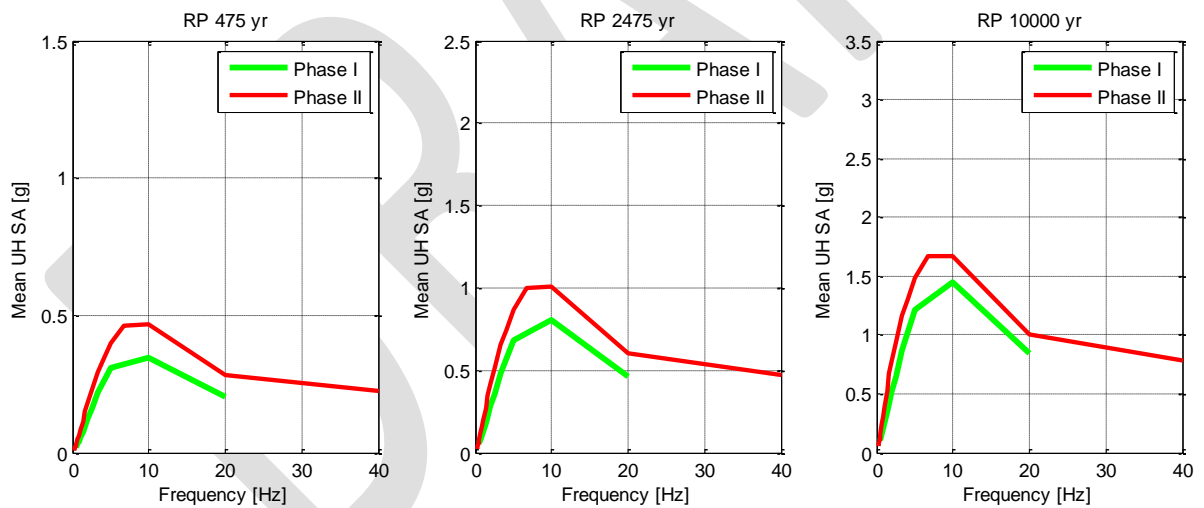


Figure 64 – TRT site. Comparison between Phase I and Phase II mean UH spectra

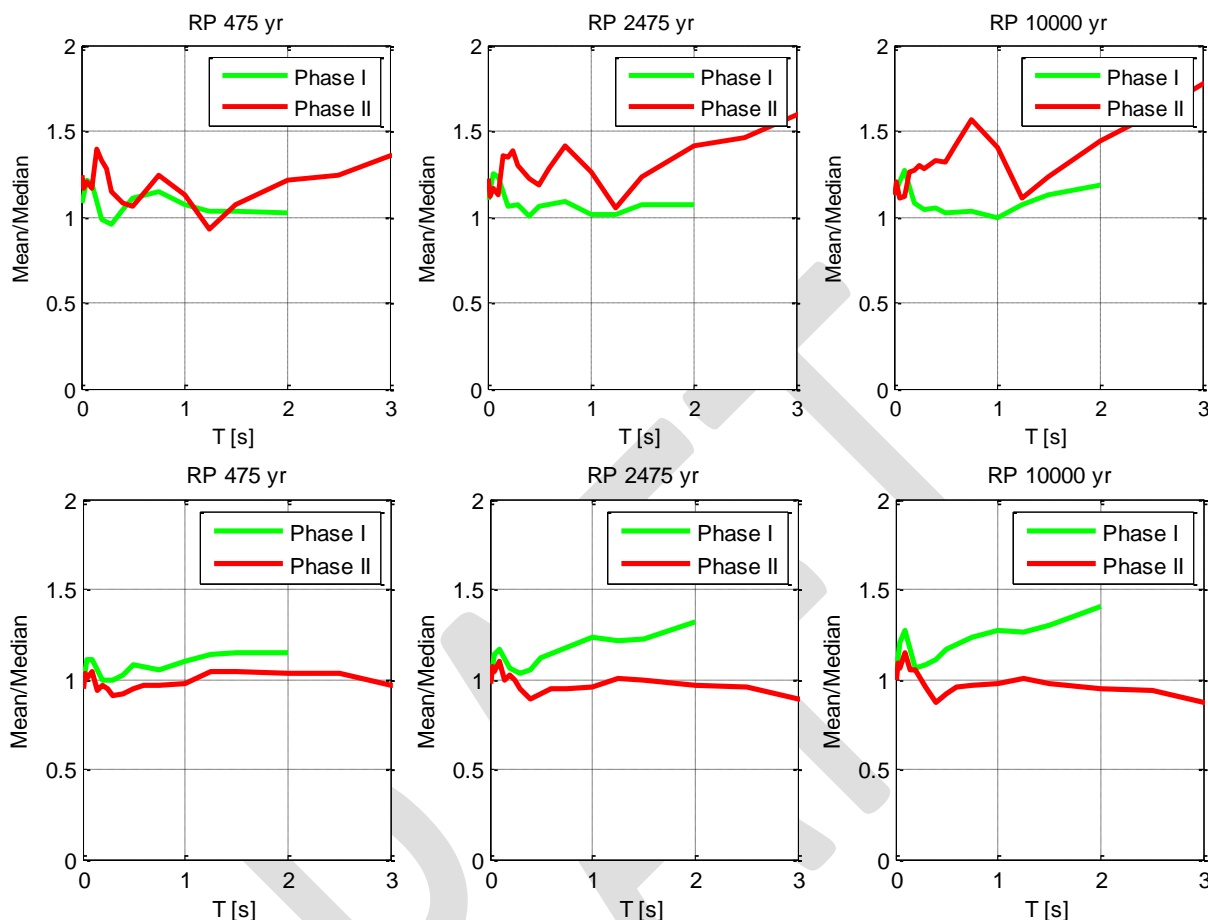



Figure 65 – Comparison between Phase I and Phase II statistical measures of LT spreads, represented by the mean/median ratios of response spectrum ordinates, for NVL (top row), CAS (middle row), and TRT (bottom row), at the three indicated return periods (RP).

As regard the variability affecting the present Phase 2 hazard estimates, a representation of it is proposed in Figure 65, in terms of mean/median ratios, and compared with that associated to the Phase I results. Results are quite site dependent: while for NVL and TRT the ratio is about 1 at all periods, for CAS this is significantly different and always above 1. These curves show that the variability of results in this Phase 2 tend to be generally lower for NVL and TRT, but not for CAS site.



	<p>Research and Development Programme on Seismic Ground Motion</p> <p>CONFIDENTIAL</p> <p><i>Restricted to SIGMA scientific partners and members of the consortium, please do not pass around</i></p>	<p>Ref : SIGMA-2013-D4-94 Version : 01</p> <p>Date : October 2013 Page :</p>
--	---	--

## 12. Conclusions (tentative)

The work documented in this Deliverable is intended as an update and extension of the previous year's work (2012, Sigma Phase I).

Herein, we have dealt with a few tasks that were just outlined in Phase I, and deemed to deserve further consideration in the following phase. These tasks concerned:

- the updating of the earthquake catalogue and of magnitude conversion relationships;
- the use of the single station sigma approach to account for local variability of site response in PSHA;
- the use of a fault (+ background) model;
- the updating of the GMPEs and of the gridded seismicity model of the logic tree;
- the use of different approaches to account for site effects in PSHA, relying on the conceptual background provided


Concerning the influence of the catalogue and conversion relations, we decided to introduce a few changes with respect to Phase I work, which led us to increase the minimum magnitude considered in the estimation of seismicity parameters and hazard analyses. These changes have been shown to lead to slightly more conservative hazard evaluations.

The use of the so-called single station sigma, or non ergodic, approach has been shown to affect the hazard estimates in different ways, depending on how the site correction terms and the single site sigmas combine with the standard deviations of the GMPEs at use. We found that the overall effect of this approach has been to decrease substantially the severity of hazard estimations at one of the test sites (CAS).

The introduction of a fault-based model, based on the latest updates of the Composite Seismogenic Sources of the DISS3 database in the Po plain region, allowed us to test different ways of treating fault rupture and integration when a characteristic earthquake representation is of concern. We considered this representation in the perspective of a time-independent process (as for all the LT branches), fulfilling a specific request of the SC. The results of the fault + background modeling turned out to be in close agreement with those yielded by the AS branches of the LT, for two of our test sites.

The final results from the LT analyses for ground type C, B and A conditions, for the sites of interest (the same as in Phase I), show for the 10,000 years RP a decrease in mean hazard level with respect to Phase I, with the largest reductions obtained for ground type A, while for ground type C the reduction is substantial only at CAS. There is no reduction for TRT.

As regards the extent of the associated uncertainty, Figure 55 suggests some increase at short periods ( $T < 0.2$  s) on ground type A, but a significant decrease at larger periods. On ground types B and C similar considerations apply, except at CAS where the variability in Phase II


	<p>Research and Development Programme on Seismic Ground Motion</p> <p>CONFIDENTIAL</p> <p><i>Restricted to SIGMA scientific partners and members of the consortium, please do not pass around</i></p>	<p>Ref : SIGMA-2013-D4-94 Version : 01</p> <hr/> <p>Date : October 2013 Page :</p>
--	---	--

increases. This aspect is now being explored. We interpret the fact that the mean/median ratio tends to 1 at periods > about 0.5 s as an indication that the LT has a good structure and weight distribution, apt to reduce the influence of outliers from individual branches.

Special care has finally been devoted to the use and comparison of different approaches to account for site effects in PSHA. This task has not been completed yet; more advanced results will be shown and discussed at the next SC meeting (Lyon, 13-15 November 2013), fully exploiting the output of the closely related Deliverable D3-96 and the final version of the present Deliverable will be released after the meeting.


The indications from the present results, illustrated in Sect. 9, are that application of the site specific approach (PSHA at rock plus SAF based on 1D analyses) will be far more effective than the fully probabilistic approaches for reducing the level of the hazard estimation (where data-based non ergodic analyses are not feasible).

DRAFT


	<p>Research and Development Programme on Seismic Ground Motion</p> <p>CONFIDENTIAL</p> <p><i>Restricted to SIGMA scientific partners and members of the consortium, please do not pass around</i></p>	<p>Ref : SIGMA-2013-D4-94 Version : 01</p> <p>Date : October 2013 Page :</p>
--	---	--

### 13. References


- Akinci, A. (2010). HAZGRIDX: earthquake forecasting model for  $ML \geq 5.0$  earthquakes in Italy based on spatially smoothed seismicity. ANNALS OF GEOPHYSICS, 53, 3, 2010; doi: 10.4401/ag-4811
- Akkar, S. and Bommer, J., 2010. Empirical Equations for the Prediction of PGA, PGV, and Spectral Accelerations in Europe, the Mediterranean Region, and the Middle East. Seismological Research Letters, Vol. 81, No. 2 pp. 195--206.
- Atkinson G. and D Boore (2011). Modifications to Existing Ground-Motion Prediction Equations in Light of New Data, Bulletin of the Seismological Society of America, Vol. 101, 1121–1135.
- Atzori S., Merryman Boncori J., Pezzo G., Tolomeri C., Salvi S. (2012). Secondo Report analisi dati SAR e modellazione della sorgente del terremoto dell'Emilia. INGV (in Italian).
- Basili R, Kastelic V, Valensise G, DISS Working Group 2009 (2009) DISS3 tutorial series: Guidelines for compiling records of the Database of Individual Seismogenic Sources, version 3. Rapp Tecn INGV 108:20 (<http://istituto.ingv.it/1-ingv/produzione-scientifica/rapporti-tecnici-ingv/archivio/rapporti-tecnici-2009/>).
- Basili R, Valensise G, Vannoli P, Burrato P, Fracassi U, Mariano S, Tiberti MM, Boschi E (2008) The database of individual seismogenic sources (DISS), version 3: summarizing 20 years of research on Italy's earthquake geology. Tectonoph 453:20–43 doi:10.1016/j.tecto.2007.04.014(database open for consultation at <http://diss.rm.ingv.it/diss/>).
- Bethmann, F., N. Deichmann, P. Martin Mai (2011). Scaling Relations of Local Magnitude versus Moment Magnitude for Sequences of Similar Earthquakes in Switzerland, Bulletin of the Seismological Society of America, Vol. 101, No. 2, pp. 515–534, April 2011, doi: 10.1785/0120100179.
- Bindi, D., F. Pacor, L. Luzi, R. Puglia, M. Massa, G. Ameri, R. Paolucci (2011). Ground motion prediction equations derived from the Italian strong motion database. Bull Earthquake Eng (2011) 9:1899–1920, doi: 10.1007/s10518-011-9313-z.
- Bouchon, M. and Aki, K. (1967) "Scaling Law of Seismic Spectrum." Journal of Geophysical Research, Vol. 72, No. 4 pp. 1217—1231.
- Boore, D.M. (2003). Simulation of Ground Motion Using the Stochastic Method. Pure appl. geophys. 160 (2003) 635–676.

	<p>Research and Development Programme on Seismic Ground Motion</p> <p>CONFIDENTIAL</p> <p><i>Restricted to SIGMA scientific partners and members of the consortium, please do not pass around</i></p>	<p>Ref : SIGMA-2013-D4-94 Version : 01</p> <p>Date : October 2013 Page :</p>
--	---	--

- Boore, D.M. (1983). Stochastic simulation of high-frequency ground motions based on seismological models of the radiated spectra, *Bull. Seism. Soc. Am.*73, 1865–1894.
- Burrato, P., F. Maesano, G. Valensise (2012). Review of active faulting in the Po Plain, SIGMA-2012-D1-27, June 30 2012.
- Burrato, P., F. Maesano, G. Valensise (2013). Preliminary regional earthquake source models of the Po Plain, based on full 3D definition of active faults, SIGMA-2013-D1-67, January 31 2013.
- Cadet, H., P.-Y. Bard, A. Rodriguez-Marek (2012). Site effect assessment using KiK-net data: Part 1. A simple correction procedure for surface/downhole spectral ratios. *Bull Earthquake Eng* (2012) 10:421–448. DOI 10.1007/s10518-011-9283-1.
- Castro, R., F. Pacor, F. Pacor, R. Puglia, G. Ameri, J.Letort, M.Massa, L. Luzi (2013). The 20 and 29 May, 2012, Emilia Earthquakes (Northern Italy) and the Main Aftershocks: S-wave Attenuation, Acceleration Source Functions and Site Effects, *Geophysical Journal International*, submitted.
- Cauzzi, C. and Faccioli, E., 2008. Broadband (0.05 to 20 s) prediction of displacement response spectra based on worldwide digital records. *Journal of Seismology*, Vol. 12, No. 4 pp. 453-475.
- Chen, L., E. Faccioli (2013). Single-station standard deviation analysis of 2010-2012 strong-motion data from the Canterbury region, New Zealand, BEE, accepted for publication.
- Chiou, B. and Youngs, R., 2008. An NGA Model for the Average Horizontal Component of Peak Ground Motion and Response Spectra. *Earthquake Spectra*, Vol. 24, No. 1 pp. 173-215.
- Convertito, V., Emolo, A., and Zollo, A. (2006). Seismic-Hazard Assessment for a Characteristic Earthquake Scenario: An Integrated Probabilistic-Deterministic Method. *Bulletin of the Seismological Society of America* 96(2), 377-391.
- Delavaud, E., Cotton, F., Akkar, S., Scherbaum, F., Danciu, L., Beauval, C., Drouet, S., Douglas, J., Basili, R., Sandikkaya, M.A., Segou, M., Faccioli, E., Theodoulidis, N., 2012. Toward a ground-motion logic tree for probabilistic seismic hazard assessment in Europe, *J Seismol*, DOI 10.1007/s10950-012-9281-z.
- DISS Working Group (2010), Database of Individual Seismogenic Sources (DISS), Version 3.1.01: A compilation of potential sources for earthquakes larger than M 5.5 in Italy and surrounding areas, <http://diss.rm.ingv.it/diss/>, © INGV 20092010 - Istituto Nazionale di Geofisica e Vulcanologia –All.


	<p>Research and Development Programme on Seismic Ground Motion</p> <p>CONFIDENTIAL</p> <p><i>Restricted to SIGMA scientific partners and members of the consortium, please do not pass around</i></p>	<p>Ref : SIGMA-2013-D4-94 Version : 01</p> <p>Date : October 2013 Page :</p>
--	---	--

- Faccioli E, Chen L (2012) Single-station standard deviation for probabilistic seismic hazard analyses at representative sites in the Po Plain, Northern Italy. Proc. Workshop in Honor and Memory of Prof. Giuseppe Grandori, November 5, 2012, Milan , Italy.
- Faccioli, E. (2012). Recent evolution and challenges in the Seismic Hazard Analysis of the Po Plain region, Northern Italy, Bull Earthquake Eng. DOI 10.1007/s10518-012-9416-1.
- Faccioli E, Bianchini A, Villani M (2010) New ground motion prediction equations for  $T > 1s$  and their influence on seismic hazard assessment. Proceedings of the University of Tokyo Symposium on Long-period Ground Motion and Urban Disaster Mitigation, Tokyo, Japan.
- Field EH, Johnson DD, Dolan JF (1999) A mutually consistent seismic-hazard source model for Southern California. Bull Seismol Soc Am 89:559–578.
- Gasperini, P., B. Lolli, G. Vannucci (2013). Empirical Calibration of Local Magnitude Data Sets Versus Moment Magnitude in Italy. Bulletin of the Seismological Society of America, Vol. 103, No. 4, pp. 2227–2246, August 2013, doi: 10.1785/0120120356.
- Graves, R., Jordan, T., Callaghan, S., Deelman, E., Field, E., Juve, G., Kesselman, C., Maechling, P., Mehta, G., Milner, K., Okaya, D., Small, P., and Vahi, K. (2011). CyberShake: A Physics-Based Seismic Hazard Model for Southern California. Pure Appl. Geophys, Gutenberg, B., and Richter, C.F., (1956), Magnitude and energy of earthquakes, Annals of Geophysics, 9, pp. 1-15.
- Grünthal, G.; Whalstrom, R.; Stromeyer, D. 2009a. The unified catalogue of earthquakes in central, northern and northwestern Europe (CENEC)-updated and expanded to the last millenium. Journal of seismology ; 13, 4,517-541.
- Grünthal, G.; Stromeyer, D. ; Whalstrom, R. 2009b. Harmonization check of Mw within the central, northern and northwestern European earthquake catalogue. Journal of seismology ; 13, 4,613-632.
- Gruppo di Lavoro MPS (2004). Redazione della mappa di pericolosità sismica prevista dall'Ordinanza PCM del 20 marzo 2003. Rapporto Conclusivo per il Dipartimento della Protezione Civile, INGVMilano-Roma, aprile 2004, 65 pp. + 5 appendici.
- Hanks TC, Kanamori H (1979) A moment magnitude scale. J Geophys Res 84:2348–2350. doi:10.1029/JB084iB05p02348.
- Jara, J.M. and Rosenblueth, E. [1988]"Probability distribution of times between characteristic subduction earthquakes." Earthquake Spectra, Vol. 4 pp. 499 -- 529.

	<p>Research and Development Programme on Seismic Ground Motion</p> <p>CONFIDENTIAL</p> <p><i>Restricted to SIGMA scientific partners and members of the consortium, please do not pass around</i></p>	<p>Ref : SIGMA-2013-D4-94 Version : 01</p> <p>Date : October 2013 Page :</p>
--	---	--

- Lombardi, A.M., W. Marzocchi (2010). A double-branching model applied to long-term forecasting of Italian seismicity ( $ML \geq 5.0$ ) within the CSEP project. ANNALS OF GEOPHYSICS, 53, 3, 2010; doi: 10.4401/ag-4762.
- Malagnini, L., R. B. Herrmann, I. Munafo', M. Buttinelli, M. Anselmi, A. Akinci, and E. Boschi (2012). The 2012 Ferrara Seismic Sequence: Regional Crustal Structure, Earthquake Sources, and Seismic Hazard, Geophys. Res. Lett., doi:10.1029/2012GL053214, in press.
- Motazedian, D. and Atkinson, G.M. [2005]"Stochastic Finite-Fault Modeling Based on a Dynamic Corner Frequency." Bulletin of the Seismological Society of America, Vol. 95, No. 3 pp. 995--1010. doi:10.1785/0120030207.
- Ordaz M., Jara J.M., Singh S.K. (1991) Riesgo sísmico y espectros de diseño en el estado de Guerrero. Technical Report, Instituto de Ingenieria, UNAM, Mexico City.
- Pacor F.,Luzi L., Massa M., Bindi D. (2012). Ranking of available GMPEs from residual analysis for northern Italy and definition of reference GMPEs. SIGMA Project, Deliverable SIGMA-2012-D2-53-02.
- Pacor F.,Luzi L., D'Amico M., Puglia R. and Bindi D. (2013a). Updating and analysis of strong-motion database of Northern Italy through the residual analysis between empirical predictions and observations in the Po plain region. SIGMA ENEL Project, Deliverable SIGM0002-2013.
- Pacor F.,Luzi L., Puglia R., D'Amico M. (2013b). CALIBRATION OF GMPEs FOR PO PLAIN REGION. SIGMA ENEL Project, Deliverable SIGMA-2013-D2-72.
- Peruzza, L., Pace, B., Cavallini, F. [2008] "Error propagation in time-dependent probability of occurrence for characteristic earthquakes in Italy", Journal of Seismology, DOI 10.1007/s10950-008-9131-1.
- Pondrelli S., Salimbeni S., Morelli A., Ekström G., Postpischl L., Vannucci G. and Boschi E., European-Mediterranean Regional Centroid Moment Tensor Catalog: solutions for 2005-2008, Phys. Earth Planet. Int., in press, 2011.
- Pondrelli, S., S. Salimbeni, A. Morelli, G. Ekström, M. Olivieri and E. Boschi, 2010, Seismic moment tensors of the April 2009, L'Aquila (Central Italy) earthquake sequence, Geophys. J. Int., doi: 10.1111/j.1365-246X.2009.04418.x
- Rodríguez-Marek, A., Montalva, G., Cotton, F. and Bonilla, F. (2011). Analysis of single-station standard deviation using the KiK-net data, Bull. Seismological Soc. America, 101(3), June 2011, pp. 1242–1258.
- Rovida, A., R. Camassi, P. Gasperini, M. Stucchi (eds.), 2011. CPTI11, the 2011 version of the Parametric Catalogue of Italian Earthquakes. Milano, Bologna, <http://emidius.mi.ingv-it/CPTI>.



	<p>Research and Development Programme on Seismic Ground Motion</p> <p>CONFIDENTIAL</p> <p><i>Restricted to SIGMA scientific partners and members of the consortium, please do not pass around</i></p>	<p>Ref : SIGMA-2013-D4-94 Version : 01</p> <p>Date : October 2013 Page :</p>
--	---	--

- Villani, M., E. Faccioli, M. Ordaz, M. Stupazzini (2012). High resolution seismic hazard analysis in a complex geological configuration: the case of Sulmona (Central Italy) basin, submitted.
- Villani, M. (2010). High resolution SHA in the vicinity of earthquake sources, PhD Thesis, RoseSCHOOL, IUSS Pavia (Italy).
- Wells, DL, K.J. Coppersmith (1994) New empirical relationships among magnitude, rupture length, rupture width, rupture area, and surface displacement. Bull Seismol. Soc Am 84(4):974–1002.
- Zhao, J. X., Zhang, J., Asano, A., Ohno, Y., Oouchi, T., Takahashi, T., Ogawa, H., Irikura, K., Thio, H. K., Somerville, P. G. and Y. Fukushima, 2006. Attenuation relations of strong ground motion in Japan using site classification based on predominant period. Bull. Seism. Soc. Am., Vol. 96 No. 3, pp. 898–913.
- Zonno, G., R. Basili, F. Meroni, G. Musacchio, P. Martin Mai, G. Valensise (2012). High-frequency maximum observable shaking map of Italy from fault sources, Bull Earthquake Eng. DOI 10.1007/s10518-012-9346-y.

## APPENDIX A

### New Gutenberg-Richter correlations for all the SSZ areas at study

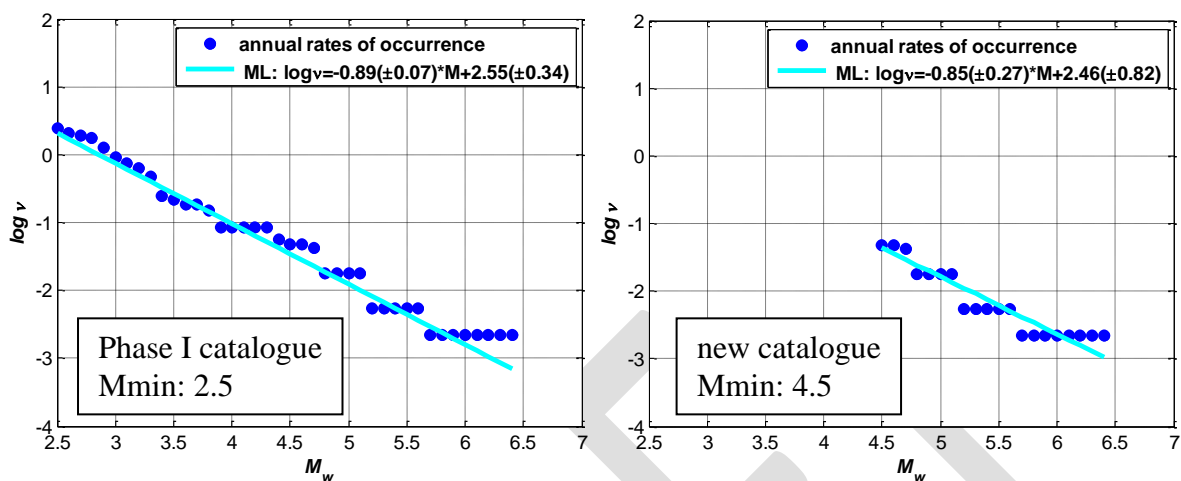


Figure A.1 –GR parameters for SSZ 901.

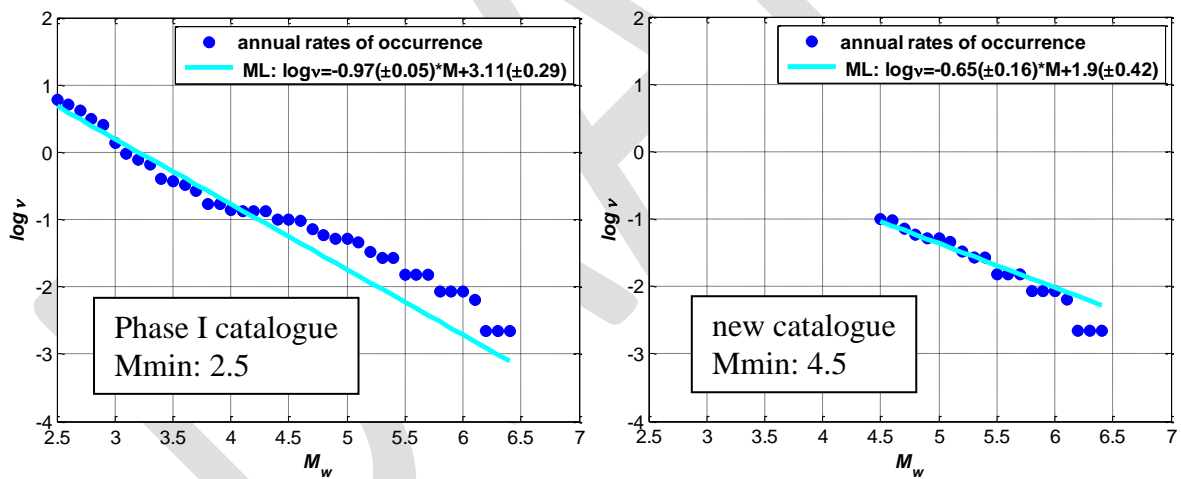


Figure A.2 –GR parameters for SSZ 902.

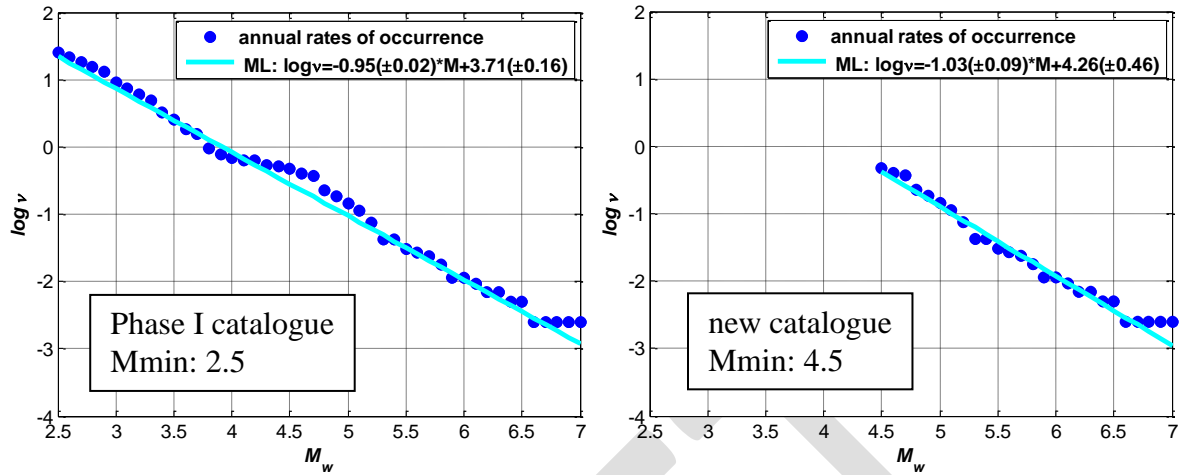


Figure A.3 –GR parameters for SSZ 905.

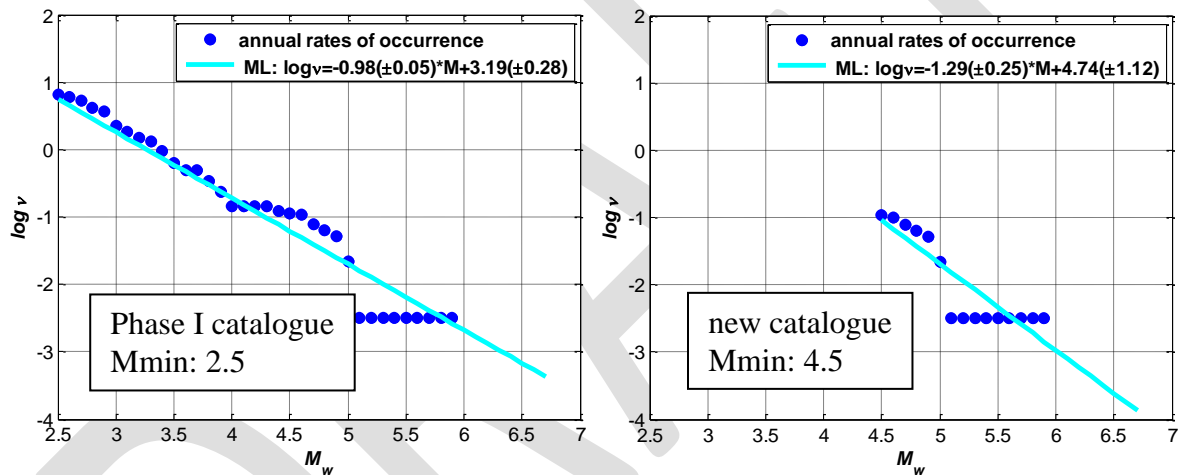


Figure A.4 –GR parameters for SSZ 906.

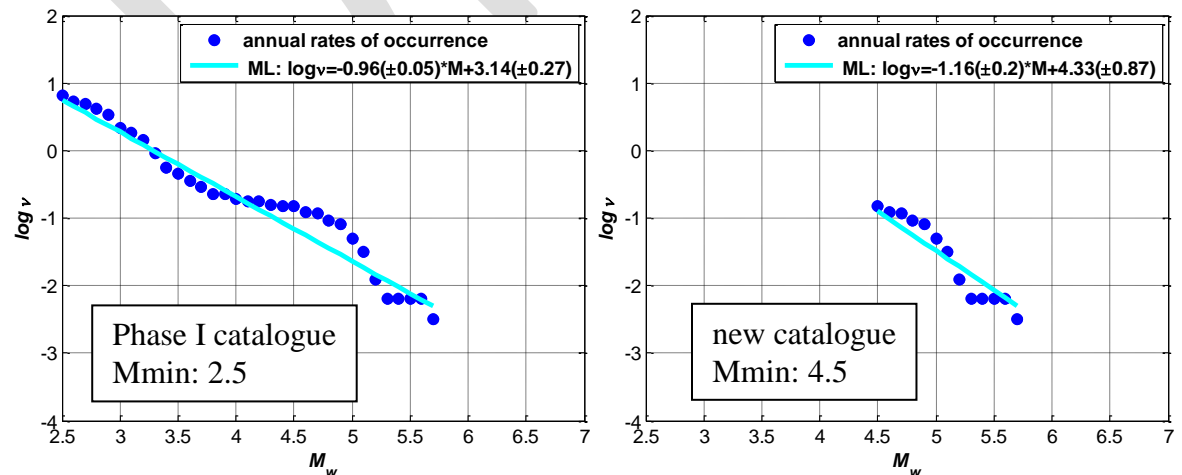


Figure A.5 –GR parameters for SSZ 907.

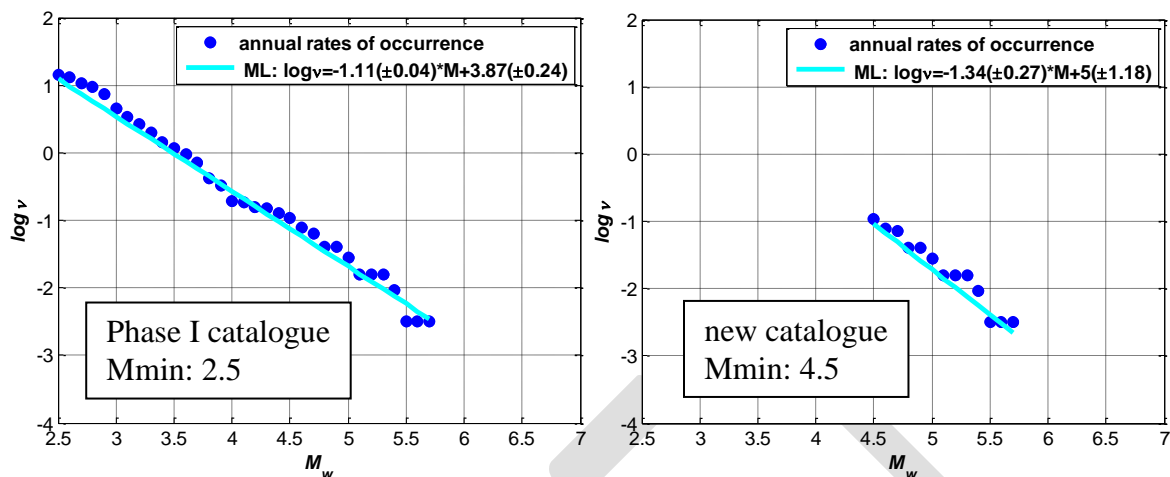


Figure A.6 –GR parameters for SSZ 908.

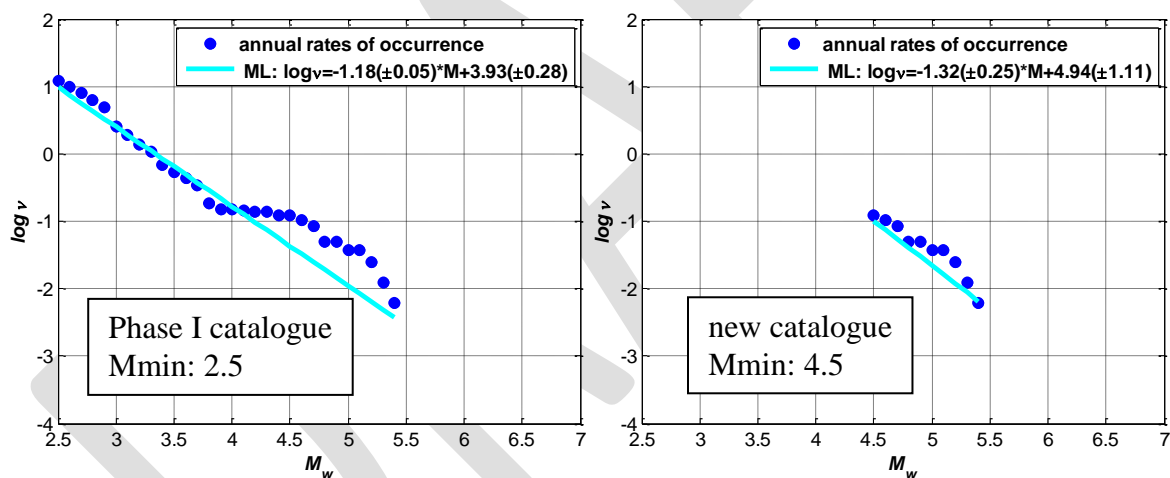


Figure A.7 –GR parameters for SSZ 909.

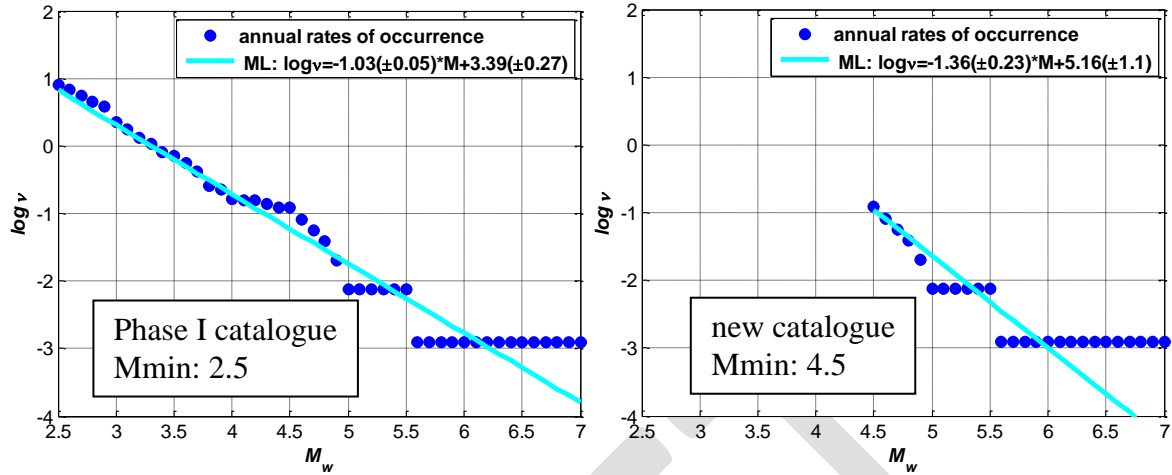


Figure A.8 –GR parameters for SSZ 910.

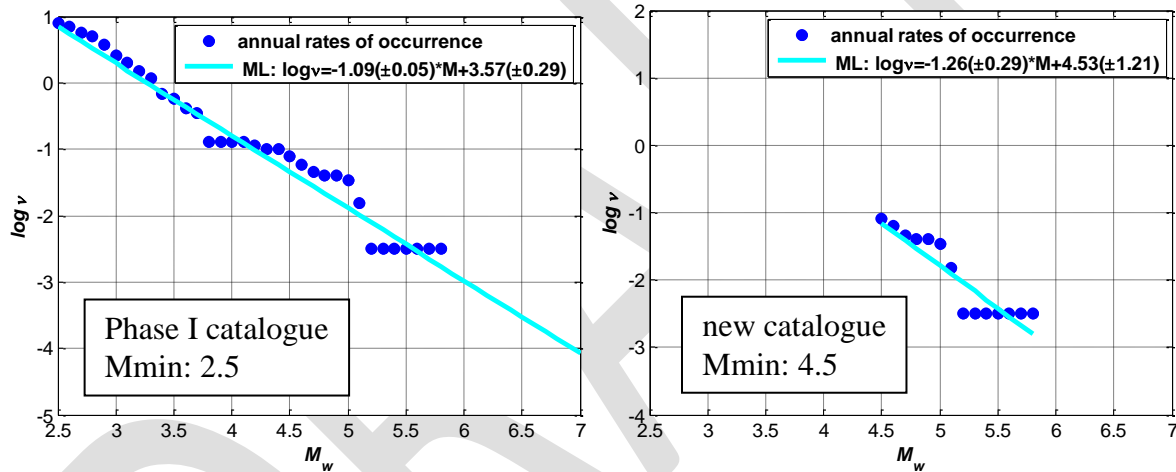


Figure A.9 –GR parameters for SSZ 911.

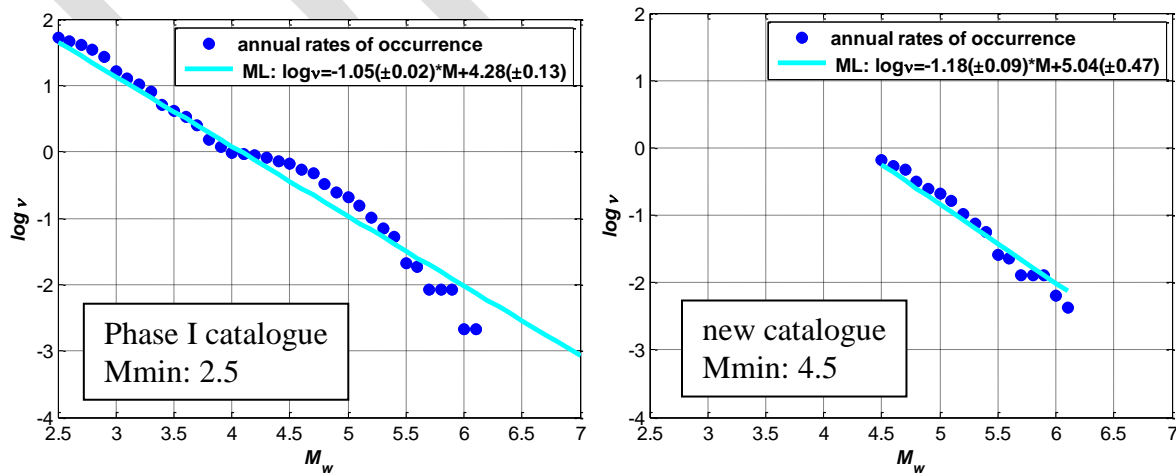


Figure A.10 –GR parameters for SSZ 912+913+914.

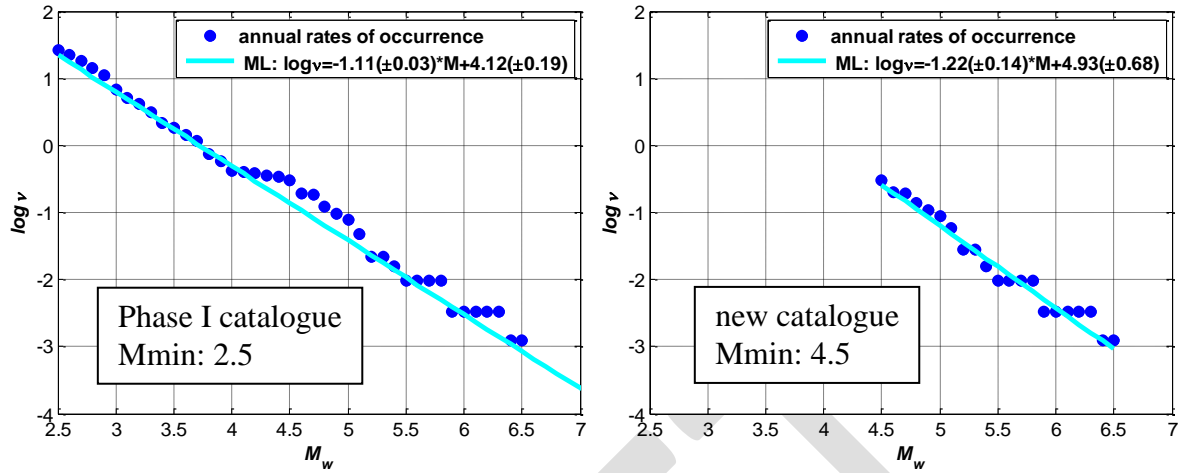


Figure A.11 –GR parameters for SSZ 915.

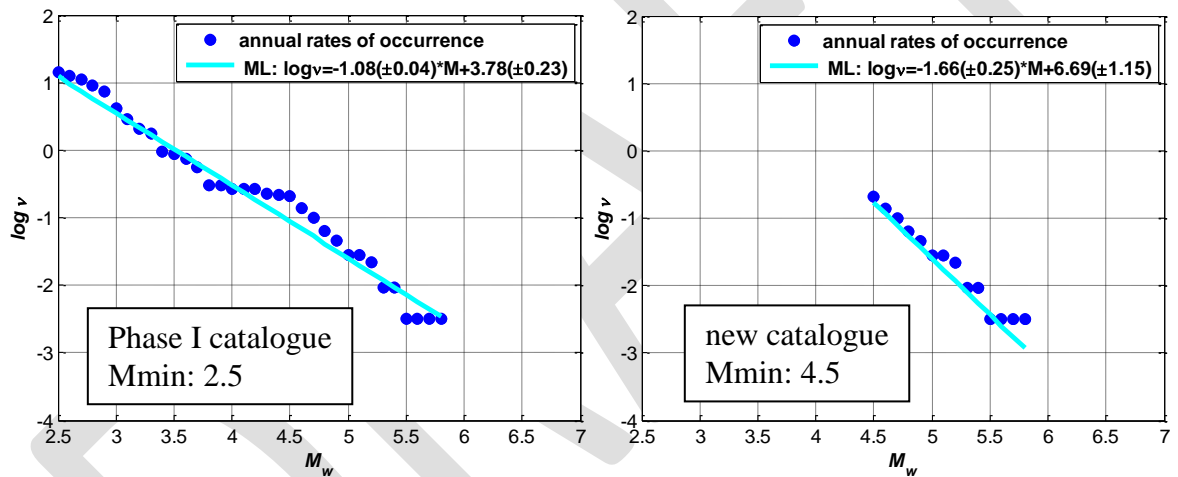


Figure A.12 –GR parameters for SSZ 916.



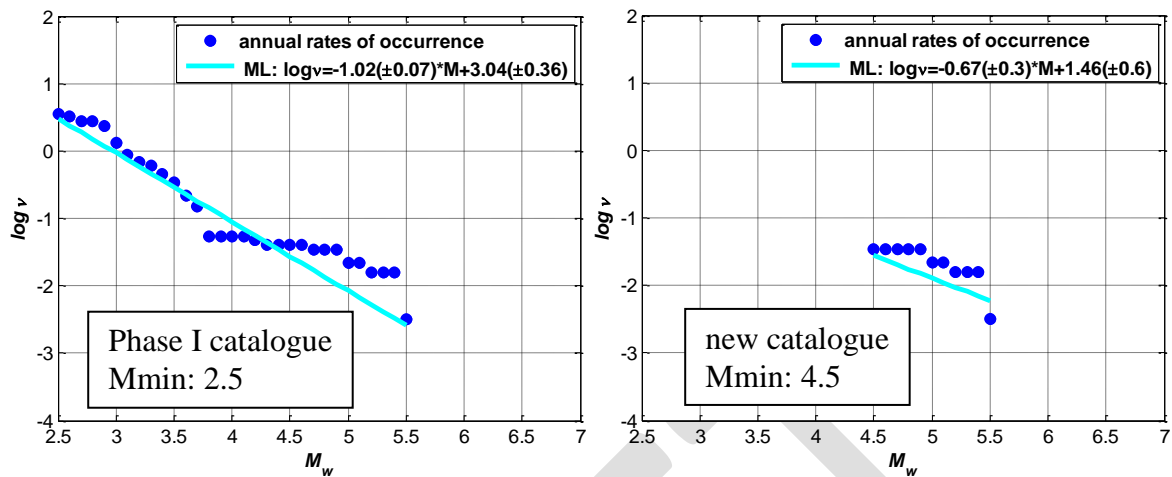


Figure A.13 –GR parameters for the subduction zone (*slab*).

DRAFT

# **SITE SPECIFIC PROBABILISTIC STUDY FOR PO PLAIN AREA**

**Report by E. Faccioli, M. Vanini and R. Paolucci**

*Review by G. Woo*

*Member of the SIGMA Scientific Committee*

*14 November 2013*

## **GENERAL SUMMARY**

This report is notable and highly commendable for exploring, in multiple modelling aspects of PSHA, avenues for using new information, understanding and methodology. As a research document, the report provides PSHA practitioners with some ideas for future application, and encourages further research in the same direction.

It is widely accepted that any innovative development in PSHA has to be thoroughly tested and validated before it might be considered for actual use in a nuclear safety context. So a substantial amount of further research, data accumulation and analysis may need to be undertaken before implementation of some of the ideas in an actual nuclear PSHA. However, the results are already of value in sensitivity analysis and stress testing.

Some specific comments are listed below.

### **5.1. Method of ground motion residual analysis**

*The use of the so-called single station sigma, or non ergodic, approach has been shown to affect the hazard estimates in different ways, depending on how the site correction terms and the single site sigmas combine with the standard deviations of the GMPEs at use. We found that the overall effect of this approach has been to decrease substantially the severity of hazard estimations at one of the test sites (CAS).*

The use of a single station sigma is the ideal preferred objective of every seismic hazard analyst. There is an expectation that there might be a sigma reduction of 0.1 ~ 0.2. But there is a practical question over whether this is really justifiable now, based on existing evidence, especially when hazard estimations may be considerably reduced.

### **6.3 Faults**

*Moreover, CRISIS allows a slip-predictable behaviour in time that is modelled assuming, after Jara and Rosenblueth (1988), that the expected value of the magnitude of the characteristic earthquake ( $E(M)$ ) grows with the time elapsed since the last characteristic event.*

Recognizing that fault magnitudes may be quite moderate, it would be instructive to see the strength of the evidence for assuming slip-predictable behaviour for the regional faults being modelled. A more recent reference than from 1988 would be helpful in building confidence.

### **6.4. Recurrence time**

*The “ideal” situation for a given fault segment would obviously be to carry a long list of associated earthquakes with clear neo-tectonic markers, so that statistics could be derived directly from observations. The actual observations of multiple, characteristic events on the same fault segment in Italy are definitely few, mostly represented by recent active sources in Central Apennines.*

Recognizing that the characteristic earthquake hypothesis has come under particular scrutiny and criticism in the past few years, and that the supportive Italian data are rather limited, a more robust defence of adopting this model might have been expected.

### **6.6. Modelling faults with an alternative approach**

*As a matter of comparison and validation of the adopted modeling of faults sources, with special regard for near field locations, we implemented a very recent novel approach for probabilistic seismic hazard analyses, in which deterministically computed ground motion is introduced, in replacement of the empirically predicted values of GMPEs. This approach, thoroughly discussed in Villani et al. (2012) and Villani (2010), to which we refer for details, was first proposed by Convertito et al. (2006), who used a predominantly far field approximation for generating the deterministic ground motions. Moreover within the SCEC's CyberShake Project (Graves et al., 2011) 3D simulations and finite fault rupture descriptions in the low frequency range have been used to compute seismic hazard analyses in Southern California.*

It is very commendable and far-sighted for the authors to have implemented this novel approach for probabilistic seismic hazard analysis. This methodology will supersede GMPE's at some stage in the future, especially in some geological environments.

But, to use an American saying, is this method ‘ready for prime time’? Tom Jordan, SCEC, thinks not yet, according to a recent conversation I had with him in late October 2013. Over time, issues, e.g. over resolution at higher frequencies, will doubtless be sorted out, but the current capability remains open to question.

### **6.6.3. Approach used for hazard computations with Composite Sources**

*Each CSS is partitioned into faults of equal size, consistent with the associated characteristic magnitude  $m_C$  on the basis of the Wells and Coppersmith (1994) relations, and the CSS representative focal mechanism.*

The adequacy of the 1994 Wells and Coppersmith relations is questionable, given the current basic research being undertaken to return to the primary evidence, revise the underlying dataset and update these relations. The uneven quality of the data taken by Wells and Coppersmith makes the continued use of these relations a convenience that is increasingly hard to justify.

## **8. Logic Tree**

*As to the weights assigned to the different earthquake source model branches, we relied on the very recent results of the statistical performance of several hazard models for Italy tested vs. strong motion observations (<https://sites.google.com/site/ingvdpc2012progettos2/home>), with the highest scores gained by the same type gridded seismicity model used herein. For AS and FS+BG models, the results of separate analyses did not give us any reason to assign different weights, as shown in Sect. 6.5.*

I positively endorse the scientific principle of relying on statistical performance tests for assigning model weights. The result that the gridded seismicity weight (0.6) is higher than for the model-based seismicity (0.4) is very interesting, and might serve as a guide to seismic hazard assessments elsewhere. Typically, the relative weight accorded to a zoneless seismicity model is significantly lower than 0.5, reflecting more a collective adherence towards Cornell-McGuire tradition than any empirical scientific justification.

## **9. Accounting for site effects**

*More significant, however, is that the use of both SAFs leads to decreasing the values of the site specific spectra below the bedrock values at periods  $0 < T < 0.2$  s, mostly due to non-linear effects.*

It would be instructive to have some more detailed and explicit explanation of this result, to ensure that it is not a numerical artefact of the high-frequency resolution of the computation.

## Project SIGMA

# SITE SPECIFIC PROBABILISTIC STUDY FOR PO PLAIN AREA

(Ref : SIGMA-2013-D4-94)

*Review by : Jean B. Savy  
October 29, 2013*

### 1. Scope of the work reviewed

This is a review of the work documented in EDF Ref: SIGMA-2012- D4-94 by Ezio Faccioli, Manuela Vanini and Roberto Paolucci. This work is to be presented at the CS6 of November 13<sup>th</sup> to 15<sup>th</sup>, 2013, in Paris.

The reviewed report is an update and extension of a Phase I PSHA analysis for the Po plain area. The authors took each part of the entire chain of models and methods and updated parameters in the view of new or better data more recently available, and updated the methods to the most recently published state-of-the-art methods. The goal was to produce estimates of PSHA using the best available methods and use the best data, without necessarily producing new methods, or new data, thereby creating a new standard for PSHA.

### 2. Review approach

The main goal of this study was not to do more research to develop new methods but rather it was to make use of the best methods and data to produce a state-of-the-art analysis, and in the process, update the results of Phase I. The authors chose to use existing methods, in some cases improving on them, computer codes and data sets that are well documented and published in technical journals. As a result, my review concentrated on the following:

- Relevance and documentation of the methods and tools selected
- Implementation of those methods and tools
- Contextualization, relative to other WPs
- The general conclusions of the study
- General form

### 3. General review conclusions

In my opinion the authors have performed a state-of-the-art PSHA, pulling together the most advanced and tested methods and data bases available to date for the Po plain area. The use of Single-Station parameters was convincingly demonstrated as providing a robust and, generally, reduced estimate of ground-motion predictions.

As a PSHA practitioner myself, I can say that I did not agree with all the choices made in this study, for many of these choices are subjective, sometimes arbitrary, but what I reviewed made sense and was rational, although it sometimes lacked clarity and /or documentation.

The main technical comments concern the estimation and implementation of uncertainties in the seismicity parameters (G-R a and b's), the assignment of weights on the seismicity branches of the Logic trees, and finally the lack of attempt to discuss or reconcile the maximum magnitude estimates in the overlapping areas with neighboring countries.

The reviewed document is well written. An abstract and an executive summary should be added as recommended at the last CS meeting.

#### 4. General comments

- *Relevance and documentation of the methods and tools selected*  
The methods and tools selected reflect the latest in research but in several cases it is taken for granted without explaining the rationale, and without explaining the concepts, advantages and limitations. This is especially the case for the selection of the weights in the Logic Tree where the results of a recent study was used to come up with those weights, but a review of the referenced study did not provide the information that was eventually used in this study.
- *Implementation of those methods and tools*  
Once methods, and tools, were selected, they were implemented properly.
- *Contextualization, relative to other WPs*  
There was no attempt to put the results of this work within the context of SIGMA, which is somewhat understandable, since this study appears to be mostly self-contained. However, some of the very good work done here can be used in other WPs, such as the implementation of the scoring of PSHA models by Albarello et al. method, or the hybrid method of using EXSIN code in lieu of attenuation relationships for small events and small distances.
- *The general conclusions of the study*  
Although section 12 "Conclusions" is tentative in the reviewed report, it rightly points in the direction of one of the main goals of SIGMA which is the improvements in the estimates of hazard from using the Single-Station (non-ergodic) approach to estimating the ground-motion.
- *General form*  
The report is well organized and well written. Only missing are an abstract and an executive summary to follow the recommendations of the last CS.

#### 5. Detailed comments

1. *Phase I WP4 work*
  - No comments.
2. *Phase II work*



- No comments.
3. *Catalogue and magnitude conversions*
- The conversions shown in the report do not mention any uncertainty. What would be the uncertainty on Mw at the boundaries of the range of magnitudes, and how would that affects the estimate of uncertainties in the a's and b's estimates in the next section?  
This may not have much influence on the hazard for low return periods, but it certainly does for the return period of interest in SIGMA, that is  $10^4$  and  $10^5$  years.
  - The uncertainties in the a's and b's are substantial. How was this epistemic uncertainty taken in consideration?. Are the a's and b's used in the analysis, or are the earthquakes considered as purely characteristic? Table 1 shows alternative choices for Mmax, with its associated  $\lambda_{M>4.5}$  but no uncertainty on b. If that uncertainty was considered, it must be explained how it was used in the PSHA calculation code.
4. *Catalogue and magnitude conversions*
- No comments.
5. *The single station sigma*
- $\delta S_2 S_s$  is an epistemic uncertainty that in theory should be dealt in the same way as other epistemic uncertainties, such as by adding a branch in the logic tree. Was this considered? What would be the effect on the results?
  - Page 24 top paragraph, 4<sup>th</sup> line: replace “(see Figure 14)” by “(see Figure 18)”
6. *Model-based description: faults + background*
- Page 29 it is mentioned that “appropriate tests” were performed to verify that screening out the faults with peak response spectrum accelerations less than 0.03g was fine. Can a few details be given on the type of tests? What GMPE(s)?, Was it on the basis of median, mean, how many  $\sigma$ 's, etc.?
  - Page 30, section 6.2, second sentence:  
“*This area has been chosen in order to cover the low seismicity ( $M_w$  4.5 - 5.4) not accounted for by fault modelling.*”  
What was the method used to determine whether an earthquake belongs to a fault or not?
  - Page 31 after Figure 23, the following sentence is ambiguous:  
“*The G-R parameters for this area have been computed has shown before, selecting events from the updated catalogue, starting from a minimum value of 4.5 up to a maximum of 5.4 (158 events in all) and relying on the same completeness periods defined in Sigma Phase I.*”  
Does it mean that other sources within (the composite sources) do not have events in [4.5-5.4]?
  - Table 2 page 32: How is the uncertainty in the bi-linear reoccurrence curves handled?
  - Page 34: The Jara and Rosenblueth study, mentioned in reference to support the slip-predictable model, was essentially developed and tested with data from subduction zones. Furthermore the use of a time-dependent model implies that the results must be specifically developed for given windows of time, with a choice of starting date. This is not discussed in the report, as all the results are given in terms of annual probabilities. Is there an intention to use this kind of model in the future? Is there enough data for this purpose?
  - Table 3, page 35: The central value of the characteristic magnitude ( $M_c$ ) is certainly not known without uncertainty. The generic model shown in Figure 27 does show a  $\Delta M$  on either side of  $M_c$ , but table 3 does not give this value. The report should explain how the model is used, and specifically what is the  $\Delta M$ .
  - Section 6.6.3 brings several questions:

- Figure 35 shows the distribution of earthquakes on the faults. Since we allow the same  $M_c$  to be anywhere on the fault with equal probability, aren't we running the risk of underestimating the ground-motion in cases where the site is in the middle such as for CAS and NVL?
  - Since we are doing so much additional work, can't we just develop specific functions of attenuation for these cases and use them as GMPEs in the code?
  - Going one step further, if we now have the tools to do this type of hazard analysis by generating artificial earthquakes by simulation of events on the faults, can't we do the entire analysis that way? One advantage would be to introduce the site effects directly on the "actual" ground-motion rather than on an averaged-out prediction (GMPEs).
7. *Gridded seismicity.*
- Aybige Akinci's paper shows a large uncertainty on the  $b$  values (G-R). Furthermore it does not include a large sample of very large/rare events that are needed for the predictions of ground-motion in the  $10^4$  or  $10^5$  year return period range that are the return periods of interest for large and critical facilities. Thus the comparison, and indeed the validity, of these types of approaches are limited. They are well suited for testing the validity of other methods, such as the standard PSHA approach, for return periods probably up to a few thousand years, but are not well suited for larger return periods.
8. *Logic tree*
- Page 50: Should give a brief explanation of the scoring method developed by Albarello et al. which is referenced in the document as:  
<https://sites.google.com/site/ingvdpc2012progettos2/home>),  
This reference does not actually give the scores and does not either give any indication on how a weight could be assigned to a set of models. (There might be another reference that I could not obtain). Thus the authors need to describe the rationale for choosing the weights they chose on the logic tree shown in Figure 44.  
The description of the scoring methods and data used, plus the fact that we are interested in large return periods, make me strongly disagree with the choice made of 40% for the model-based seismicity and 60% for the gridded model. I think the choice is justifiable for low return periods but not for large ones for which the reverse is more justifiable in my opinion.  
Should the weight of the branches be modulated by the choice of return period?
9. *Accounting for site effects*
- Page 53, last paragraph. What return period was used to calculate the UH spectra for which the compatible records were selected?  
This is important because for large return periods the ground-motion is likely to be high and the soil behavior is likely to be non-linear. For lower return period this is probably not likely to occur. Therefore the calculations of response at the site must be done for the intended return period, and if necessary several different analyses must be done for each of the required return periods.
10. *Results of logic tree for ground type A*
- Figure 46: Results seem strange because the uncertainty in the hazard does not increase with acceleration, as we would expect. Is there a simple explanation to this?
  - Figure 52, 53 and 54 give a good summary of the improvements over Phase I.
  - Figure 55, on the other hand is not a good indicator of the improvements. It is misleading to display the change in variability by a ratio of mean/median because making a ratio when the values are small emphasizes the extent of the arithmetic difference between the two values. Why not simply show the difference between the 16<sup>th</sup> and 84<sup>th</sup> percentiles?
11. *Results of logic tree for ground type C and B*

- No comments
12. *Conclusions (tentative)*
- This section restates the outline of the work performed without clearly enumerating the important results and conclusions of the various parts of the study.
  - This section should also make the link with the other WPs , in particular with WP2 for the very good work on single-station uncertainty, and WP4 for the model testing and scoring.

Respectfully submitted, October 29, 2013.

Jean Savy